

**Forschungszentrum Karlsruhe**  
Technik und Umwelt

**Wissenschaftliche Berichte**  
FZKA 6385

**The Second Advanced Lead  
Lithium Blanket Concept  
Using ODS Steel as Structural  
Material and SiC<sub>f</sub>/SiC Flow  
Channel Inserts as Electrical  
and Thermal Insulators  
(Task PPA 2.5)**

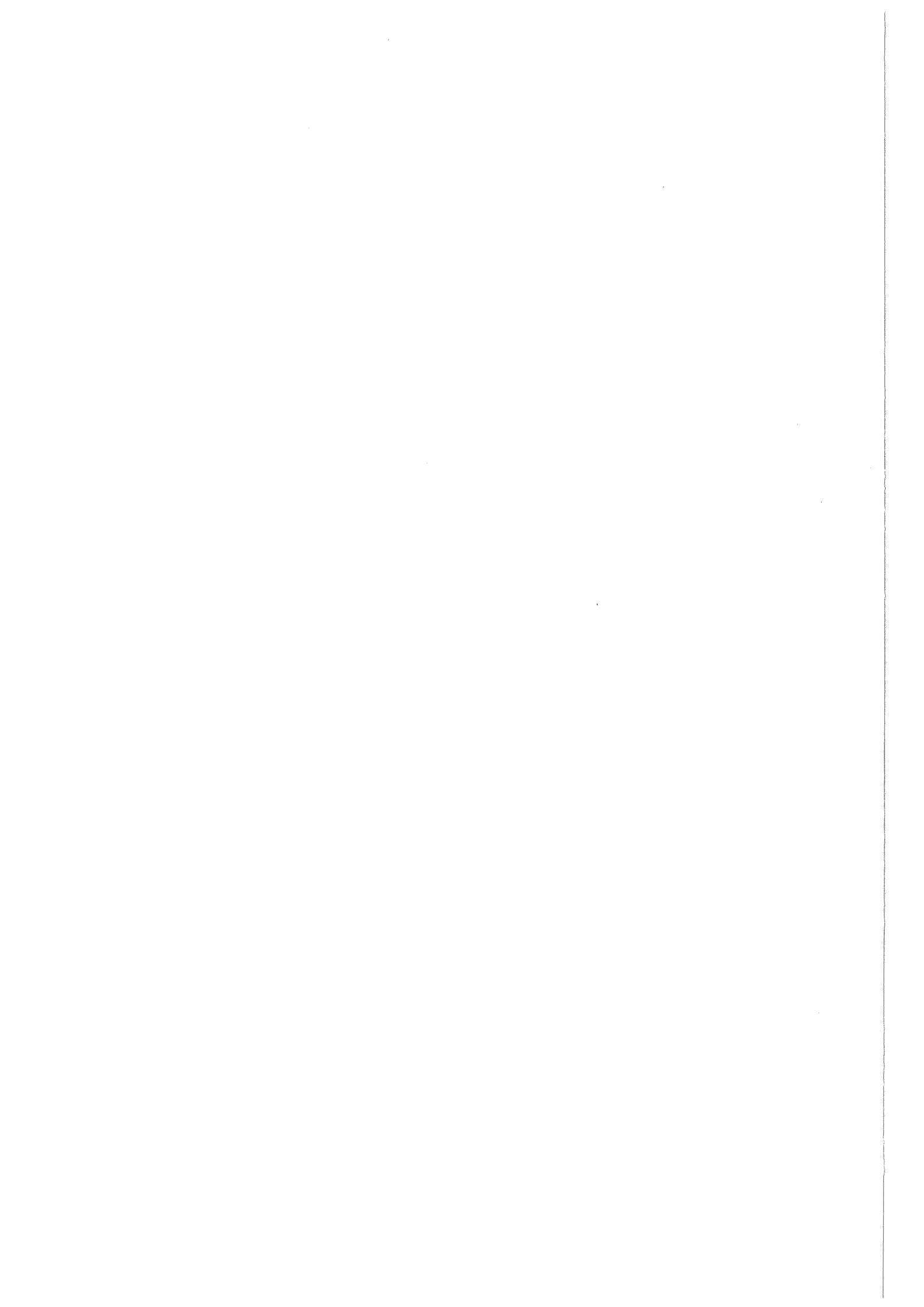
**Final Report**

**P. Norajitra, L. Bühler, U. Fischer,  
K. Kleefeldt, S. Malang, G. Reimann,  
H. Schnauder, G. Aiello, L. Giancarli,  
H. Golfier, Y. Poitevin, J. F. Salavy**

**Institut für Materialforschung  
Projekt Kernfusion**

**Dezember 1999**

---



# **Forschungszentrum Karlsruhe**

Technik und Umwelt

Wissenschaftliche Berichte

**FZKA 6385**

## **The Second Advanced Lead Lithium Blanket Concept Using ODS Steel as Structural Material and SiC<sub>f</sub>/SiC Flow Channel Inserts as Electrical and Thermal Insulators (Task PPA 2.5)**

**Final Report**

**P. Norajitra, L. Bühler, U. Fischer, K. Kleefeldt, S. Malang, G. Reimann,  
H. Schnauder, G. Aiello\*, L. Giancarli\*, H. Golfier\*, Y. Poitevin\*,  
J.F. Salavy\***

Institut für Materialforschung  
Projekt Kernfusion

*\* CEA/Saclay, DRN/DMT/SERMA, 91191 Gif-sur-Yvette, France*

Forschungszentrum Karlsruhe GmbH  
1999

**Als Manuskript gedruckt**  
**Für diesen Bericht behalten wir uns alle Rechte vor**  
**Forschungszentrum Karlsruhe GmbH**  
**Postfach 3640, 76021 Karlsruhe**  
**Mitglied der Hermann von Helmholtz-Gemeinschaft**  
**Deutscher Forschungszentren (HGF)**  
**ISSN 0947-8620**

## **Abstract**

Preparatory work on the advanced dual coolant (A-DCL) blanket concept using SiC<sub>f</sub>/SiC flow channel inserts as electrical and thermal insulators has been carried out at the Forschungszentrum Karlsruhe in co-operation with CEA as a conceptual design proposal to the EU fusion power plant study planned to be launched in 2000 within the framework of the EU fusion programme with the main objective of specifying the characteristics of an attractive and viable commercial D-T fusion power plant.

The basic principles and design characteristics of this A-DCL blanket concept are presented and its potential with regard to performance (neutron wall load, lifetime, availability) is discussed in this report. The results of this study show that the A-DCL blanket concept has a high potential for further development due to its high thermal efficiency and its simple concept solution.

## **Das zweite Advanced Blei-Lithium-Blanketkonzept mit ODS-Stahl als Strukturmaterial und SiC<sub>f</sub>/SiC-Strömungskanaleinsätzen als elektrische und thermische Isolierungen**

### **Zusammenfassung**

Für die geplante, ab 2000 zu startende Reaktorstudie im Rahmen des EU Fusionsprogramms wurde im Forschungszentrum Karlsruhe in Zusammenarbeit mit CEA eine vorbereitende Studie für das Advanced Dual Coolant (A-DCL) Blanketkonzept als Konzeptvorschlag zur Weiterentwicklung durchgeführt mit dem Hauptziel, die Charakteristiken eines attraktiven und entwicklungsfähigen (D-T)-Fusionsleistungsreaktors zu spezifizieren.

Das Grundprinzip und die Designcharakteristik dieses A-DCL Blanketkonzeptes sind in diesem Bericht dargestellt, und sein Potential hinsichtlich der Leistung (Neutronen-Wandbelastung, Lebensdauer, Verfügbarkeit) wird diskutiert. Die Ergebnisse dieser Vorstudie zeigen, daß das A-DCL Blanketkonzept aufgrund seines hohen Wirkungsgrades und seiner einfachen Konzeptlösung ein hohes Potential zur Weiterentwicklung besitzt.

## Table of Contents

<b>1.</b>	<b>Introduction</b>	<b>1</b>
<b>2.</b>	<b>Main features</b>	<b>2</b>
<b>3.</b>	<b>Methods of calculation and results</b>	<b>2</b>
<b>3.1</b>	<b>Neutronic calculations</b>	<b>2</b>
<b>3.2</b>	<b>Material data</b>	<b>3</b>
<b>3.3</b>	<b>Thermohydraulic layout, temperature and stress analyses</b>	<b>3</b>
<b>3.3.1</b>	<b>Temperature constraints and coolant temperatures</b>	<b>3</b>
<b>3.3.2</b>	<b>Thermohydraulic layout</b>	<b>3</b>
<b>3.3.3</b>	<b>Temperature and stress analyses</b>	<b>4</b>
<b>3.4</b>	<b>Power conversion system and thermal efficiency</b>	<b>5</b>
<b>4.</b>	<b>Open issues</b>	<b>6</b>
<b>5.</b>	<b>Lifetime, maintainability and reliability</b>	<b>6</b>
<b>6.</b>	<b>Conclusions</b>	<b>7</b>
<b>7.</b>	<b>References</b>	<b>8</b>
<b>8.</b>	<b>Nomenclature</b>	<b>9</b>
	<b>Appendices</b>	<b>39</b>

## 1. Introduction

In the framework of the EU power plant study planned to start in 2000, preparatory work based on an advanced dual coolant (A-DCL) blanket concept [1] has been carried out at the Forschungszentrum Karlsruhe (FZK) in co-operation with CEA (Subtask PPA 2.5.2, silicon carbide composite SiC<sub>f</sub>/SiC related issues) as a proposal for further blanket development. The basic principle of a dual coolant blanket concept is the use of a helium-cooled ferritic steel structure and a self-cooled eutectic lead-lithium alloy Pb-17Li serving both as breeder material and coolant and thus allowing a relatively simple construction. However, this advantage is counteracted by magneto-hydrodynamic (MHD) problems caused by the interaction of liquid metal flow and the strong magnetic field in the fusion reactor. In a previous EU blanket study for DEMO [2] coating of the duct walls with an insulating layer was considered a promising solution of these problems and it needs to be developed.

The A-DCL blanket concept is based on the use of oxide dispersion-strengthened (ODS) steel as structural material and SiC<sub>f</sub>/SiC flow channel inserts (FCIs) as electrical and thermal insulators as proposed in ARIES-ST study [3] and in Ref. [4]. This avoids the need for insulating coatings on the steel structure inside the liquid metal flow channels (for MHD reasons) and allows a high exit temperature of the lead-lithium, which gives the potential for a high efficiency of the power conversion system. In this case, the SiC<sub>f</sub>/SiC FCIs have no structural function (i.e. no static pressure difference between the inside and outside of the insert walls is expected). Therefore, neither a high strength nor a high thermal conductivity (i.e. a strong thermal barrier is favoured) of this material is required. Moreover, the use of ODS ferritic steel as structural material allows for an about 100 K higher temperature limit of the first wall in comparison with MANET steel ( $T_{\text{max-MANET-FW}} \leq 550^{\circ}\text{C}$ , [5]) used in the earlier EU DCL blanket concept for DEMO. For these reasons a higher neutron wall loading (resulting in higher power densities and surface heat load) could be allowed together with an enhancement of the thermal efficiency up to a value of  $\approx 46\%$  using a closed-cycle helium gas turbine in the power conversion system.

The goal of this study is to evaluate the potential of this A-DCL blanket concept with regard to a high thermal efficiency and blanket performance limitations in terms of maximum neutron wall load, maximum surface heat flux, maximum power density, maximum structural temperature, availability and lifetime. On the basis of specified power reactor parameters (geometry, power, and neutron source distribution) for a base case given by UKAEA Culham and characterised by an average neutron wall load of  $2.22 \text{ MW/m}^2$ , the following working steps have been performed:

1. Neutronic calculations to determine the tritium breeding potential, the blanket power generation and the power density distribution for the base case.
2. Fixing of the temperature constraints for this A-DCL concept.
3. Thermohydraulic layout calculation for the coolant media concerning mass flow rate, coolant temperature rises, heat transfer and pressure losses for the base case and further cases with higher blanket performance by linear extrapolation of the power densities and surface heat flux.
4. Corresponding temperature calculations for the first wall and the breeding zone including Pb-17Li, channel inserts, and steel structure. Determination of heat exchange between Pb-17Li and He and iterative corrections of the thermohydraulic data.
5. MHD calculations for the Pb-17Li flow (velocity profile, pressure loss) for correction of the near-wall heat transfer in the Pb-17Li flow.
6. Evaluation of the maximum allowable power limits for the FW and the blanket breeding zone leading to the definition of the A-DCL reference case with a considerably higher power density than that in the base case.
7. Temperature calculations for the FW, and for the blanket breeding zone for the A-DCL reference case.
8. Thermomechanical analyses for the first wall and the SiC<sub>f</sub>/SiC flow channel inserts for the A-DCL reference case.
9. Evaluation of the thermal efficiency and assessment of the availability and life time for the A-DCL reference case.

## 2. Main features

The structural design of an A-DCL outboard blanket segment is shown in Fig. 1 as a cut-out at the torus equatorial zone in an isometric representation with a radial depth of about 1 m, a toroidal width of about 1.4 m and a poloidal height of about 12 m. The whole blanket structure is made of ODS ferritic steel. The U-shaped first wall having a total thickness of 44 mm (Fig. 2), together with the ODS steel grids forming the Pb-17Li coolant channels and the shielding structure, makes up a stiff segment box. Within the first wall (FW) and side wall radial-toroidal helium coolant channels (30x20 mm<sup>2</sup>, rad.xpol., Fig. 3) with 24 mm poloidal channel pitch and 4 mm poloidal thick webs are passed by 14 MPa helium gas in alternating directions. The counter-flowing helium gas contributes to achieving a uniform temperature distribution in the external structure and, hence, to minimising the thermal stresses. Besides, separation of the helium supply systems 1 and 2 guarantees emergency cooling upon failure of a coolant system.

Within the segment box, radial-poloidal and toroidal-poloidal plates are welded together to form stiffening grids which also act as Pb-17Li flow separators (about 335 x 240 mm<sup>2</sup> tor.-rad. rectangular channels, Figs. 2, 5) and are rigidly welded to the external structure. At present, only the diffusion welding method is recommended e.g. in Ref. [6, 7] for the ODS joints (Fig. 4). The blanket box is not expected to withstand the maximum helium coolant pressure because the use of a passive accident management scheme (pressure suppression system) is foreseen. The Pb-17Li, besides having the function of a tritium breeder and neutron multiplier, acts as a coolant as well. The Pb-17Li outlet temperature is determined by compatibility issues and, for efficiency reasons, needs to be maximised. Because of the high magnetic field present in the blanket region (~7 Tesla), the Pb-17Li needs to be electrically insulated from the steel wall despite the relatively low flow velocity (max. 0.5 m/s). This is achieved by adding SiC<sub>f</sub>/SiC channel inserts (about 5 mm thick) which also act as thermal insulators (in order to maximise the Pb-17Li temperature without exceeding the allowable steel temperature). In this concept the most important specific requirements for SiC<sub>f</sub>/SiC which has no direct structural functions are a low electrical conductivity and low thermal conductivity, together with a compatibility with Pb-17Li at high temperatures. To keep the steel temperature sufficiently low, the ODS steel grids are cooled by 14 MPa helium gas after the first wall cooling (Fig. 5).

The helium coolant gas enters the upper blanket segment at 300°C and is routed four times (Fig. 3) on its way downwards in a meandering flow through the segment walls containing the parallel coolant channels by means of a header system. After the last passage the helium temperature at the lower outlet of the segment walls attains a value of 440°C. On its flow upwards, it is passed through the channel arrays in the steel grids with U-shaped coolant channels (Figures 4, 5) and heated up to 480°C before leaving the blanket top.

The liquid metal Pb-17Li enters the top end of the blanket at 460°C, flows downwards through the four channels in the front zone and is heated to 630°C at the blanket bottom (Figures 1, 2, 6). It is then diverted into the two rear channel zones containing eight channels altogether, where it flows back to the top at lower velocity and leaves the blanket at 700°C.

## 3. Methods of calculation and results

### 3.1 Neutronic calculations

Based on the PPA2 reactor parameters (geometry, size, power and neutron source distribution) for the base fusion machine provided by UKAEA Culham neutronic calculations [8] (Appendix 1) have been performed with the MCNP Monte Carlo code using a 7.5 degree torus sector model including the intermediate gaps (Fig. 7) to determine the tritium breeding potential, and to provide the nuclear heating input data, i.e. the blanket power generation and the power density distribution in the blanket, for the subsequent thermohydraulic and thermomechanical calculations. Table 1 shows the neutronic calculation results serving as base case for the following reactor study with a TBR (without ports) of 1.09, an energy multiplication factor of 1.11, and maximum power densities in steel, Pb-17Li and SiC<sub>f</sub>/SiC of 18, 13 and 5 MW/m<sup>3</sup>, respectively. The corresponding radial profiles of the power density are shown in Fig. 8. The average neutron wall loads for the outboard and the overall blanket segments amount to 2.51 and 2.22 MW/m<sup>2</sup>, respectively. For the linear extrapolation of the blanket power in the thermohydraulic and thermomechanical calculations the ratio of avg. heat flux/avg. neutron wall load of 0.17 and the surface flux peaking factor (max./avg.) of 1.3 have been taken into account. The extrapolated maximum power densities for the outboard blanket segments as a function of the average neutron wall load are shown in Fig. 9.

### 3.2 Material data

Since the material data for ODS steel are not yet available, the comparable data of the ferritic steel T91 [9, 10, 11, 12] (Table 2) were taken, e.g. the thermal conductivity  $\lambda$  (400-600°C)  $\approx$  29 W/mK, thermal expansion coeff.  $\alpha \approx 12.0 \cdot 10^{-6}$  1/K and specific heat  $c_p \approx 750$  J/kgK. For stress evaluation according to the RCC-MR code [10, 11], the  $S_m$  values of T91 are assumed on the temperature level shifted upwards by 100 K (see Ref. [13]), e.g.  $S_{m,t-ODS} \approx 174/146/101$  MPa at 500/600/700 °C, respectively, with  $t \approx 10^4$ h (Table 3).

For Pb-17Li the same data as applied for the DEMO calculations [5] are used, e.g.  $\lambda$  (600°C)  $\approx$  19 W/mK and  $c_p$  (600°C)  $\approx$  187 J/kg-K (Table 3).

Present knowledge concerning the SiC<sub>f</sub>/SiC related issues [14] (Appendix 2, 2A) is as follows:

1. Thermal conductivity: The low thermal conductivity of  $< 2$  W/mK could be achieved easily.
2. Electrical conductivity: The electrical conductivity recently measured at JRC/Ispra for CERASEP<sup>®</sup>N2- is about  $500 \Omega^{-1}m^{-1}$ .
3. Sealed surface to avoid the infiltration of Pb-17Li: The possibility of applying a SiC-coating during the densification phase, as a final step, has already been proved by industry. R&D is required in order to verify the lifetime of such a coating (need of limiting the occurrence and the size of cracks).
4. Compatibility with Pb-17Li at high temperature: The only experimental data available (obtained in JRC/Ispra) have shown a compatibility between SiC<sub>f</sub>/SiC and static Pb-17Li at 800°C for a few thousand hours. Pb-17Li infiltration was not fully checked in the experiment. Further R&D is therefore required to check the effects of Pb-17Li velocity and to verify whether infiltration occurs. Longer operating times also have to be achieved.
5. Maximum achievable length of the channel inserts: At present the maximum possible length of the FCI would be about 3.5 m (furnace size).

In the following calculations the thermal conductivity  $\lambda$  of 2 W/mK and the electrical conductivity  $\sigma$  of  $500 \Omega^{-1}m^{-1}$  for SiC<sub>f</sub>/SiC are assumed on a preliminary basis.

### 3.3 Thermohydraulic layout, temperature and stress analyses

#### 3.3.1 Temperature constraints and coolant temperatures

Two temperature limits are relevant for the blanket layout: a) the maximum temperature of the ODS steel, which is expected on the plasma facing surface of the FW at the equatorial plane of the outboard segments, should not exceed 650 °C due to a strong decrease of its creep rupture strength beyond this temperature; b) the maximum interface temperature between the ODS and the stagnant Pb-17Li should not exceed 500 °C due to corrosion. To adapt to these boundary conditions, the coolant temperatures were chosen as follows:  $T_{He, inlet} = 300$  °C (in consideration of the secondary He circuit in the power conversion system),  $T_{He, outlet} = 480$  °C;  $T_{Pb-17Li, inlet} = 460$  °C (in consideration of the pinch point) and  $T_{Pb-17Li, outlet} = 700$  °C. The following detailed thermomechanical analyses were carried out for the outboard blankets because their thermal loads are higher than those at the inboard blankets, especially at the equatorial plane of the torus where the highest power densities together with the peak surface heat flux are expected.

#### 3.3.2 Thermohydraulic layout

Based on a linear extrapolation of the surface heat flux and the neutron power from the base case, the thermohydraulic calculations were carried out for a range of the maximum surface heat flux between 0.1-1.5 MW/m<sup>2</sup> (corresponding to a range of average neutron wall load of 0.45-6.79 MW/m<sup>2</sup>). After fixing the coolant inlet and outlet temperatures (see above), the helium and Pb-17Li mass flow rates were pre-determined in a first step, omitting the heat exchange between the helium and Pb-17Li coolants. In a next step, the amount of this heat exchange was determined in detail by means of the

temperature field calculations (see next section), thus leading back to a correction of the mass flow rates which were found to be less than 2% because of a strong heat insulating effect of the SiC<sub>f</sub>/SiC FCIs with the chosen property. Moreover, in order to enhance the heat transfer coefficient  $\alpha_{\text{He/wall}}$  and, hence, to keep the maximum steel temperatures below the allowable limit, two surfaces of the He channels, excluding the web surfaces, are artificially roughened (Figures 3, 4). As a result,  $\alpha_{\text{He/wall}}$  is increased by a factor  $f_{\alpha}$  of 2, as assumed in the DEMO calculations. To minimise the He pressure losses for the expected larger performance in the reference case than in the base case (Table 1), a relatively high He pressure of 14 MPa was chosen, which leads to a reasonable pumping power in the He loop of about 5% for the reference case relative to the extracted power. In case of lower performance as in the base case as well as in the DEMO layout conditions [5] a He pressure of 8 MPa would be sufficient to cope with pressure losses. After this, all other thermohydraulic data, e.g. the helium mass flow with the corresponding pressure loss, pumping power (Fig. 10), as well as He velocity and heat transfer coefficient in the FW and grid channels were determined as a function of the average neutron wall load (Fig. 11). The corresponding values of mass flow, velocity and pumping power computed for the Pb-17Li coolant loop are illustrated in Fig. 12.

### 3.3.3 Temperature and stress analyses

The 2D temperature and stress calculations have been carried out with the FE code ABAQUS. To identify the blanket performance limits dictated by the temperature constraints mentioned above, two separate temperature analyses were carried out locally for the first wall and for the blanket interior. After a comparison of the limit values obtained from both cases, the smaller one was taken as a reference case for the blanket. Then, the corresponding 2D stress analysis for the FW was carried out for the reference case.

In the first wall calculations the blanket heat and neutron wall loads were varied, while the He velocity and the first wall thickness were taken as parameters (Fig. 13). From the first results a He velocity of 40 m/s was found to be reasonable in view of the pressure loss leading to a symmetrical division of the meandering flow into four passages within the external walls of the blanket. Besides, a reasonable first wall thickness between 3 and 4 mm was preferred. The results of this analysis showed that a maximum allowable peak surface heat flux e.g. of about 1.0 MW/m<sup>2</sup> for the FW of 4 mm thickness and a He velocity of 40 m/s could be achieved (Fig. 14), which corresponds to an average neutron wall load of 4.5 MW/m<sup>2</sup>. However, the maximum allowable peak surface heat flux could be even enhanced up to 1.5 MW/m<sup>2</sup> by choosing a FW thickness of 3 mm and a He velocity of about 95 m/s, without paying attention to the pressure loss. In this case, an adaptation of the construction and thermohydraulic layout has to be done more in detail, e.g. reduction of the He channel pitch to cope with the primary stresses and asymmetrical subdivision of the He passages to obtain the highest He velocity at the torus centre.

For the temperature field calculations of Pb-17Li, the "slug flow" method [5] was used, employing a coordinate system which moves at liquid metal velocity in flow direction through the channel. This leads to a quasi-steady state calculation that allows only conductive heat transfer transverse to the flow direction assuming a uniform velocity distribution over the flow cross section, while the specific heat of the adjoining solid structures is set to zero. Concerning the MHD effects, the radial velocity profile and the pressure loss of the Pb-17Li flow were calculated [15] (Appendix 3). The results show that an increase of the near-wall velocity by at least a factor of 2 (corresponding to  $\sigma = 1.0 \Omega^{-1}\text{m}^{-1}$ ) can be assumed conservatively (Fig. 15). This was taken into account when correcting the near-wall heat transfer condition, especially at the rear side of the first wall. The calculations were carried out at varying neutron wall loads under preservation of the energy balance. Fig. 16 shows the maximum ODS/Pb-17Li interface temperature at the blanket centre and at the blanket bottom end as a function of the average neutron wall load. According to higher Pb-17Li temperature at the outlet, a slightly higher interface temperature than that at the blanket centre can be recognised well at a lower neutron wall load but this difference will become less at higher blanket performance because the He cooling capacity is enhanced. Taking into account the maximum allowable interface temperature of 500°C the calculation results yield a maximum allowable limit for the average neutron wall load of about 4.0 MW/m<sup>2</sup> (corresponding to a maximum value of 5.0 MW/m<sup>2</sup>), which can be considered as the reference case of this blanket concept.

The main A-DCL blanket data for the reference case are summarised in Table 4. The corresponding values of the average and maximum surface heat loads amount to 0.68 and 0.88 MW/m<sup>2</sup>, respectively. Taking into account an overall segments surface area of 1187 m<sup>2</sup> and an energy multiplication factor of 1.15 for the blanket system (Table 1) the blanket thermal power (surface power + neutron power) of 6267 MW was determined. After an extrapolation of the pumping power of one blanket segment (1.36 MW for the He loop and 0.08 MW for the Pb-17Li loop, Figures 10 and 12) the total pumping power for this reference reactor amounts to 144 MW taking into account pump efficiencies of 0.8.

Fig. 17 shows the corresponding Pb-17Li temperature distribution in a front corner channel at the blanket bottom end and a temperature profile along a path through the walls of the grid and the SiC<sub>f</sub>/SiC FCIs. With the moderate thermal conductivity assumed for SiC<sub>f</sub>/SiC the maximum temperature gradient across the FCI wall amounts to about 180 K.

For the reference case the temperature distribution in the first wall with 4 mm thickness is shown in Fig. 18. The maximum FW temperature amounts to 617 °C which is far below the allowable value of 650 °C. The following 2D stress calculations (Figures 19, 20) for the first wall assuming generalised plane strain boundary conditions yield a maximum primary stress of 197 MPa (Fig. 19) at the front corners of the coolant channel (< allow. 261 MPa at 466 °C) and a maximum primary plus secondary stress of 413 MPa (Fig. 20) at the plasma facing surface (< allow. 418 MPa at 617 °C).

In the SiC<sub>f</sub>/SiC FCIs the primary stress is negligibly small because there is no pressure difference between inner and outer walls so that the secondary stress caused by temperature distribution in the FCIs dominates in this case. Taking into account the FCI temperature distribution for the reference case at the blanket end (see above) the corresponding stress calculations for the SiC<sub>f</sub>/SiC FCI (Fig. 21) [16] yield the maximum von Mises total stress in plane of about 93 MPa (< allow. 140 MPa), while the maximum tensile and compressive stresses over the FCI thickness reach a value of 6 and 30 MPa, respectively, which are well below the allowable limits of 110 MPa and 500 MPa (conservatively assumed), respectively. For these calculations the data of CERASEP N3.1 were used.

### 3.4 Power conversion system and thermal efficiency

A three-stage Brayton closed-cycle gas turbine (Fig. 22) was considered for the power conversion system, using both He and Pb-17Li exit temperatures. This solution offers a crucial advantage in avoiding the contact of liquid metal with water. For the secondary He loop 18 MPa He pressure and inlet and outlet temperatures of 280 °C and 650 °C, respectively, were chosen. A high He pressure does not explicitly affect the thermal efficiency of the power conversion system but it is required to simultaneously achieve a high heat exchanger efficiency and a low pressure loss ratio. The examination of the two-stage heat exchangers (He/He and Pb-17Li/He) [17] for this case resulted in a reasonable pressure loss (Table 5a), and a maximum equivalent bundle size (for reactor system with single IHX loop) OD x H of about 8 m x 10 m for the intermediate heat exchanger IHX-1 (He/He, straight tube type) with a heat transfer surface of 34,251 m<sup>2</sup> and pressure losses in the primary and the secondary loop of 0.1 and 0.4 MPa, respectively. However, the IHX bundle size determined above for a single loop could be sub-divided e.g. into six parallel loops with smaller bundles of helical tubes without additional pressure losses. Following the thermal efficiency calculations in [18] considering the parameters for this case (Table 6, case 1) the thermal efficiency amounts to 0.455. Taking into account the electrical pumping power for the blanket cooling of 144 MW in the reference case (see above), the net efficiency of the blanket cycle equals 0.44. For simplifying reasons, the thermal efficiency was determined under the assumption of a compressor compression ratio of 2 as assumed in [18] with a higher He inlet temperature level. To approach this value, the temperature level at the blanket inlet for this reference case has to be increased slightly, but it requires some thermohydraulic modification for the blanket coolant system that should be done in a detailed study.

An additional investigation for the case of integration of helium-cooled divertors into this power conversion cycle was carried out, e.g. a design solution with two separated He cooling systems (14 MPa or 8 MPa alternatively) for divertor bulk and divertor target with the inlet and outlet temperatures of 440/550 °C and 700/850 °C (Table 5b), respectively. The corresponding total divertor power for this reference case amounts to 1169 MW (58% divertor bulk, 42% divertor target) [19]. Four-stage heat exchangers are required for this case with a maximum equivalent bundle size for a single IHX loop (see above) OD x H of about 8 m x 9 m and pressure losses in the primary and the secondary loop of 0.2 and 0.5 MPa [17], respectively. In this case the corresponding thermal efficiency of 0.48 (Table 6,

case 2) was estimated under the same assumption mentioned above, leading to a net efficiency for the blanket and divertor coolant cycles of about 0.46, which is about 5 % higher than that in the case without integration of the divertor power. Besides the net efficiency enhancement, this solution also offers a choice of appropriate materials for different divertor components, e.g. tungsten for the divertor target with the highest thermal loads and ferritic steel for the divertor bulk with moderate temperature. However, the use of separate cooling systems requires more expenditure for an additional coolant loop.

For the blanket coolant access a double wall tube construction (Pb-17Li in inner tubes/He in outer tubes) was used in order to prevent tritium permeation by a He barrier in the outer tube. Moreover, an additional SiC<sub>f</sub>/SiC innermost tube provides for a thermal barrier by separating the hot Pb-17Li flow with a maximum temperature of 700 °C from the inner tube wall. This allows the use of steel as coolant tube material because the temperature of the double wall tube can be kept below 500 °C.

#### **4 Open issues**

Since the A-DCL blanket concept is an advanced version of the DEMO DCL blanket concept which had been under development in the EU for several years before, the same reliable computation techniques and the same Pb-17Li properties are used. The material properties of SiC<sub>f</sub>/SiC known at present are supposed to meet the requirements for these purposes, because the SiC<sub>f</sub>/SiC FCIs have no structural functions at all to cope with. Open issues regarding the SiC<sub>f</sub>/SiC material are the fabrication techniques, e.g. achieving a sealed surface to avoid the infiltration of Pb-17Li, production of a maximum FCI length (reduced number of joints), achievement of low thermal and electrical conductivity (enhances the thermal efficiency).

For the ODS steel structure the open issues primarily consist in the strength data, the fabrication and welding methods. The assumption of the strength values of comparable ferritic steels having to be shifted to a 100 K higher temperature level to achieve the value for ODS as recommended in [13] has to be examined. However, the result of the temperature calculations for the reference case has shown that the maximum structure temperatures beyond 550°C (a temperature limit e.g. for EUROFER) occur within a thin layer of about 2 mm on the plasma facing surface of the FW. This should allow a further solution, choosing EUROFER as base material for the whole steel structure that contains a thin layer of ODS steel plated on the plasma facing surface of the FW. In this case, detailed investigation on fabrication methods for ODS/EUROFER joining (e.g. hot isostatic pressure (HIP), explosion welding etc.) is required. In addition, R&D work on out-of-pile and in-pile experiments is required for both SiC<sub>f</sub>/SiC and ODS.

#### **5 Lifetime, maintainability and reliability**

Since the SiC<sub>f</sub>/SiC FCIs have no structural functions, it can be supposed that the ODS steel structure plays a decisive role for the lifetime of the blankets. The lifetime prediction [20] assuming a displacement damage for ODS of 150 dpa yields an average neutron fluence of 15.1 MWa/m<sup>2</sup>, corresponding to either 6.8 FPY at 2.22 MW/m<sup>2</sup> or 3.78 FPY at 4.0 MW/m<sup>2</sup>.

At the present state of the reactor study, a detailed reliability analysis cannot be performed yet. The similar DEMO DCL blanket concept study yields e.g. an overall availability of > 86% and even > 98% for the external cooling circuits, taking into account the redundancy principle [21]. For the A-DCL blanket concept, however, the following crucial reasons allow to assume a higher reliability than that of DEMO: No possibility of water-liquid metal reactions, higher strength of the structural material, and advanced state of today's diffusion welding technology.

## 6 Conclusions

The advanced dual coolant (A-DCL) blanket concept is characterised by its simple construction, simple function, as well as by its high thermal efficiency. The goal of this study is to investigate the potential of this blanket concept. Two temperature constraints for the FW (creep rupture strength) and the Pb-17Li breeding zone (corrosion) were taken into account. The latter was found to be decisive for the power limitation of this blanket concept. Detailed neutronic, thermohydraulic, thermomechanical and MHD calculations were carried out under the assumption of the specified PPA2 geometry and power for the base case (2.22 MW/m<sup>2</sup> average neutron wall load) and with an extrapolation of some material data for SiC/SiC and ODS steel. The calculations yielded a maximum allowable average neutron wall load of 4.0 MW/m<sup>2</sup> (corresponding to 0.9 MW/m<sup>2</sup> max. surface heat load) for the reference case which is about 80% higher than the base case value. Assuming a three-stage Brayton gas turbine cycle for the power conversion system, a net efficiency for the blanket cycle of 44% was obtained. In case of integration of the He-cooled divertor into the power conversion system in order to exploit its waste heat the net efficiency for the blanket and divertor cycle could even be increased to about 46%. The max. allowable peak surface heat load for the FW could be enhanced to a value of about 1.5 MW/m<sup>2</sup> (a margin for e.g. peaking factor uncertainty) by reducing the FW thickness and increasing the He velocity. The results of this study show that the A-DCL blanket concept has a high potential for further development due to its high thermal efficiency and its simple concept solution that may have some open issues which are expected to be solved easily.

## Acknowledgements

This work has been performed in the framework of the Nuclear Fusion Project of the Forschungszentrum Karlsruhe and is supported by the European Union within the European Fusion Technology Program.

## 7 References

- [1] P. Norajitra, "The Second Advanced Lead Lithium Blanket Concept Using ODS Steel as Structural Material and SiC<sub>f</sub>/SiC Flow Channel Inserts as Electrical and Thermal Insulators (Task PPA 2.5), Executive Summary", FZK-PKF Report Nr. 140, August 1999.
- [2] S. Malang, "Conceptual design of a dual coolant liquid metal breeder blanket", Fusion Technology 1994, Vol. 2, pp.1205-1208.
- [3] D. K. Sze, et al, "The ARIES-ST Blanket Design", Proceedings of the 13th Topical Meeting on Technology of Fusion Energy, Nashville, Tennessee (June 1998), to be published in Fusion Technology.
- [4] M.S. Tillack, S. Malang, "High performance PbLi Blanket", Proc. of the 17th IEEE/NPSS Symposium on Fusion Energy, San Diego, California, (Oct. 1997) 1000-1004.
- [5] P. Norajitra, "Thermohydraulics Design and Thermomechanics Analysis of Two European Breeder Blanket Concepts for DEMO", FZKA 5580, June 1995.
- [6] K. Shinozaki, H. Kuroki, Y. Nakao, "Bonding phenomena and mechanical properties of liquid phase bonded joints in Fe-base ODS alloy, MA956", Welding International (1996) 10, (10), 778-787.
- [7] M. Rees, R. C. Hurst, J. D. Parker, "Diffusion bonding of ferritic oxide dispersion strengthened alloys to austenitic superalloys", Journal of Materials Science (1996) 31, (17), 4493-4501.
- [8] U. Fischer, "Neutronic calculations for PPA reactor blanket concepts", July 1999, unpublished.
- [9] J. Wareing, A-A Tavassoli, "Assessment of martensitic steels for advanced fusion reactors", unpublished.
- [10] RCC-MR-Addendum May 1993, A3-18S, pp 451-476.
- [11] RCC-MR-Addendum November 1987, A3-18S, pp 67-94.
- [12] J.H. Fokkens, "HCPB Submodule Design, Material Parameters", ECN Report 71477/NUC/JF/mb/016286, September 1998.
- [13] S. Malang, M. Billone, "How well can we predict the behaviour of the different materials in solid breeder blankets?", Ninth International Conference on Fusion Reactor Materials (ICFRM9), Colorado Springs, Colorado, USA, October 10-15, 1999.
- [14] L. Giancarli, G. Aiello, H. Golfier, Y. Poitevin, J.F. Salavy, "On the Use of SiC<sub>f</sub>/SiC as Structural Materials for Fusion Blankets, CEA Comments and Suggestions Concerning Dual-Coolant and He-Cooled Ceramic Blankets", May 1999, unpublished.
- [15] L. Bühler, "MHD Flow in the Dual Coolant Blanket Concept", April 1999, unpublished.
- [16] L. Giancarli, H. Golfier, Y. Poitevin and J-F. Salavy, "SiC/SiC related issues for the second advanced lead-lithium concept and for the advanced HCPB concept", CEA report SERMA/LCA/RT/99-2677/A, December 1999.
- [17] H. Schnauder, "Heat exchanger design calculations for the 2<sup>nd</sup> advanced lead-lithium blanket concept (PPA2.5)", July 1999, unpublished.
- [18] S. Malang, H. Schnauder, M.S. Tillack, "Combination of a self-cooled liquid metal breeder with a gas turbine power conversion system", Fusion Engineering and Design 41 (1998), pp. 561-567.
- [19] K. Kleefeldt, personal communication, June 1999.
- [20] U. Fischer, personal communication, May 1999.
- [21] S. Malang, S. Tillac et al., "Development of Self-cooled Liquid Metal Breeder Blankets", FZKA 5581, November 1995.

## 8 Nomenclature

$c_p, c_v$ [J/kgK]	specific heat capacity
$E$ [MPa]	Young's modulus
$f_a$ [-]	Ratio of heat transfer coefficients
$H$ (m)	Height
$ID$ [m]	Inner diameter
$OD$ [mm]	Outer diameter
$P$ [W]	Power
$p$ [MPa]	Pressure
$R_m$ [MPa]	ultimate tensile strength
$R_{p0.2}$ [MPa]	yield strength
$S_m, S_{m,t}$ [MPa]	Strength
$s$ [m]	Thickness
$T$ [K]	Temperature
$\alpha$ [1/K]	Thermal linear expansion coefficient
$\lambda$ [W/mk]	Thermal conductivity
$\eta$ [-]	Efficiency
$\eta_{th}$ [-]	Thermal efficiency
$\nu$ [-]	Poisson's ratio
$\rho$ [kg/m <sup>3</sup> ]	Density
$\sigma$ [ $\Omega^{-1}m^{-1}$ ]	Electrical conductivity
$\sigma_{R,t}$ [MPa]	Creep rupture stress in time $t$
$\sigma_{1,t}$ [MPa]	1% total strain in time $t$

### Abbreviations

A-DCL	Advanced dual coolant
CEA	Commissariat à l'Energie Atomique
D	Dimension
DEMO	Demonstration reactor
Div	Divertor
D-T	Deuterium-Tritium
EU	European Union
FPY	Full power year
FCI	Flow channel insert
FW	First wall
FZK	Forschungszentrum Karlsruhe
He	Helium
HIP	Hot Isostatic Pressure
IB	Inboard
IHX	Intermediate heat exchanger
JRC	Joint Research Centre
MHD	Magneto-hydrodynamic
OB	Outboard
ODS	Dispersion-strengthened
PPA	Preparation for power plant conceptual study – plant availability
Pb-17Li	Eutectic lead-lithium alloy
pol	Poloidal
rad	Radial
SiC <sub>f</sub> /SiC	Silicon carbide composite
TBR	Tritium breeding ratio
tor	Toroidal
UKAEA	United Kingdom Atomic Energy Authority

**Table 1:** PPA2 reactor parameters and the calculated neutronic data and power for the base fusion machine [8] (Appendix 1).

<b>Plasma:</b> <ul style="list-style-type: none"> <li>- Major radius (m)</li> <li>- Minor radius (m)</li> <li>- Aspect ratio</li> <li>- Elongation</li> <li>- Triangularity</li> <li>- Fusion power (MW)</li> <li>- Nominal ratio avg. heat to avg. neutron flux</li> <li>- Surface heat flux peaking factor max./avg.</li> </ul>	 8.1 2.7 3.0 1.9 0.4 3607 0.17 1.3
<b>Blanket segments:</b> <ul style="list-style-type: none"> <li>- Inboard-/Outboard radius at torus midplane (m)</li> <li>- Number of segments (Inboard-/Outboard)</li> <li>- Toroidal outboard segment width at torus midplane (m)</li> <li>- Radial outboard segment depth incl. Shield (m)</li> </ul>	 5.25 / 10.95 32 / 48 1.42 1.3
<b>Average/max. neutron wall load (MW/m<sup>2</sup>):</b> <ul style="list-style-type: none"> <li>- Outboard</li> <li>- Inboard</li> <li>- Overall segments</li> <li>- <i>Divertor</i></li> </ul>	 2.51 / 2.79 2.05 / 2.55 2.22 0.903
<b>Surface area FW (m<sup>2</sup>):</b> <ul style="list-style-type: none"> <li>- Outboard</li> <li>- Inboard</li> <li>- Overall segments</li> <li>- <i>Divertor</i></li> </ul>	 716 471 1187 280
Energy multiplication factor (outboard blanket/blanket sytem/overall plant)	1.11 / 1.15 / 1.18
3D net tritium breeding ratio (toroidally segmented)	1.09
<b>Max. power densities in outboard blanket (MW/m<sup>3</sup>):</b> <ul style="list-style-type: none"> <li>- Steel</li> <li>- PbLi</li> <li>- SiC/SiC</li> </ul>	 18 13 5

**Table 2:** Data base of T91 steel for thermomechanics calculations [9, 10, 11, 12].

T [°C]	Thermophysical properties			Mechanical properties							S <sub>m</sub> and S <sub>m,t</sub> values (e.g. t = 1.10 <sup>4</sup> h for ITER)		
	ρ [kg/m <sup>3</sup> ]	λ [W/MK]	c <sub>p</sub> [J/kgK]	α .10 <sup>-6</sup> [1/K]	E [MPa]	ν [-]	Rp <sub>0.2</sub> [MPa]		Rm [MPa]		σ <sub>R,t</sub> [MPa]	S <sub>m</sub> [MPa]	S <sub>m,t</sub> [MPa]
							Min.	Avg.	Min.	Avg.			
20	7730	25.9	448.85	10.4	206000	0.3	400	551	580	700		193	193
50			462.76				388	535	559	675		193	193
100	7710	27.0	484.11	10.8	201000	0.3	375	516	536	648		193	193
150			503.92				367	505	525	634		193	193
200	7680	28.1	523.04	11.2	194000	0.3	362	499	519	627		192	192
250			542.34				359	495	514	621		190	190
300	7650	28.8	562.69	11.6	188000	0.3	356	490	506	612		187	187
350			584.94		185000		349	481	493	597		183	183
400	7610	29.2	609.96	11.9	181500	0.3	338	465	471	571		174	174
425											333		
450			638.61		178000		320	440	439	534	287	163	163
475											248		
500	7580	29.0	671.75	12.2	175000	0.3	293	403	395	483	213	146	146
525											181		
550			710.25		163000		255	350	340	418	151	126	105
575											123		
600	7540	28.5	754.96	12.5	151000	0.3	204	279	273	340	9	101	68

**Table 3:** Material data base for the A-DCL blanket layout.

	ODS Steel <sup>1)</sup>	Pb-17Li [5]	SiC <sub>f</sub> /SiC <sup>2)</sup> [14]
Thermal conductivity (W/mK)			
20°C	25.9	-	
200°C	28.1	-	
400°C	29.2	15.1	
600°C	28.5	19.1	2
800°C		21.1	
Therm. Expans. coeff. (*10 <sup>-6</sup> 1/K)			
20°C	10.4		4 / 2.5 <sup>3)</sup>
200°C	11.2		-
400°C	11.9		-
600°C	12.5		
800°C			
Electrical resistance (Ω.cm)			
400°C	0.881x10 <sup>-4</sup>	1.310x10 <sup>-4</sup>	
500°C	0.955x10 <sup>-4</sup>	1.352x10 <sup>-4</sup>	0.2
600°C	1.029x10 <sup>-4</sup>	1.395x10 <sup>-4</sup>	
700°C		1.438x10 <sup>-4</sup>	
Density (*10 <sup>3</sup> kg/m <sup>3</sup> ) 20°C	7730	9600	2500
Specific heat (J/kgK)			
20°C	449	192	
600°C	755	187	
Young's modulus *10 <sup>3</sup> (MPa)			200
400°C	182		
500°C	175		
600°C	151		
Poisson's ratio	0.3		0.18
Ultimate tensile strength / Sm (MPa)			Allow. Stresses [16]:
500°C	471 / 174		v. Mises sec.: 140
600°C	395 / 146		tensile: 110
700°C	273 / 101		compr.: ≥ 500
Max. working temp. / range (°C)	650 FW / 500 interface Pb-17Li	460 inl. / 700 outl	800

1) Derived from T91 data base [9, 10, 11, 12] (Table 2)

2) CERASEP N3.1 (Appendix 2)

3) in plane / over thickness

**Table 4:** Main data for the A-DCL reference case.

<b>Overall plant</b>	
Fusion power [MW]	6500
Neutron power [MW]	5200
Alpha-particle power [MW]	1300
Energy multiplication	1.18
Thermal power [MW]	7436
<b>Blanket</b>	
Blanket surface [m <sup>2</sup> ]	1187
Average neutron wall load [MW/m <sup>2</sup> ]	4.0
Max. neutron wall load [MW/m <sup>2</sup> ]	5.0
Average surface heat load [MW/m <sup>2</sup> ]	0.68
Max. surface heat load [MW/m <sup>2</sup> ]	0.88
-----	
Neutron power [MW] (1187m <sup>2</sup> x 4 MW/m <sup>2</sup> )	4748
Alpha-particle surface power [MW] (1187m <sup>2</sup> x 0.68 MW/m <sup>2</sup> )	807
Energy multiplication	1.15
Thermal power [MW] (4748 MW x 1.15 + 807 MW)	6267
-----	
<b>Coolant</b>	
Helium:	
- Inlet temperature [° C]	300
- Outlet temperature [° C]	480
- Pressure [MPa]	14
- Mass flow rate [kg/s]	2544
- Pumping power, $\eta = 0,8$ [MW]	136
Pb-17Li:	
- Inlet temperature [° C]	460
- Outlet temperature [° C]	700
- Mass flow rate [kg/s]	86586
- Pumping power, $\eta = 0,8$ [MW]	8
Secondary Helium:	
- Inlet temperature [° C]	280
- Outlet temperature [° C]	650
- Pressure [MPa]	18
-----	
Thermal efficiency (power conversion system)	0.46
Net efficiency of power conversion system (blanket cycle)	0.44
Electrical output [MW]	2757

**Table 5a:** Intermediate heat exchanger (IHX) dimensions [17] required for the reference case without integration of the divertors to the power conversion system.

	IHX-1 (blanket He)	IHX-2 (blanket LM)
Heat transfer (MW)	2381	3886
Medium:		
- Primary loop	14 MPa He	Pb-17Li
- Secondary loop	18 MPa He	18 MPa He
IHX inl./oul. Temp. (°C):		
- Primary loop	480 / 300	700 / 460
- Secondary loop	280 / 420	420 / 650
Heat transfer surface (m <sup>2</sup> )	34,251	38,839
Tube dimensions OD x s (mm)	22 x 2	18 x 2
Bundle		
- Type	helical	straight
- Equivalent size OD x H (m) <sup>1)</sup>	8.1 x 9.5	5.8 x 13
He Pressure loss (MPa):		
- Primary loop	0.1	-
- Secondary loop	0.2	0.2

<sup>1)</sup> for reactor system with single IHX loop

**Table 5b:** Intermediate heat exchanger (IHX) dimensions [17] required for the reference case with integration of helium-cooled divertors [19] to the power conversion system.

	IHX-1 (blanket He)	IHX-2 (divertor bulk)	IHX-3 (blanket LM)	IHX-4 (divertor target)
Heat transfer (MW)	2381	678	3886	491
Medium:				
- Primary loop	14 MPa He	14 (8*) MPa He	Pb-17Li	14 (8*) MPa He
- Secondary loop	18 MPa He	18 MPa He	18 MPa He	18 MPa He
IHX inl./oul. Temp. (°C):				
- Primary loop	480 / 300	550 / 440	700 / 480	850 / 700
- Secondary loop	280 / 412	412 / 443	443 / 657	657 / 680
Heat transfer surface (m <sup>2</sup> )	30,860	5,951	32,093	3,700
Tube dimensions OD x s (mm)	22 x 2	22 x 2	18 x 2	20 x 2
Bundle				
- Type	helical	straight	helical	straight
- Equivalent size OD x H (m) <sup>1)</sup>	8.0 x 8.8	4.9 x 3.5	9.2 x 5.5	5.5 x 1.5
He Pressure loss (MPa):				
- Primary loop	0.1	0.03	-	0.1
- Secondary loop	0.2	0.1	0.2	0.04

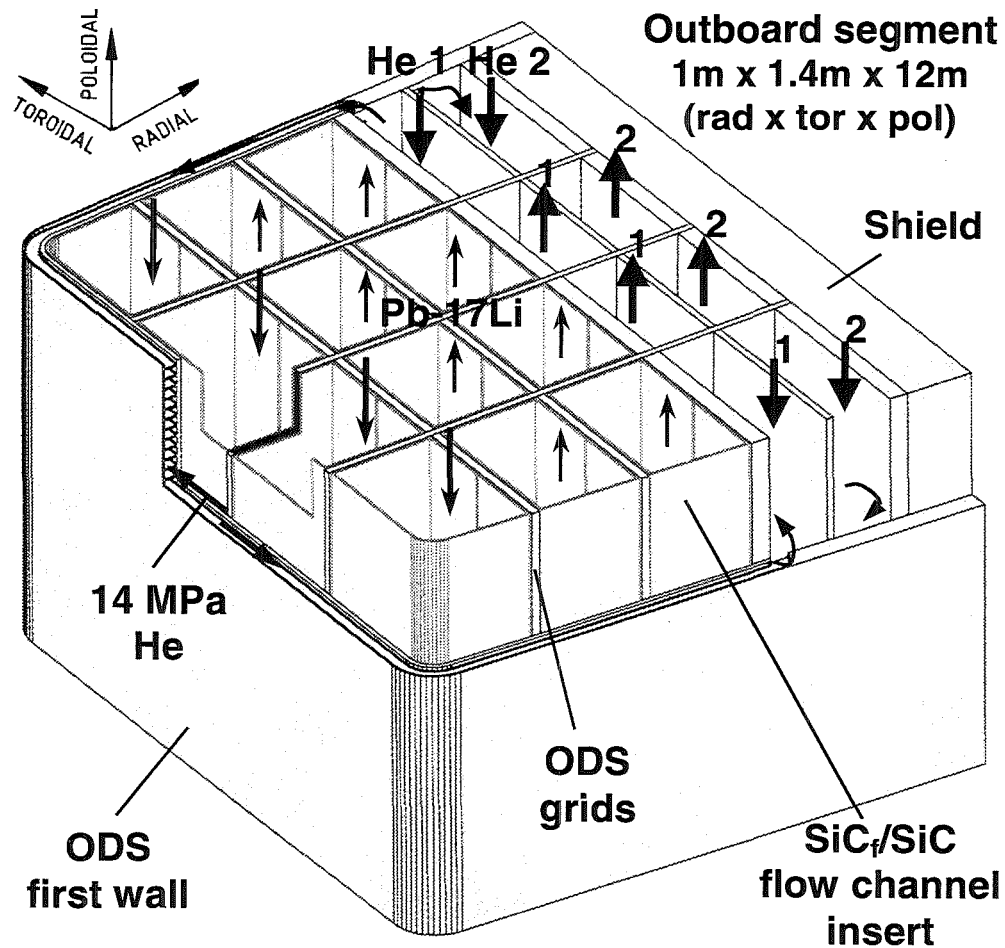
\* alternative

<sup>1)</sup> for reactor system with single IHX loop

**Table 6:** Parameters for thermal efficiency calculations for the reference case following ground rules in [18]:  
 case 1 without integration of the divertors and  
 case 2 with integration of the divertors into the power conversion system.

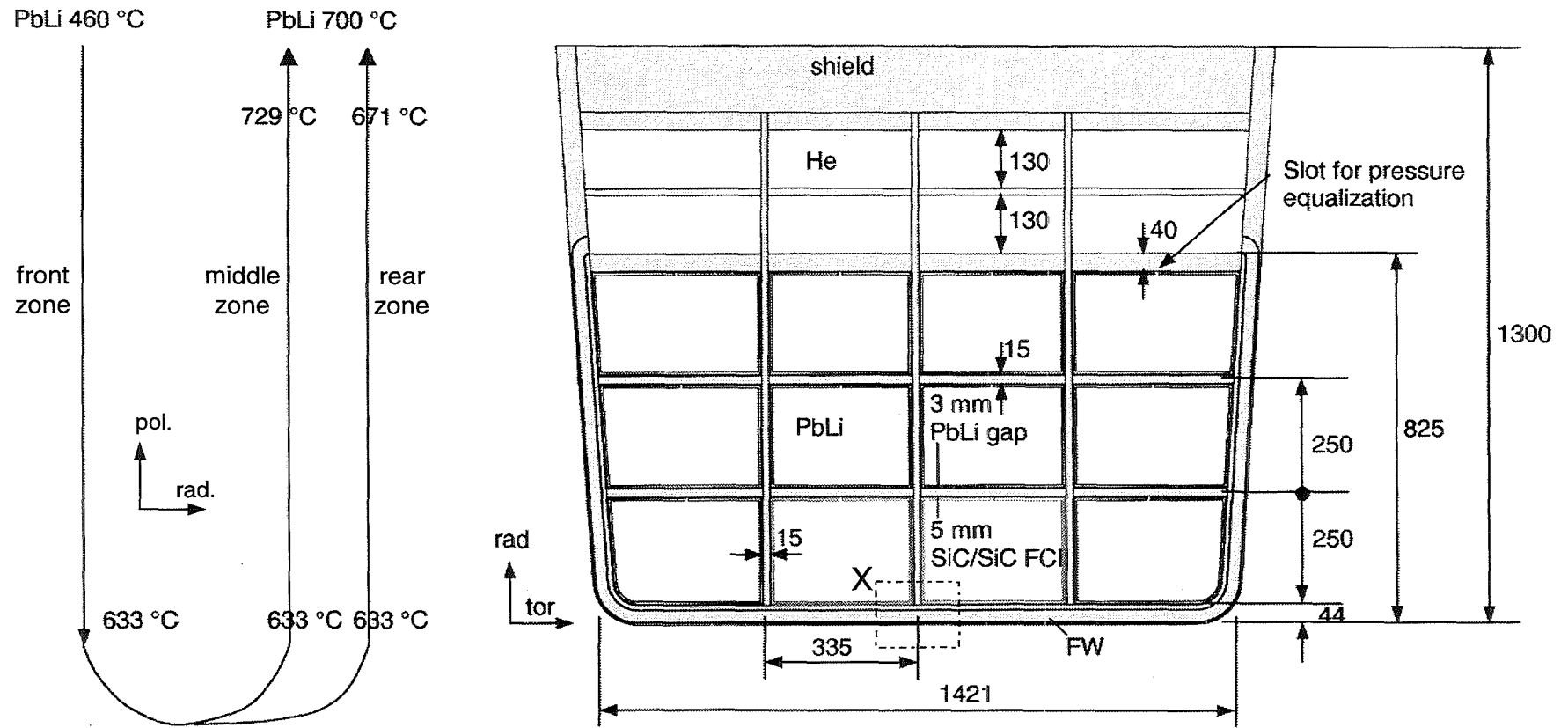
	Case 1 (without divertors)	Case 2 (with divertors)
compression ratio $r$	2	2
Turbine inlet temp. $T_0$ (K / °C)	923 / 650	953 / 680
Heat rejection temp. $T_s$ (K / °C)	308 / 35	308 / 35
Overall pressure loss ratio $\beta$	1.02	1.03
$k = c_p/c_v$ for He	5/3	5/3
Recuperator effectiveness $\eta_x$	0.96	0.96
Turbine efficiency $\eta_t$	0.92	0.92
Compressor efficiency $\eta_c$	0.92	0.92
Thermal efficiency $\eta_{th}$ <sup>1)</sup>	0.46	0.48
Net efficiency for blanket / blanket+div. cycles ( $\eta_{BI} / \eta_{B+div}$ )	0.44	0.46

$$^1) \eta_{th} = \eta_t \cdot (T_0/T_s) \cdot [1 - \beta \cdot (1/r)^{(k-1)/k}] - [(3/\eta_c) \cdot (r^{(k-1)/(3k)} - 1)] / \{ (1 - \eta_x) \cdot [(T_0/T_s) - 1 - (1/\eta_c) \cdot (r^{(k-1)/(3k)} - 1)] + \eta_x \cdot \eta_t \cdot (T_0/T_s) \cdot [1 - \beta \cdot (1/r)^{(k-1)/k}] \}$$



	Advanced DCLL	DEMO DCLL
<b>Coolants:</b>		
FW	He, 14 MPa	He, 8 MPa
Steel grids	He, 14 MPa	-
Blanket	Pb-17Li breeder (self-cooled)	Pb-17Li breeder (self-cooled)
PbLi channels	SiC <sub>f</sub> /SiC channel inserts (electr.+ thermal insulators)	Insulating coating
Structural material	ODS	MANET

**Fig. 1:** Isometric view of an A-DCL outboard blanket segment at torus centre.



Poloidal Pb-17Li flow distribution  
(see Figures 1 and 6)

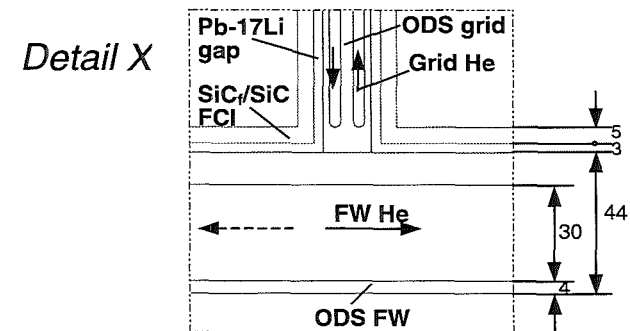


**Fig. 2:** Outboard blanket cross section at torus midplane (7.5° segment, dimensions in mm).

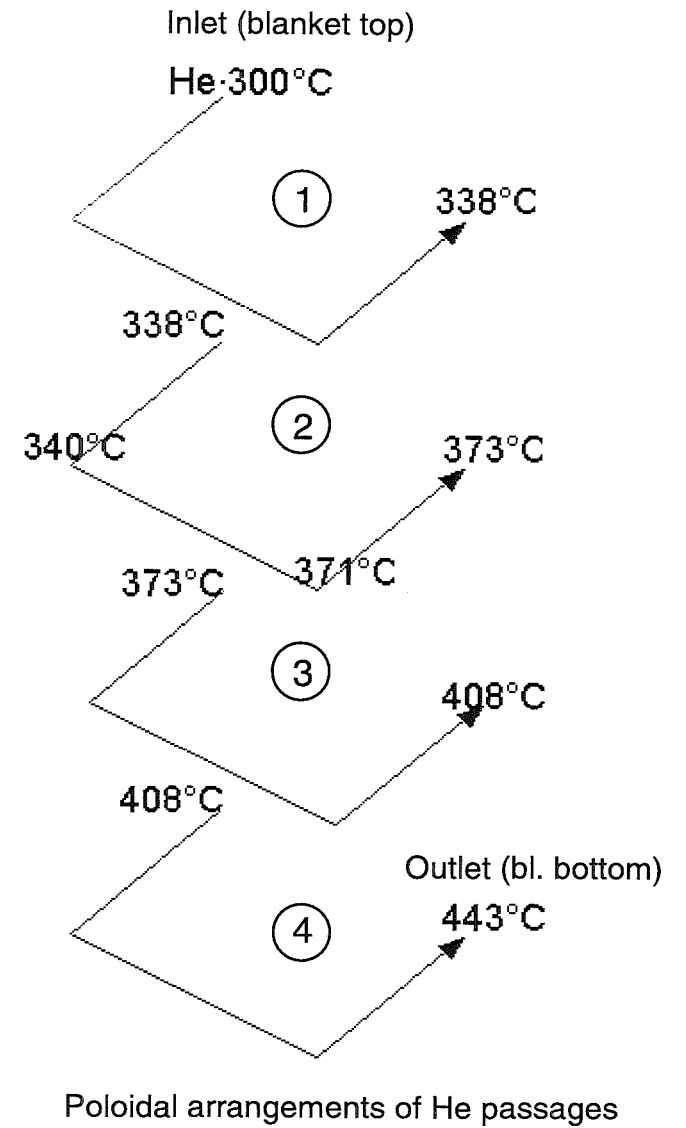
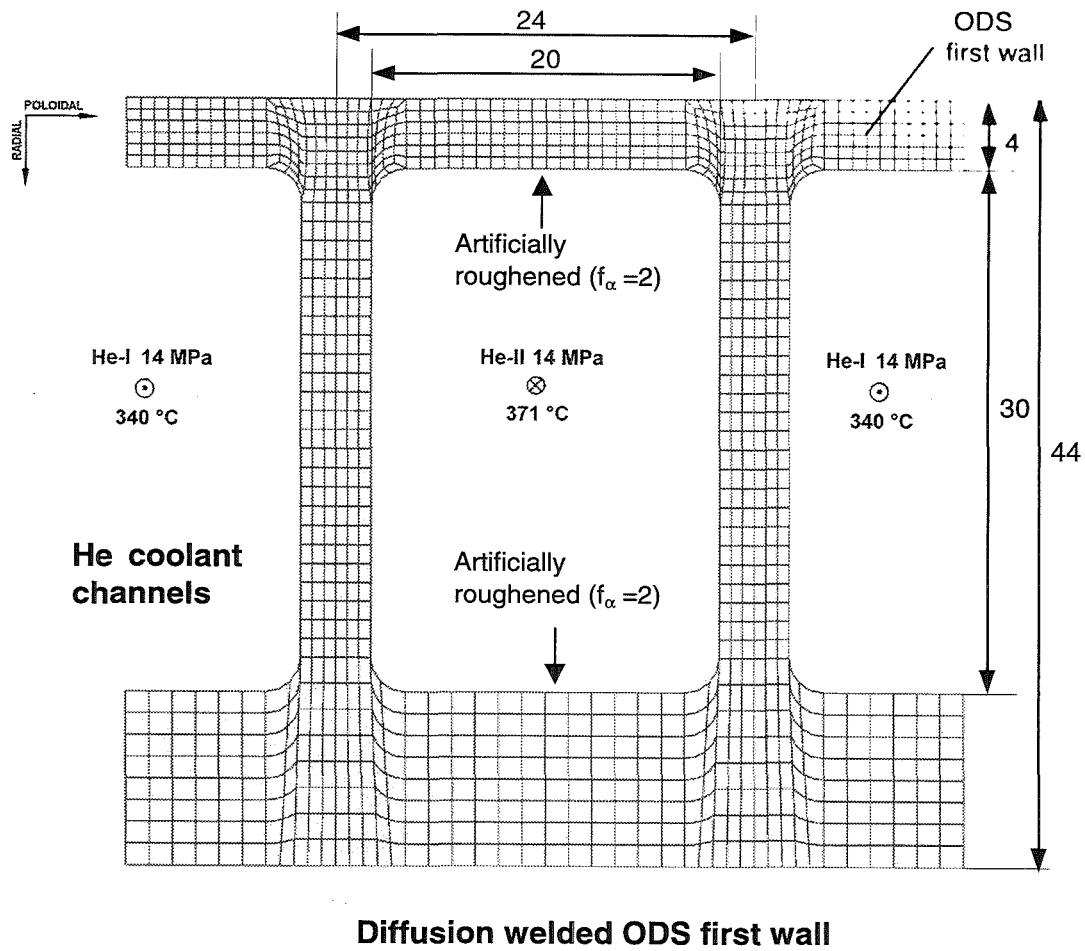
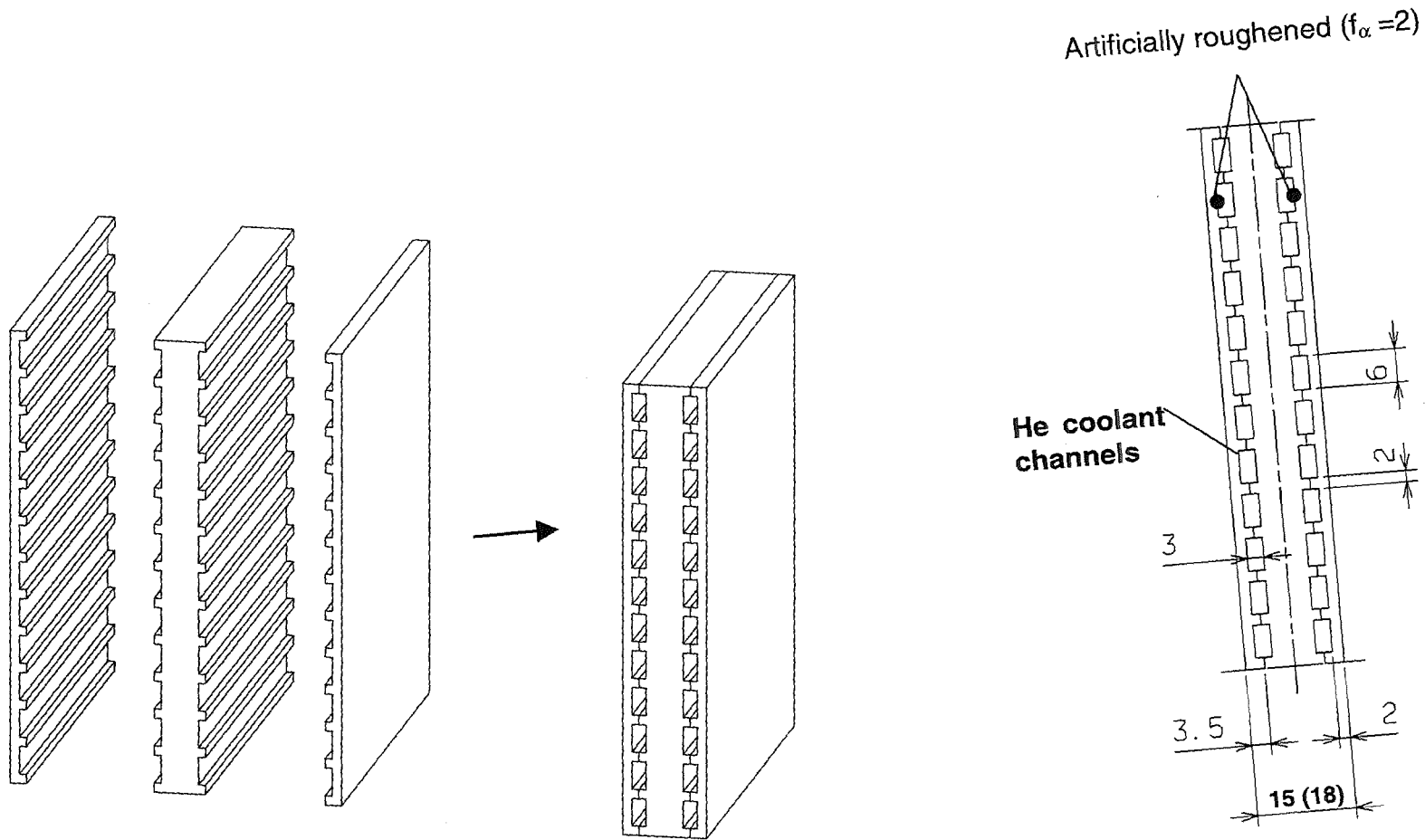


Fig. 3: First wall geometry (dimensions in mm).



### Diffusion welded ODS grids

Fig. 4: Arrangement of helium coolant channels in the grid plates.

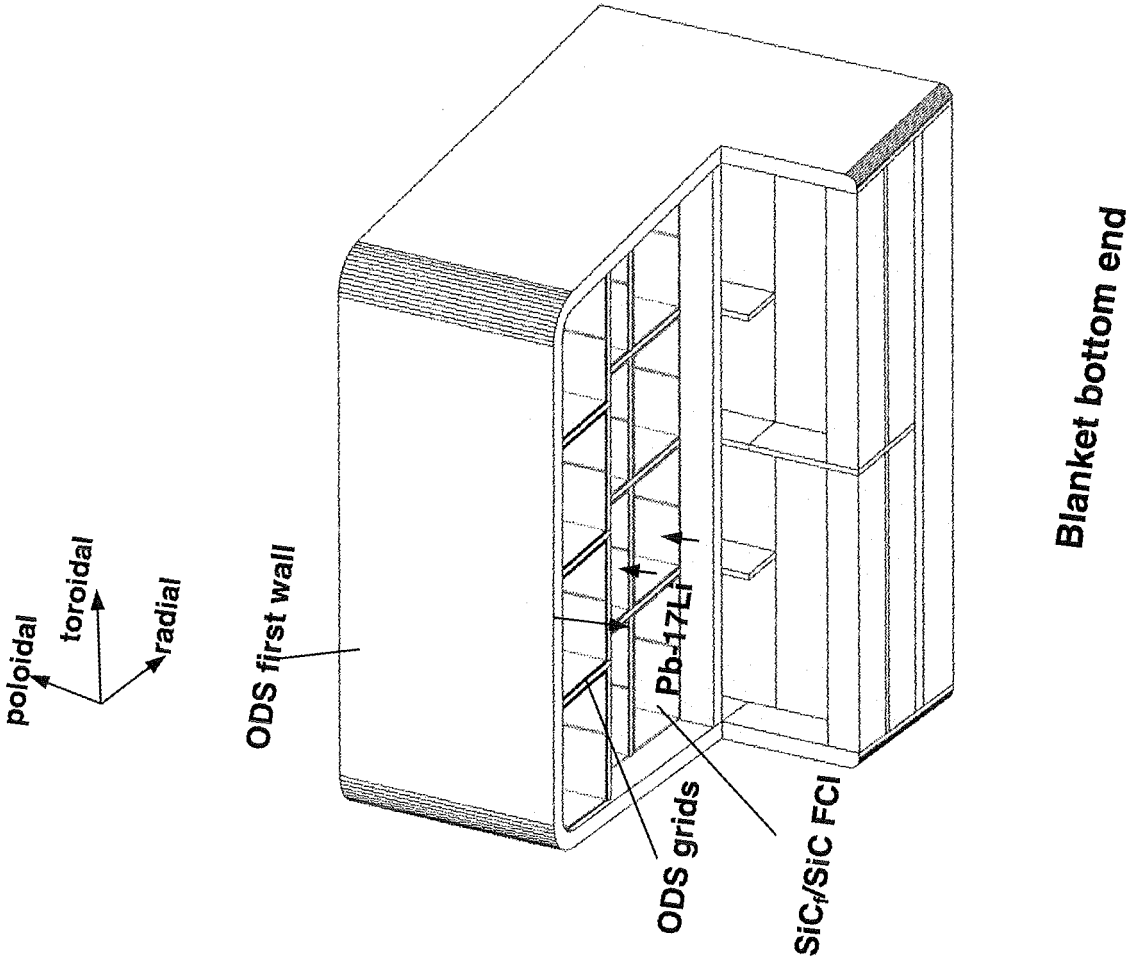
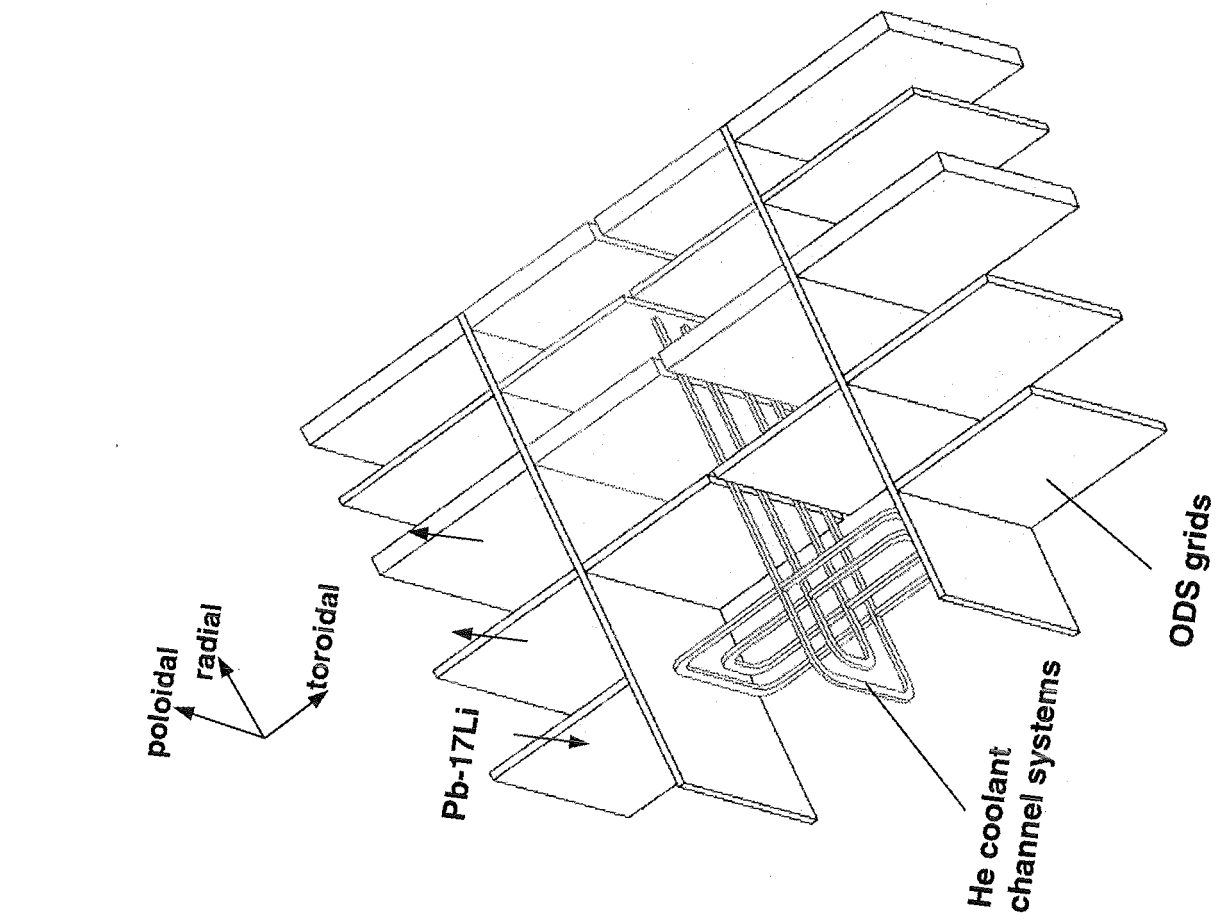
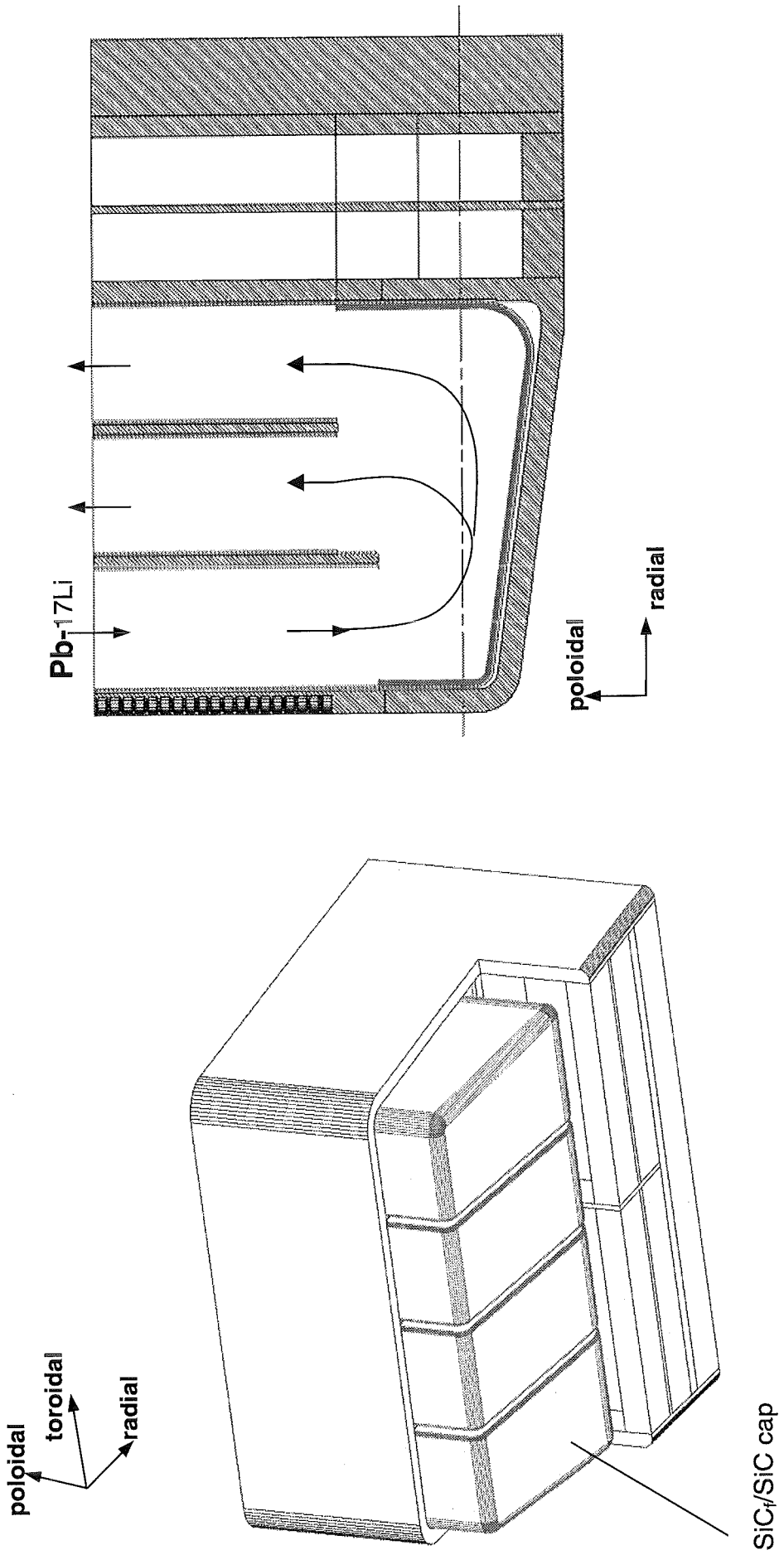


Fig. 5: Grid cooling systems.



**Fig. 6:** SiC/SiC cap construction at the blanket bottom end.

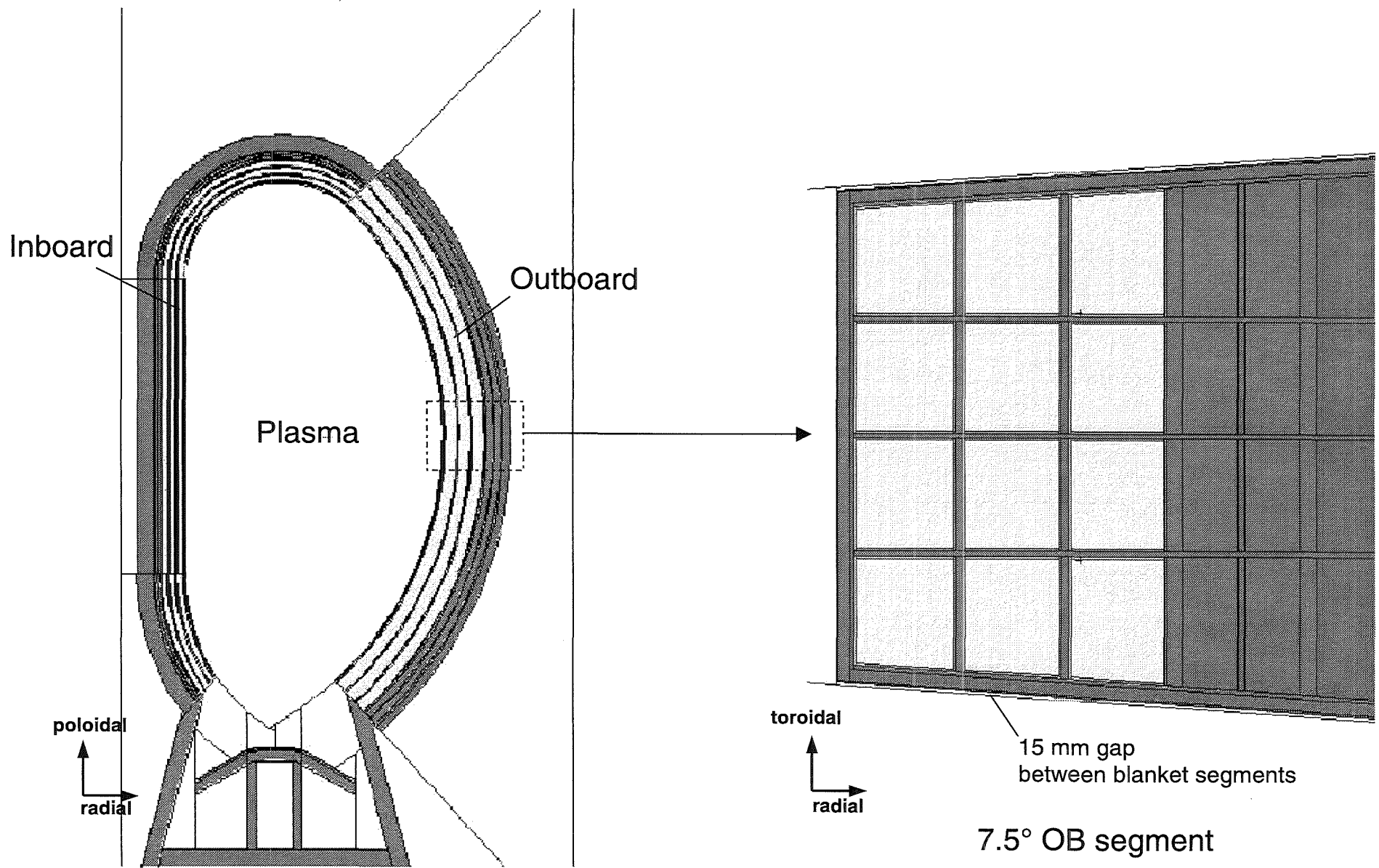
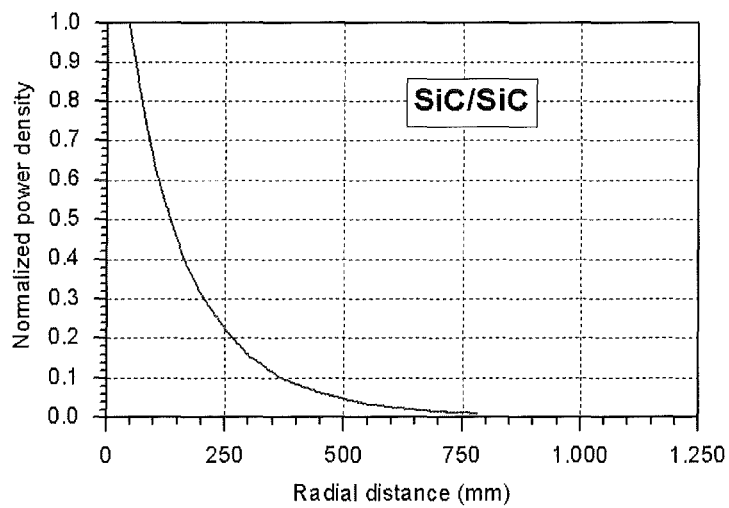
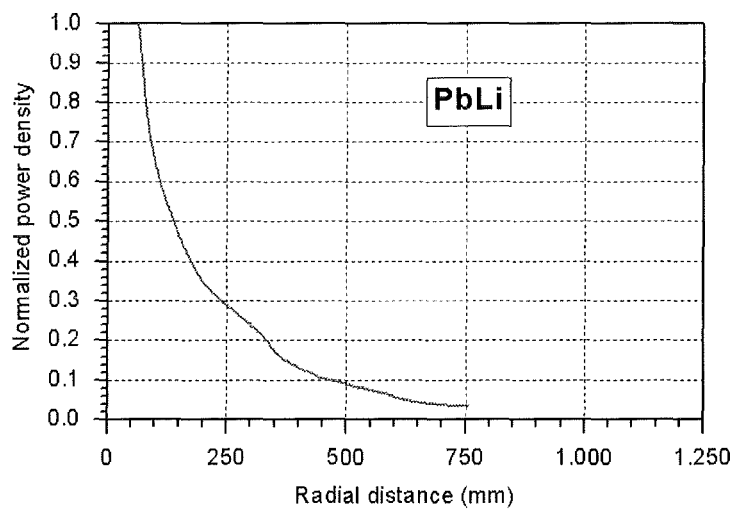
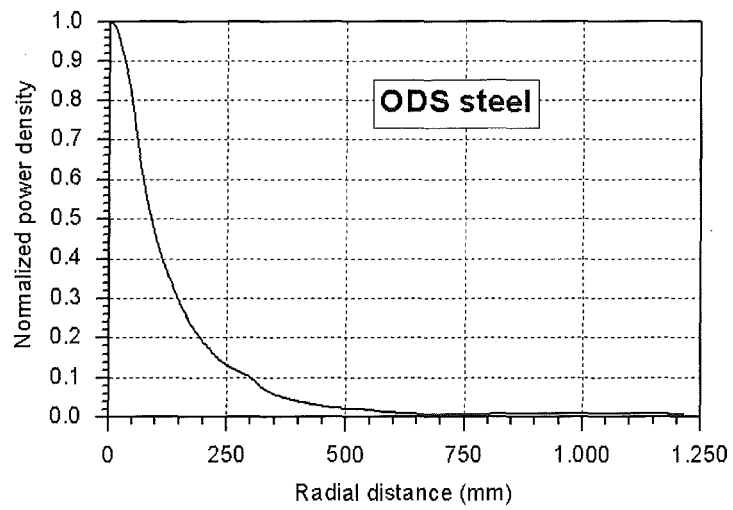
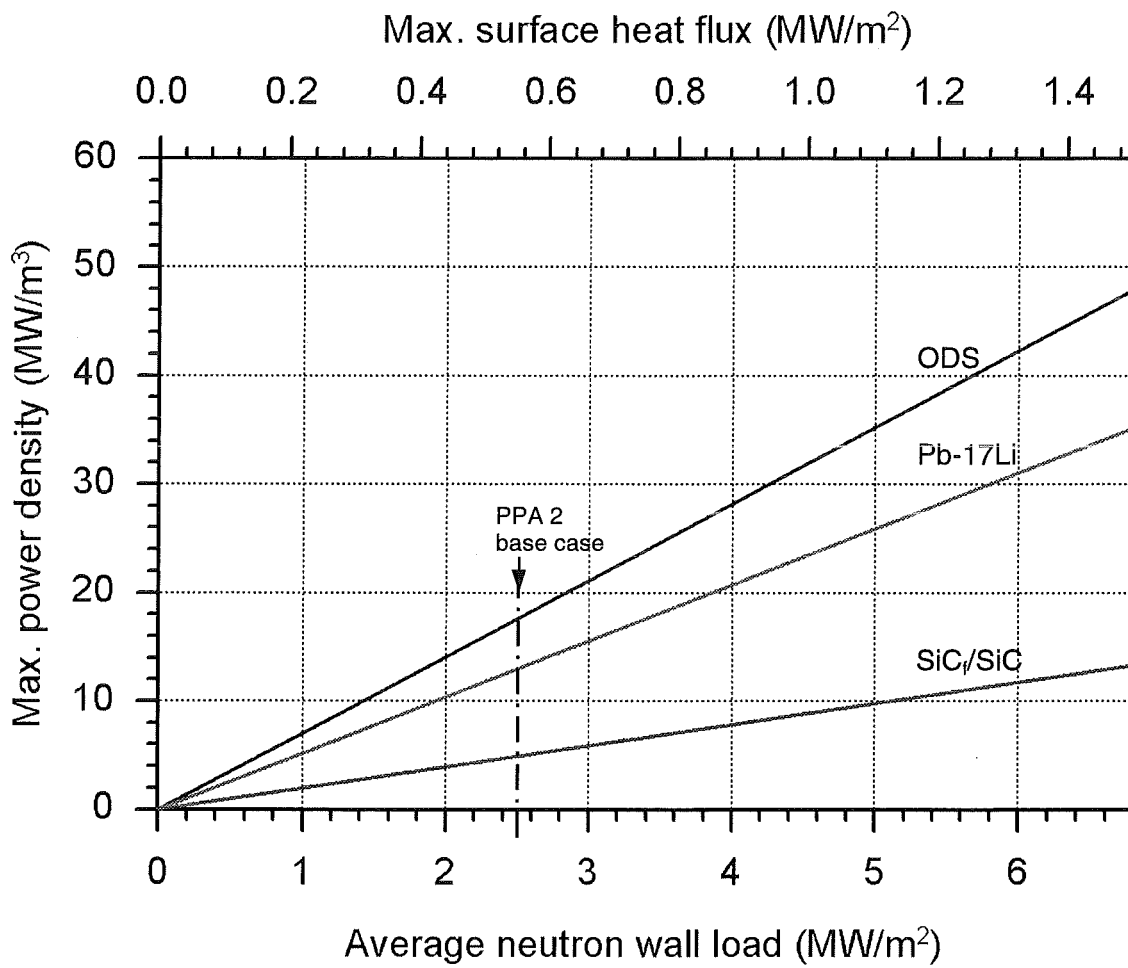


Fig. 7: PPA 2 reactor model [8].



**Fig. 8:** Radial power density distribution [8].



**Fig. 9:** Maximum power densities in ODS steel, Pb-17Li and SiC<sub>f</sub>/SiC for an outboard blanket segment as a function of average neutron wall load (linear extrapolation).

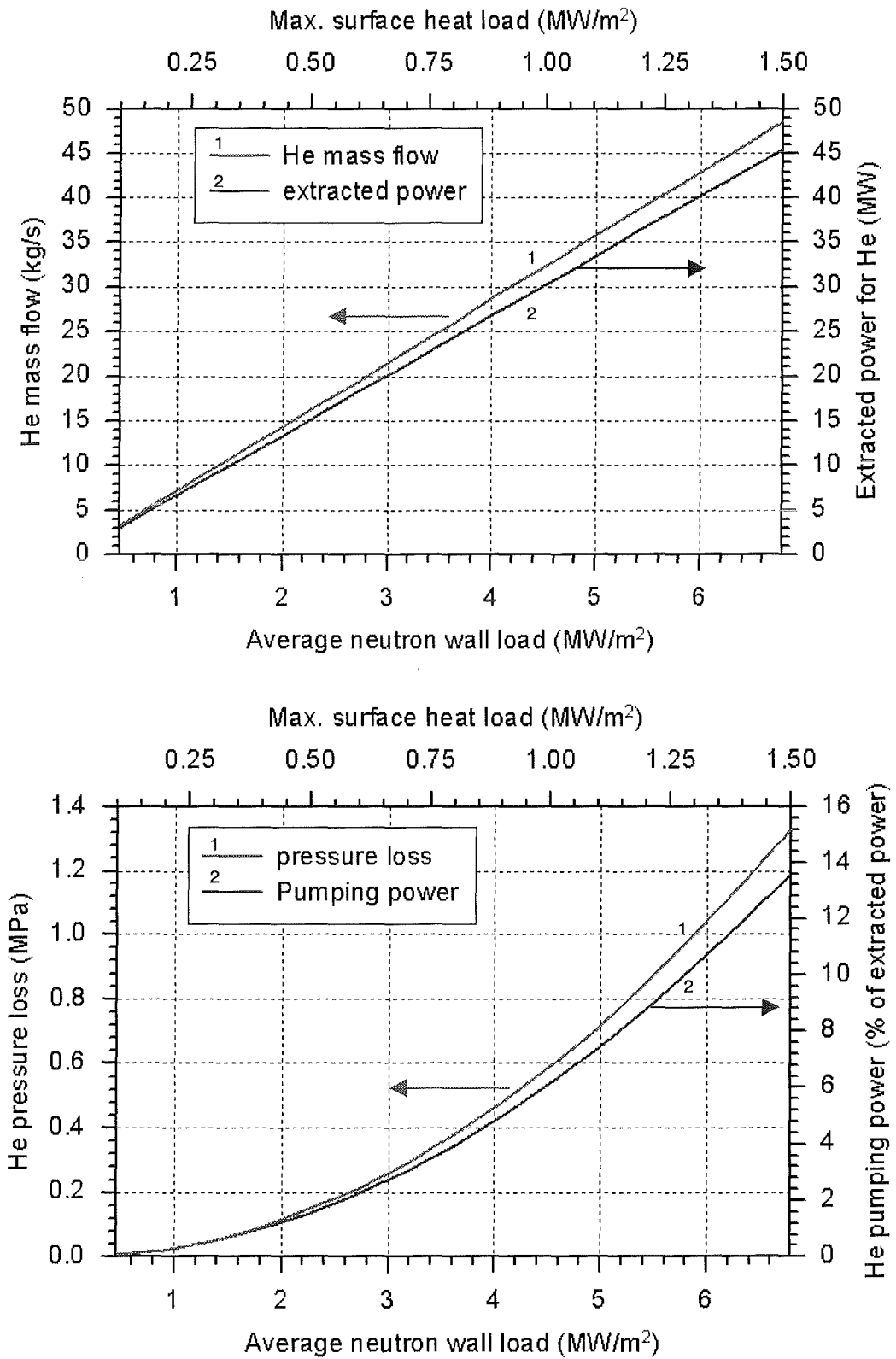


**Fig. 10:** He mass flow, extracted power, pressure loss and pumping power for an outboard blanket segment ( $T_{\text{He, in/out}} = 300/480 \text{ }^\circ\text{C}$ ) as a function of average neutron wall load.

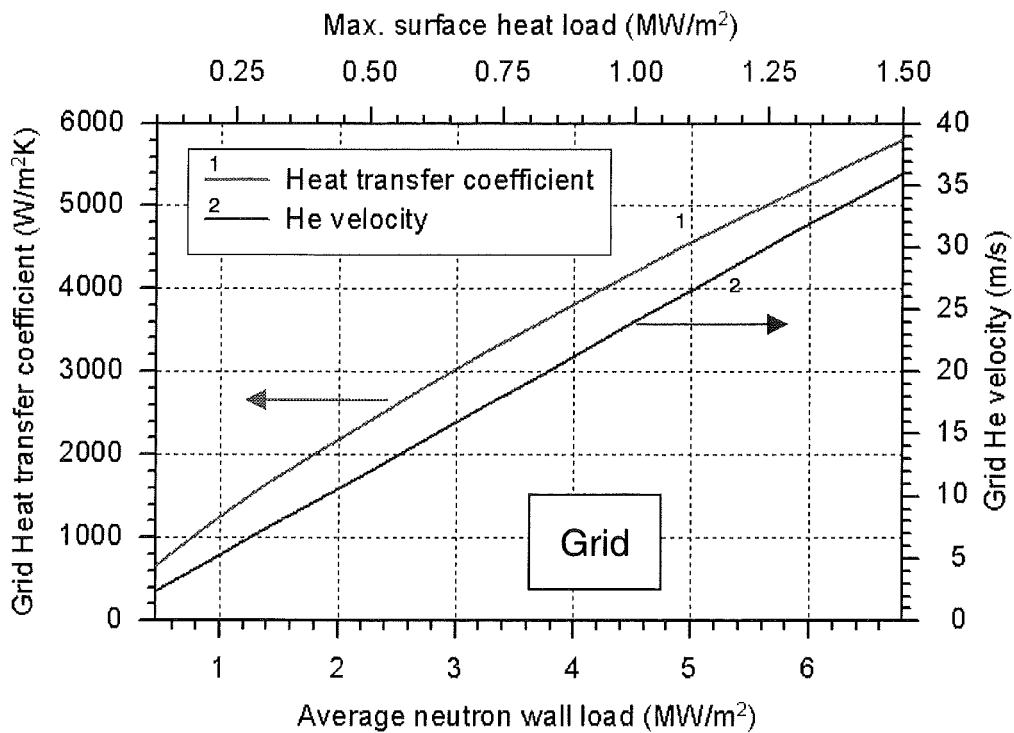
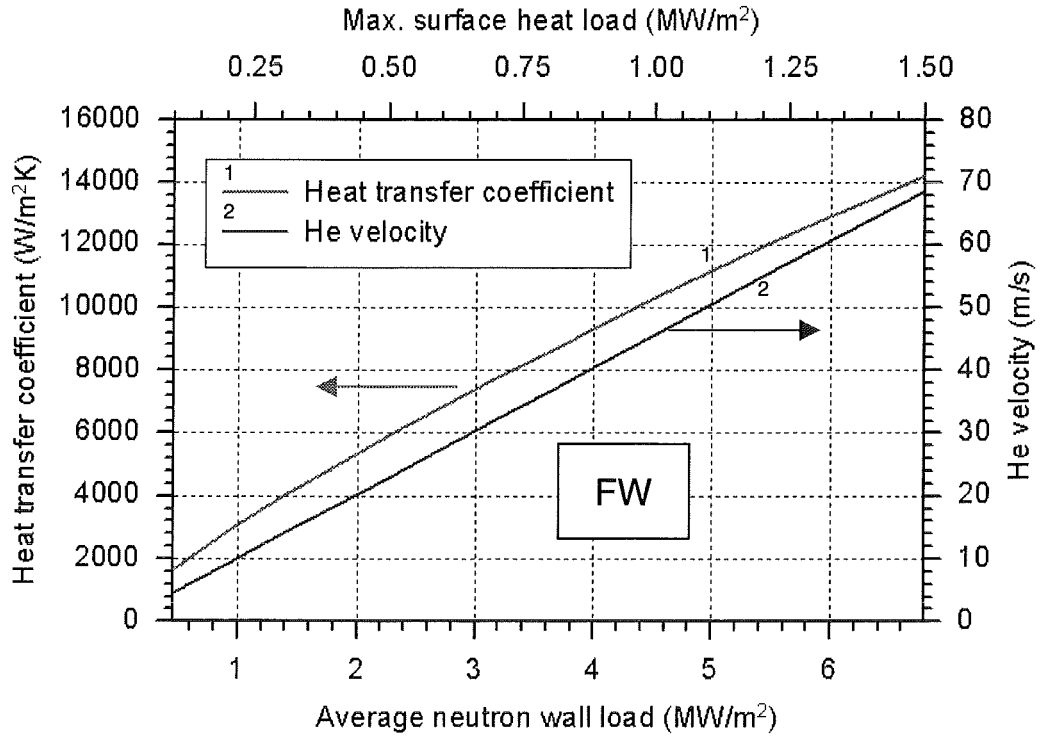


**Fig. 11:** He/wall heat transfer coefficient and He velocity ( $T_{\text{He, in/out}} = 300/480 \text{ }^\circ\text{C}$ ) in the first wall and grids coolant channels of an outboard blanket segment as a function of average neutron wall load.

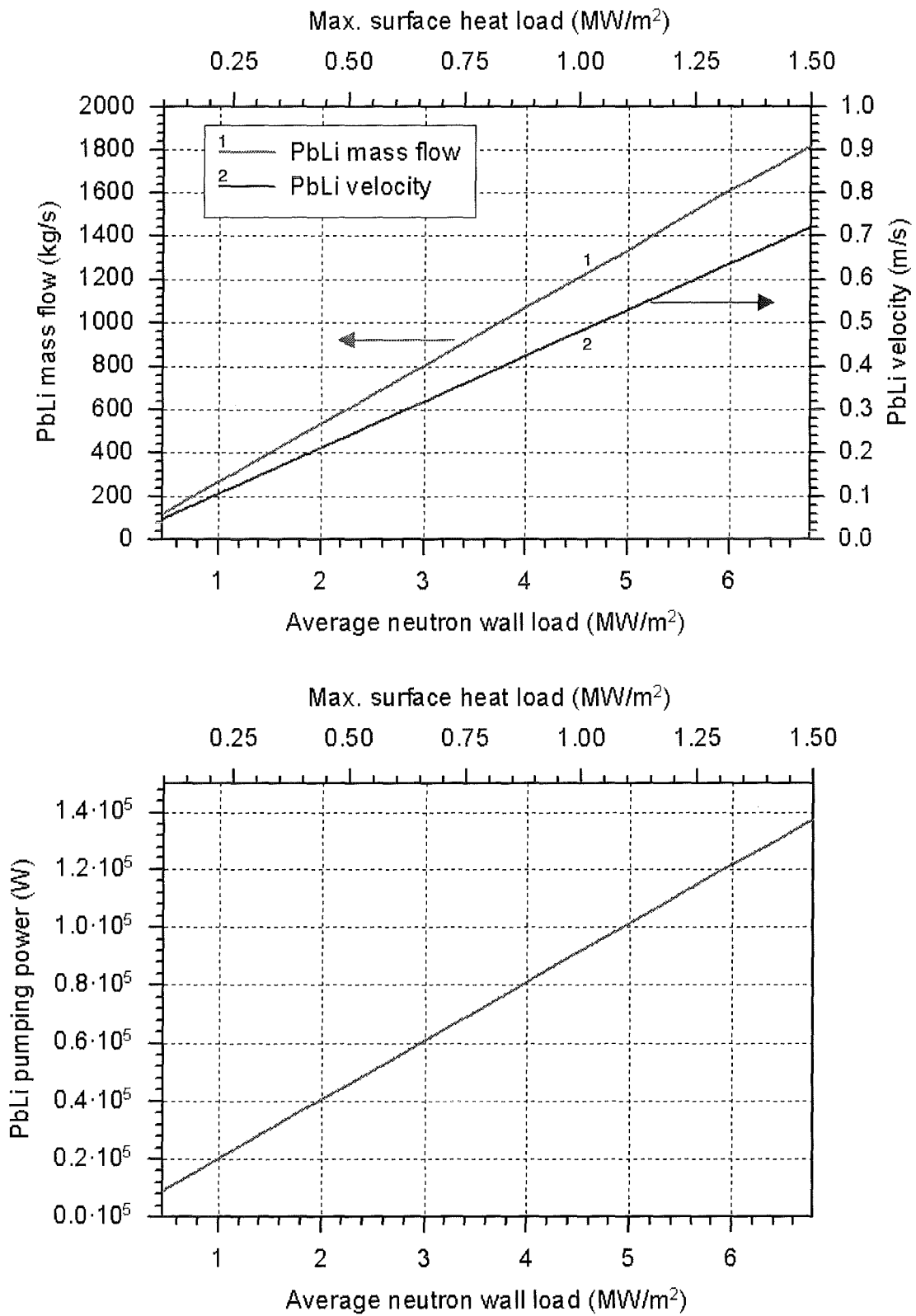


**Fig. 12:** Pb-17Li mass flow, velocity and pumping power for an outboard blanket segment ( $T_{\text{pb-17Li, in/out}} = 460 / 700 \text{ } ^\circ\text{C}$ ) as a function of average neutron wall load.

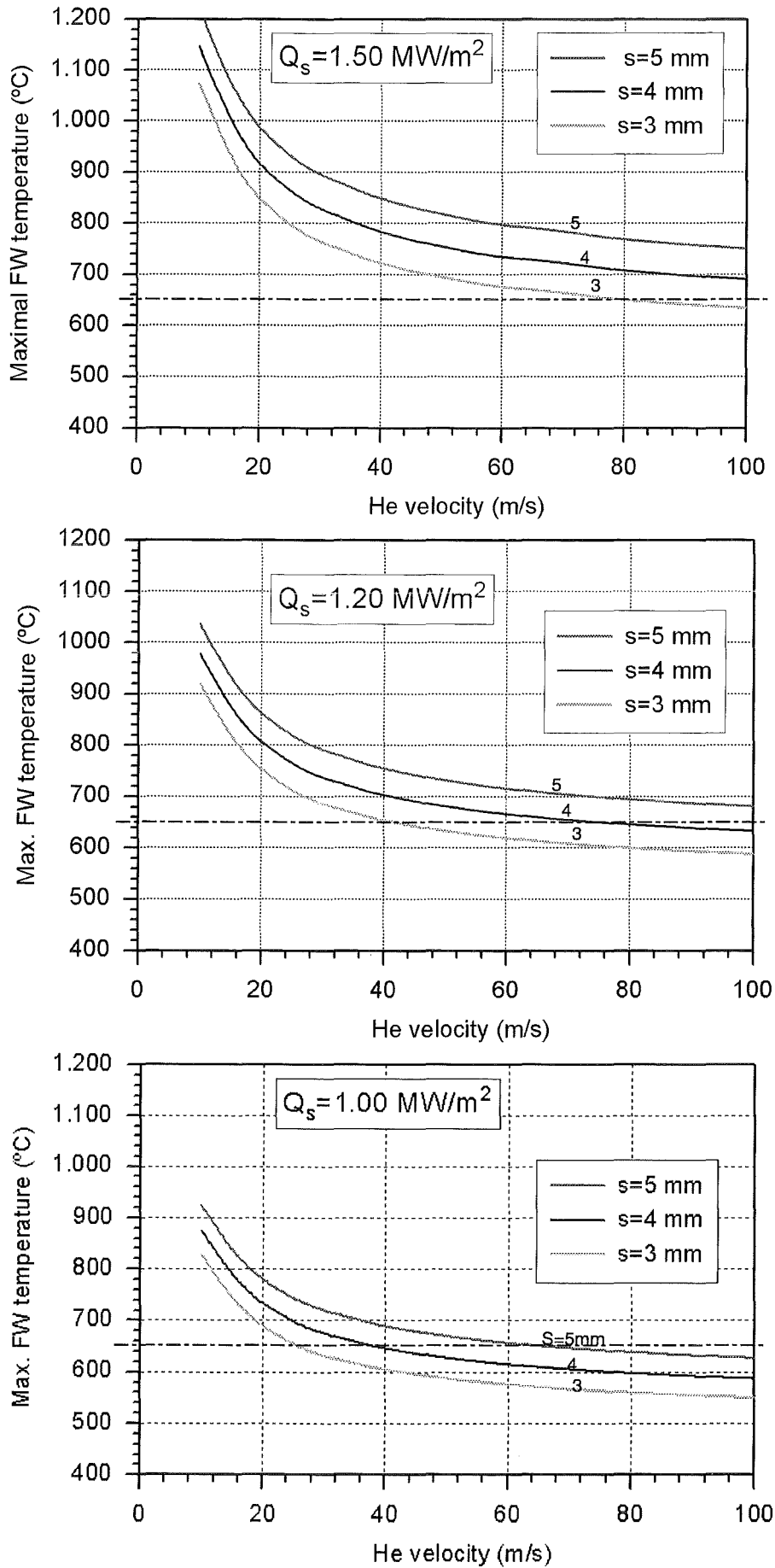


**Fig. 13:** Max. FW temperature vs He velocity (max surface heat load = 1.0, 1.2, 1.5 MW/m<sup>2</sup>)  
 FW channel 20x30 mm<sup>2</sup> (artificially roughened plasma facing wall,  $f_R=2.0$ );  
 $T_{\text{He,in/out}} = 300 / 443 \text{ }^\circ\text{C}$  (FW), 300 / 480  $^\circ\text{C}$  (blanket).

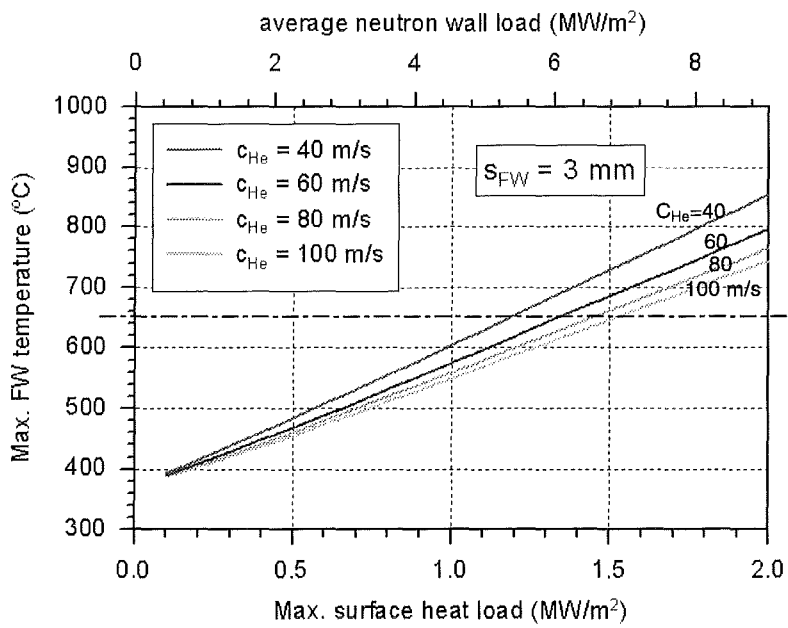
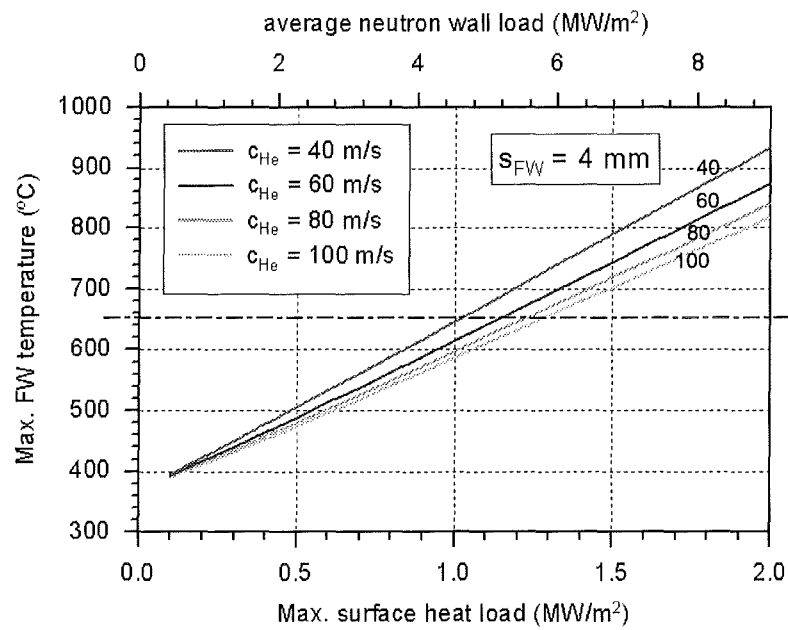
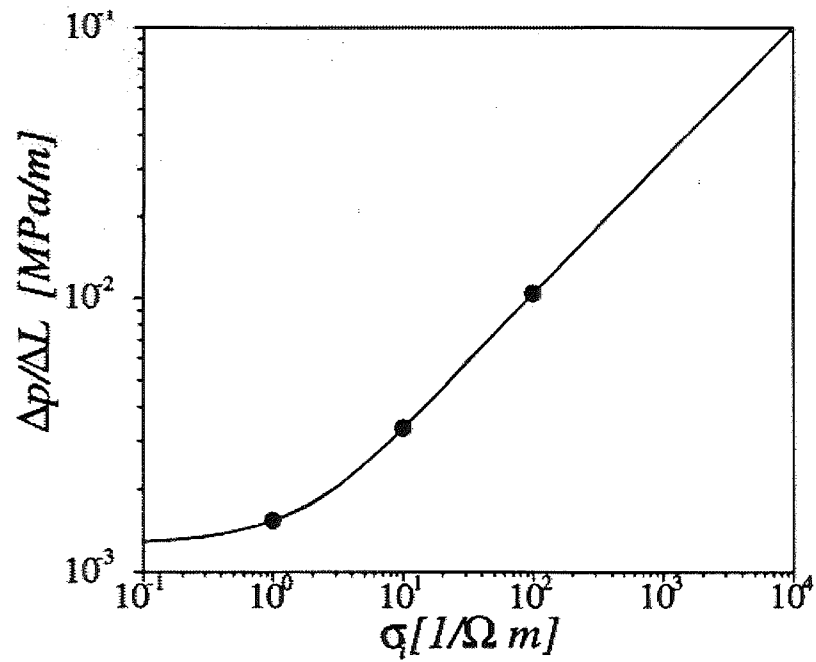
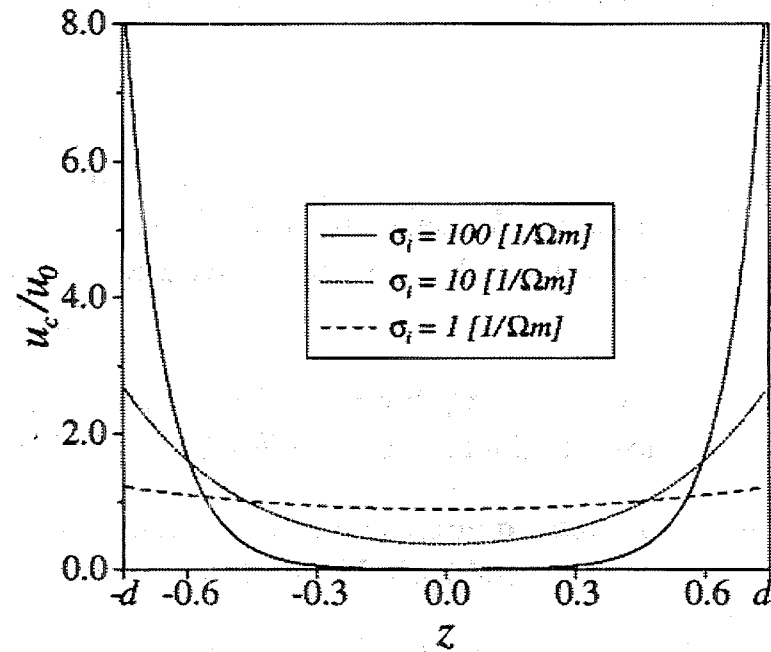


**Fig. 14:** Max. FW temperature vs max. surface heat load (FW thickness = 3, 4 mm)  
 FW channel  $20 \times 30 \text{ mm}^2$  (artificially roughened plasma facing wall,  $f_R=2.0$ );  
 $T_{He,in/out} = 300 / 443 \text{ }^\circ\text{C}$  (FW),  $300 / 480 \text{ }^\circ\text{C}$  (blanket)



MHD pressure loss



Radial velocity profile

**Fig. 15:** MHD pressure loss in the front row of PbLi as a function of the electrical conductivity of the SiC<sub>i</sub>/SiC insert and radial velocity profile perpendicular to the magnet field [15].

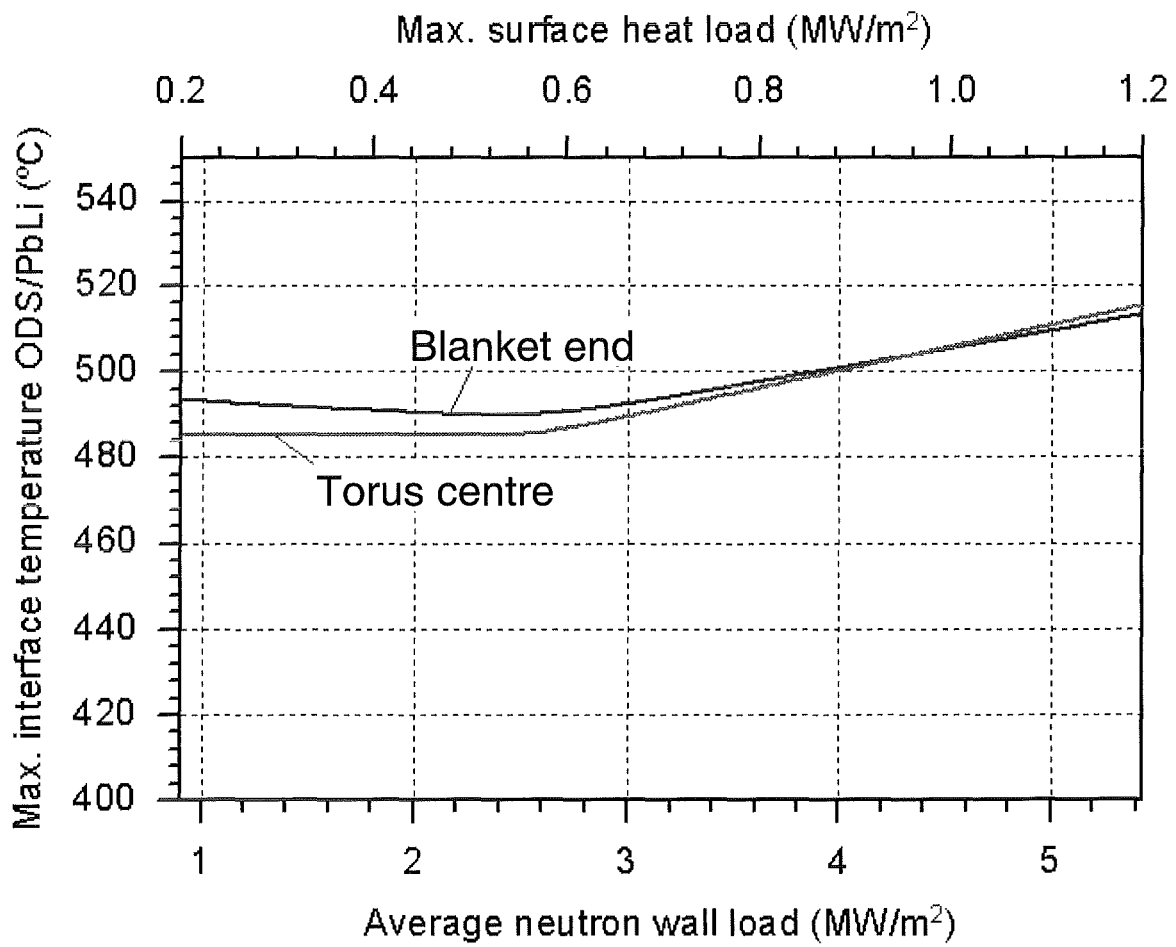
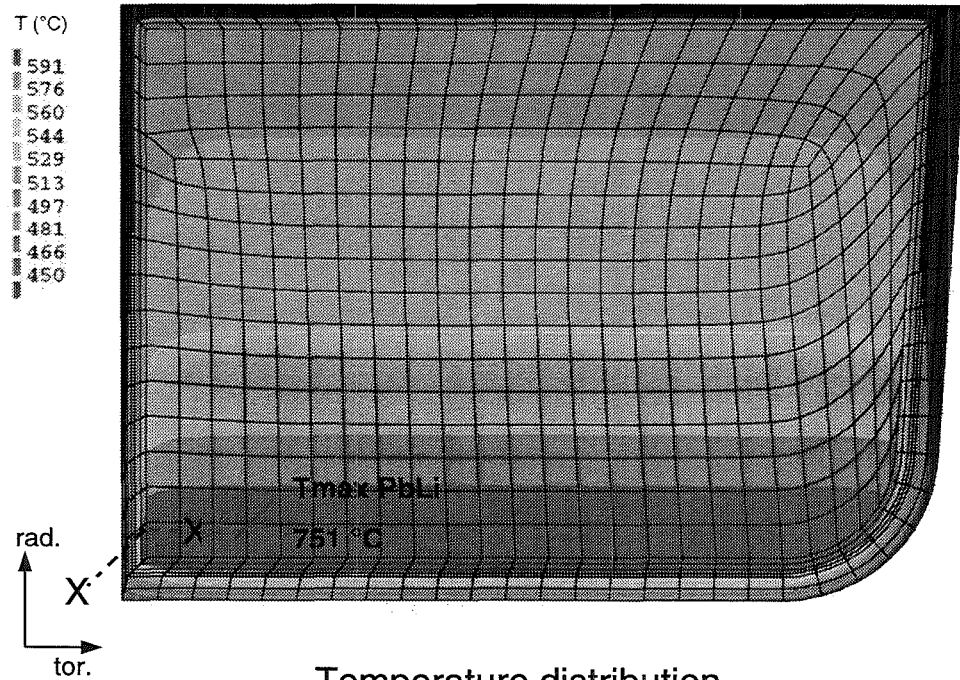
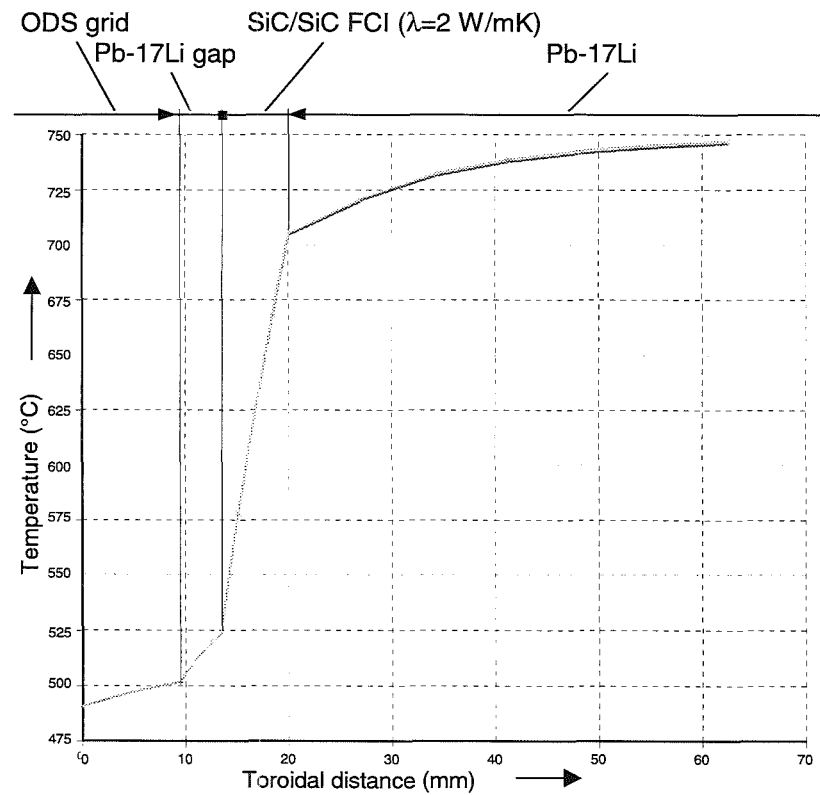


**Fig. 16:** Maximum interface temperature ODS/Pb-17Li at the torus centre and at the blanket end as a function of average neutron wall load.



Temperature distribution  
 Pb-17Li:  $T_{\max} / T_{\text{avg}} = 751 \text{ }^{\circ}\text{C} / 633 \text{ }^{\circ}\text{C}$



Temperature gradient along X-X

**Fig. 17:** Temperature distribution in a front Pb-17Li channel at the blanket end for the reference case and temperature gradient across the flow channel inserts (FCIs) along X-X.

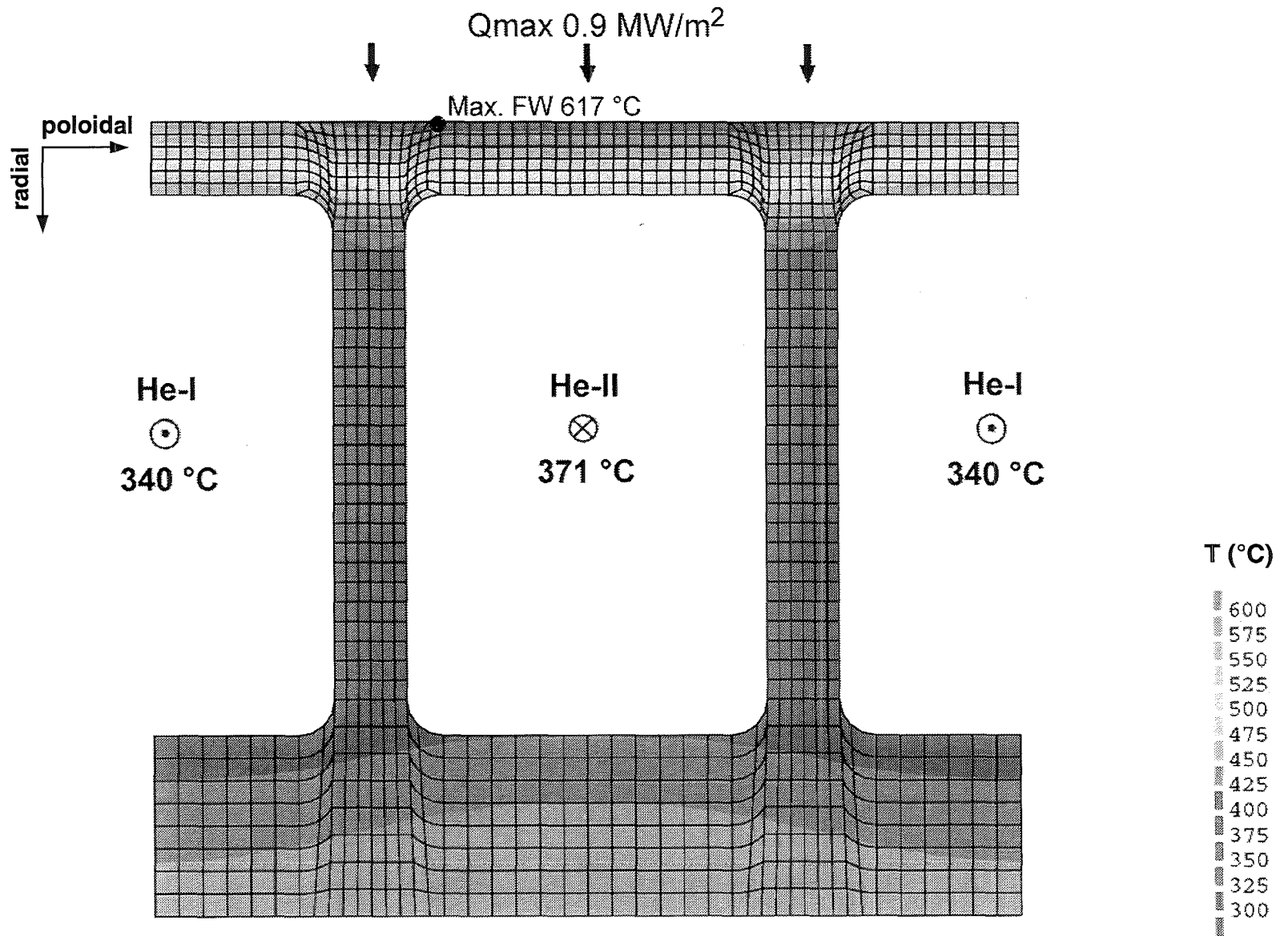


**Fig. 18:** Temperature distribution in the first wall at the torus centre for the reference case.

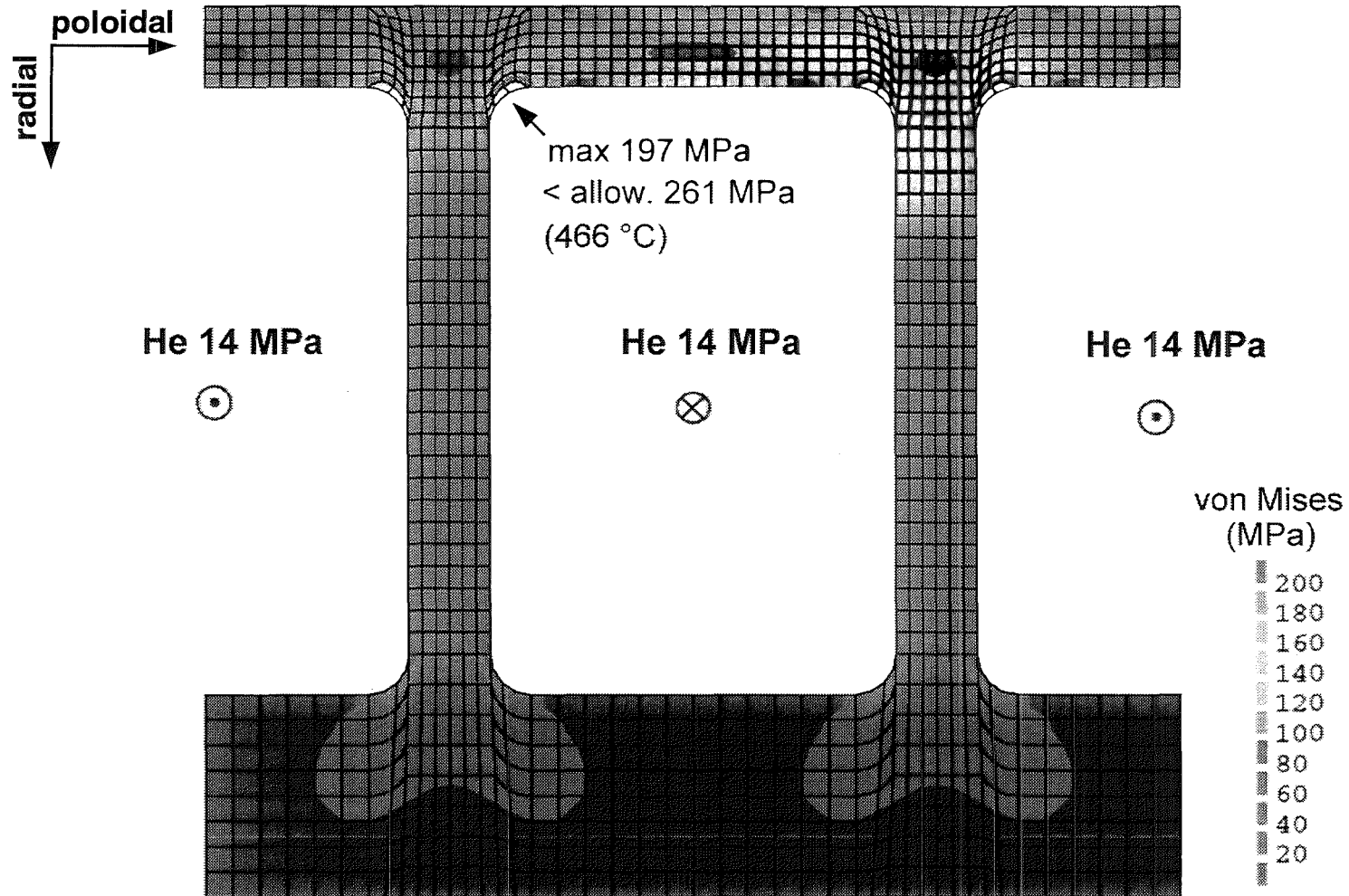


**Fig. 19:** Von Mises primary stresses in the first wall at the torus centre for the reference case.

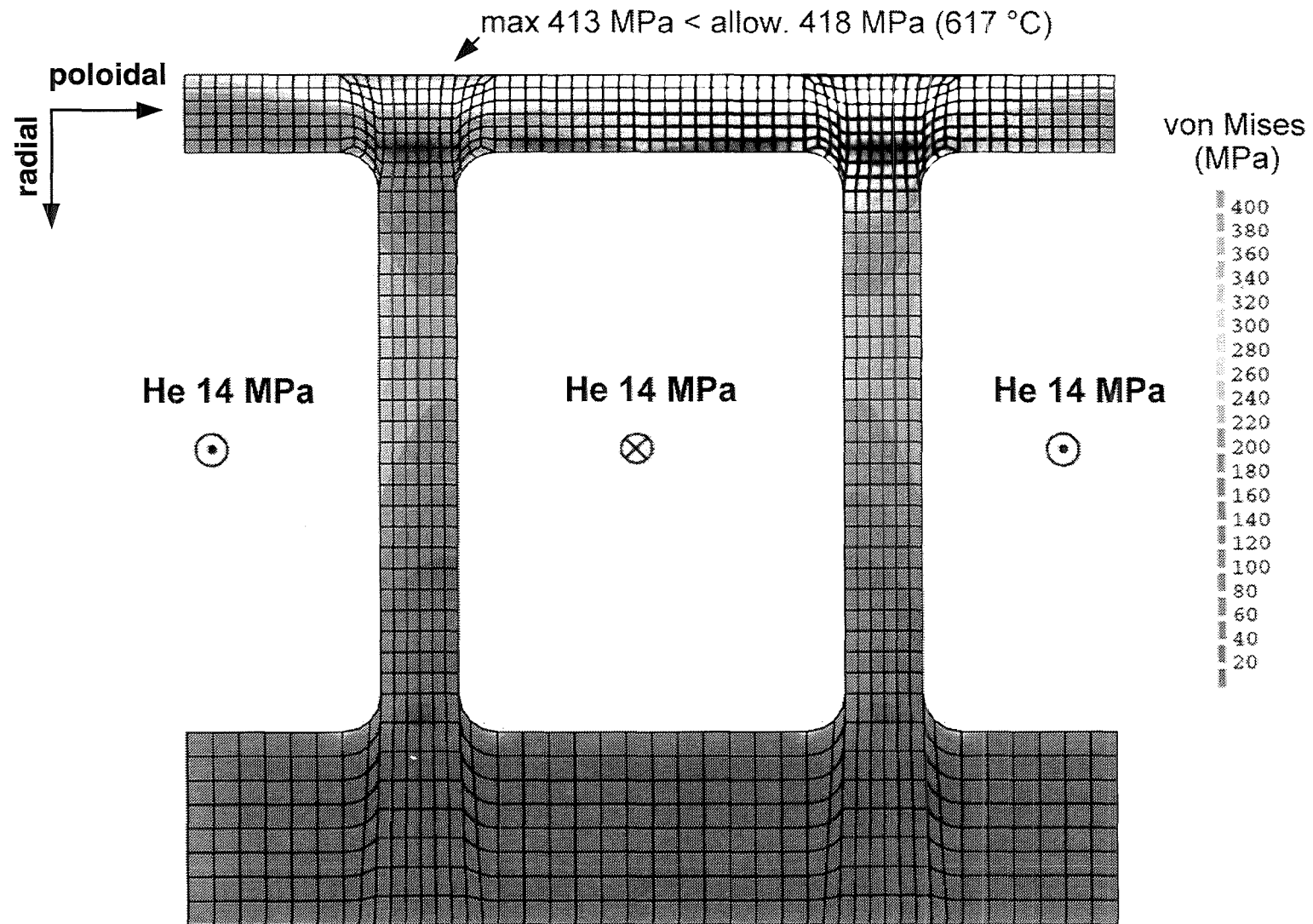


**Fig. 20:** Von Mises primary plus secondary stresses in the first wall at the torus centre for the reference case.

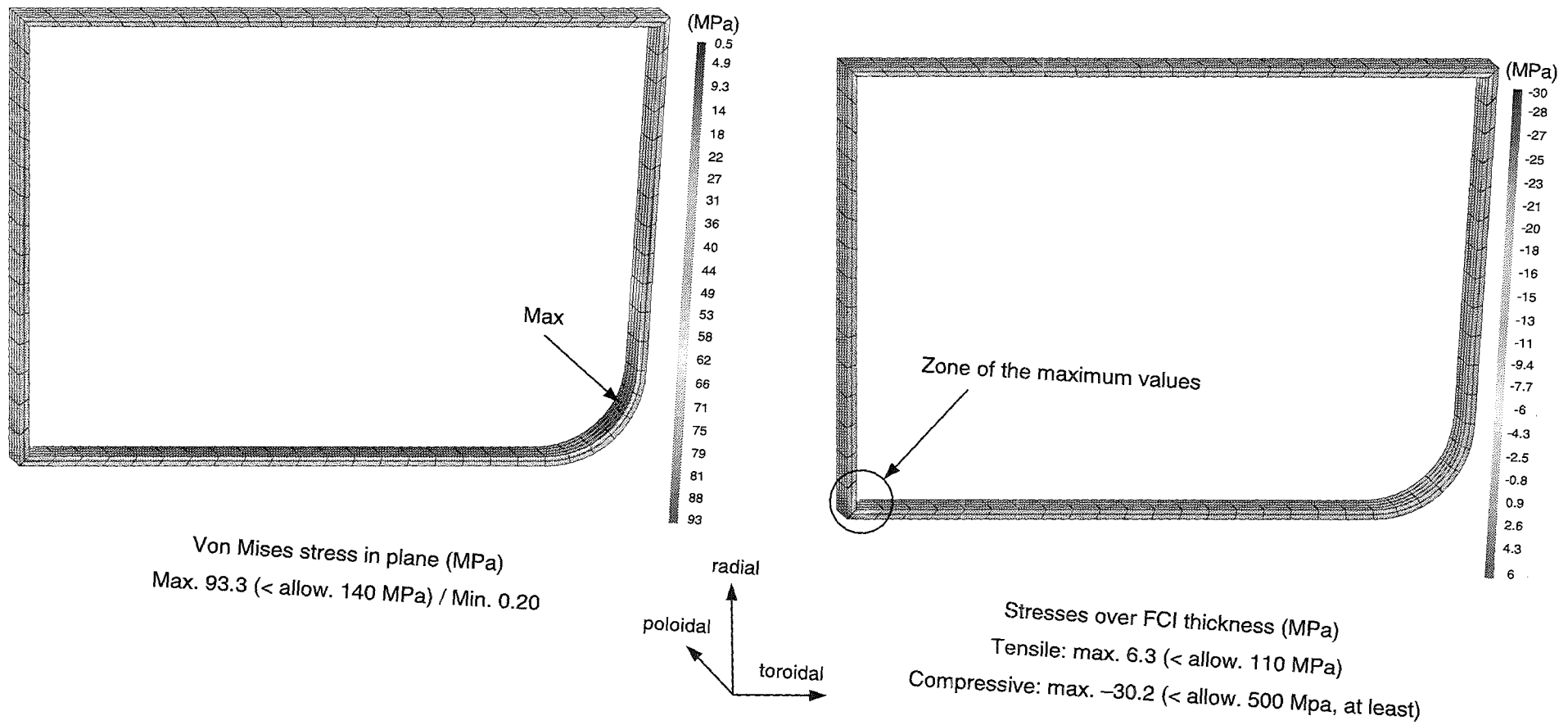


Fig. 21: Von Mises secondary stresses in the SiC<sub>x</sub>/SiC FCI (in plane and over the thickness) at the blanket end for the reference case [16].

### 3-Stage Gas Brayton Cycle

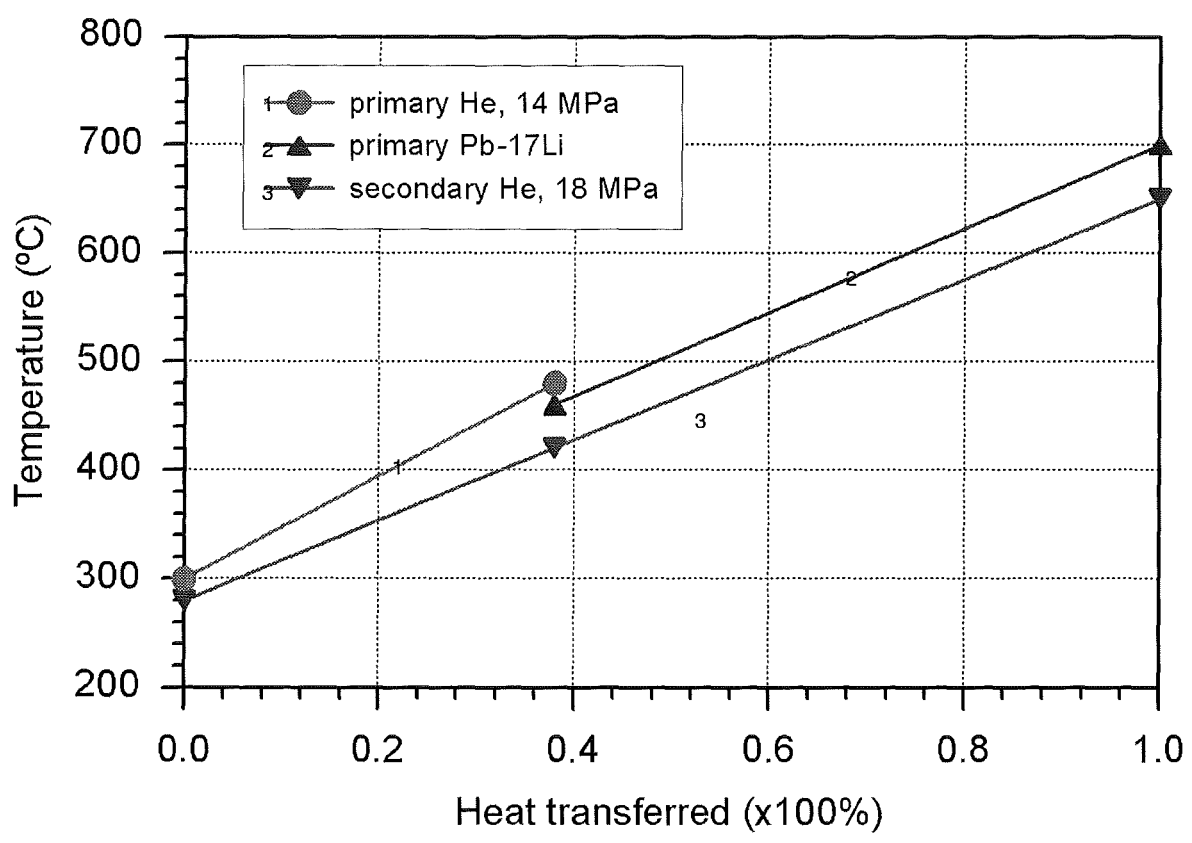
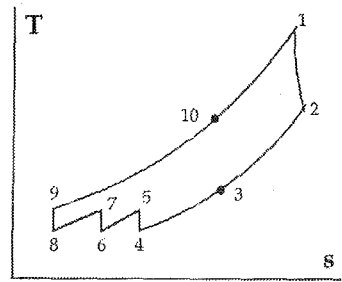
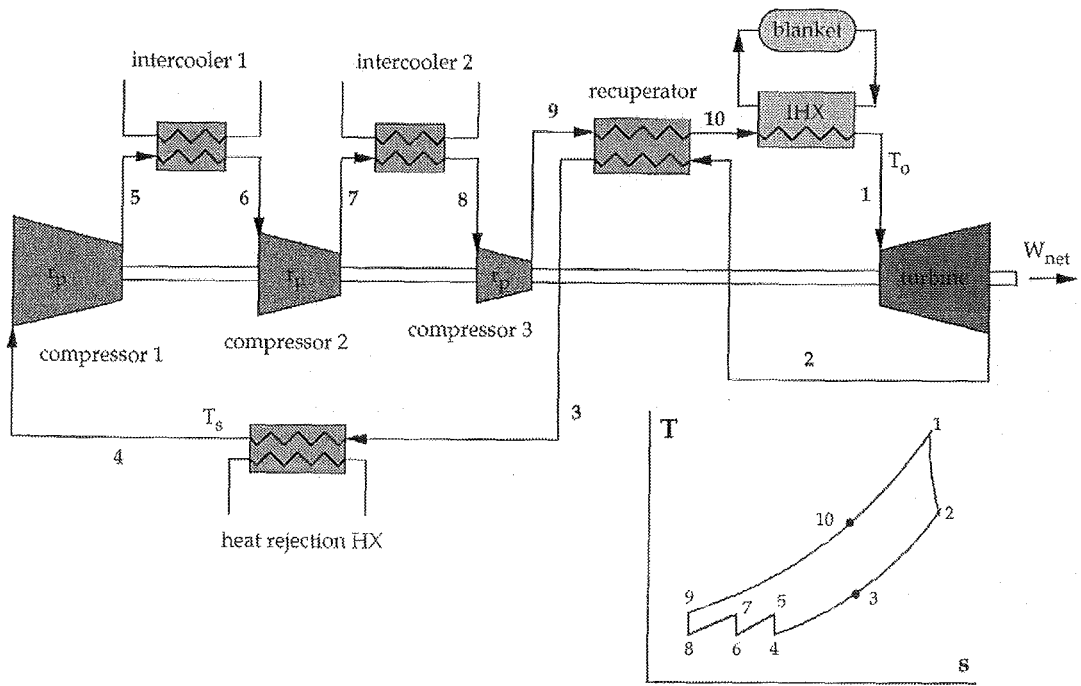
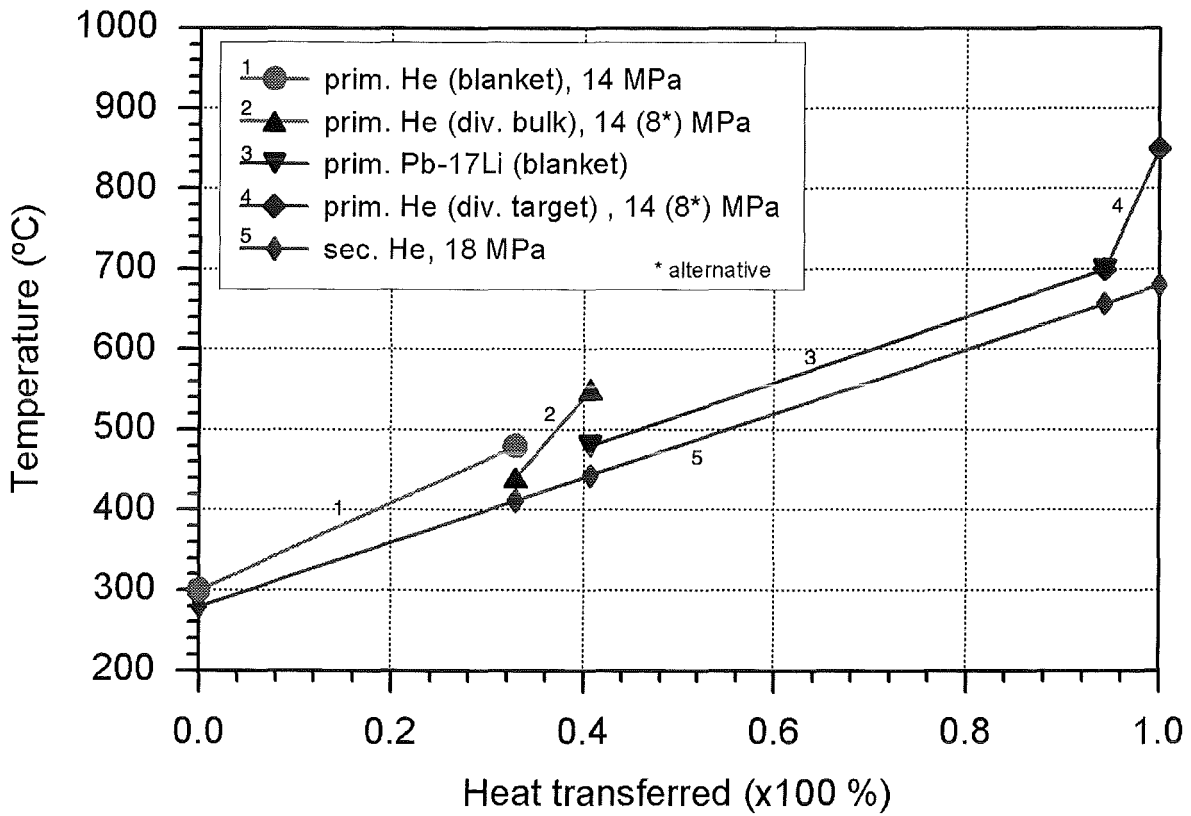


Fig. 22: Heat transfer diagram for a 3-stage gas turbine cycle net efficiency of the blanket cycle  $\eta_{Bl} = 0.44$ ).



**Fig. 23:** Heat transfer diagram for a 3-stage gas turbine cycle in case of integration of He-cooled divertors into the power conversion system (net efficiency of the blanket/divertor cycle  $\eta_{BI+Div} = 0.46$ ).

# Appendices

## Appendix 1

Draft for PPA report, V0, 6 July, 1999

### Neutronic calculations for PPA reactor blanket concepts

U. Fischer

Neutronic calculations have been performed with the MCNP Monte Carlo code [1] and nuclear data from the European Fusion File [2] to assess and optimise the breeding performance of the considered blanket concepts and provide the nuclear heating input data for the subsequent thermal-hydraulic calculations.

#### I. PPA reactor models

Based on the reactor parameters and the neutron source distribution provided by UKAEA Culham [3,4], (see Table I), a generic 7.5 degree torus sector model has been developed for the reactor variant PPA1. This model includes the plasma chamber, four poloidal blanket/shield segments, labelled I-IV, and a bottom divertor port with an integrated divertor of the SEAFP-type, see Fig. 1 for a vertical cross-section. The first wall profile has been adapted in an arbitrary way to the plasma boundary contour shape assuming a scrape-off layer of 15 cm at torus mid-plane. Suitable models of the considered PPA blanket concepts - the Dual Coolant Lithium-Lead (DCLL), the Improved (IHCPB) and Advanced Helium-Cooled Pebble Bed (AHCPB) blanket -, were integrated to the generic PPA1 reactor model when investigating the respective nuclear performance. The radial dimensions common to all blanket variants are given in Table II.

**Table I** Main reactor parameters for PPA reactor models.

	PPA1 [3]	PPA2 [5]
Plasma major radius [m]	6.73	8.10
Plasma minor radius [m]	2.24	2.7
Plasma aspect ratio	3.0	3.0
Plasma elongation	2.0	1.9
Plasma triangularity	0.36	0.4
Fusion power [MW]	2418	3607

**Table II** Radial blanket dimensions for PPA reactor models.

	PPA1	PPA2
Inboard		
First wall radius [cm]	434	525
Thickness blanket + shield [cm]	90	90
Outboard		
First wall radius [cm]	912	1095
Thickness blanket + shield [cm]	170	170

#### II. Neutron source and wall loading distribution

The neutron source distribution was provided by UKAEA Culham in the form of a numerical data array for a normalised source intensity on a 25 x 40 (r, z) regular mesh [4, 5]. These data were transformed into a cumulative probability distribution which is being used in a FORTRAN subroutine called by MCNP to sample the source neutrons.

The neutron wall loading distribution was calculated with MCNP for the voided torus sector model by scoring the number of (virgin) 14 MeV neutrons crossing the first wall. Both of the PPA reactor models were considered to compare the respective loadings and enable the extrapolation of results as described below. For the PPA2 reactor, only a simplified skeleton model was developed including plasma chamber, first wall and blanket back wall contour surfaces, and the divertor port opening. This is sufficient when calculating the neutron wall loading distribution with the proper PPA2 neutron source distribution. Table III shows the resulting average and peak values for the two PPA reactor models. The normalisation has been performed on the basis of the total fusion power as indicated for PPA1 and PPA2 above (Table I). Note that the poloidal profiles of the neutron wall loading are comparatively flat: the poloidal form factor (peak/average) amounts to no more than 1.12 for the outboard segment. In Table III, there are also given the surface areas as calculated with MCNP for the four poloidal segments. According to the MCNP reactor models, the blanket coverage amounts to 81 and 82 %, for PPA1 and PPA2, respectively.

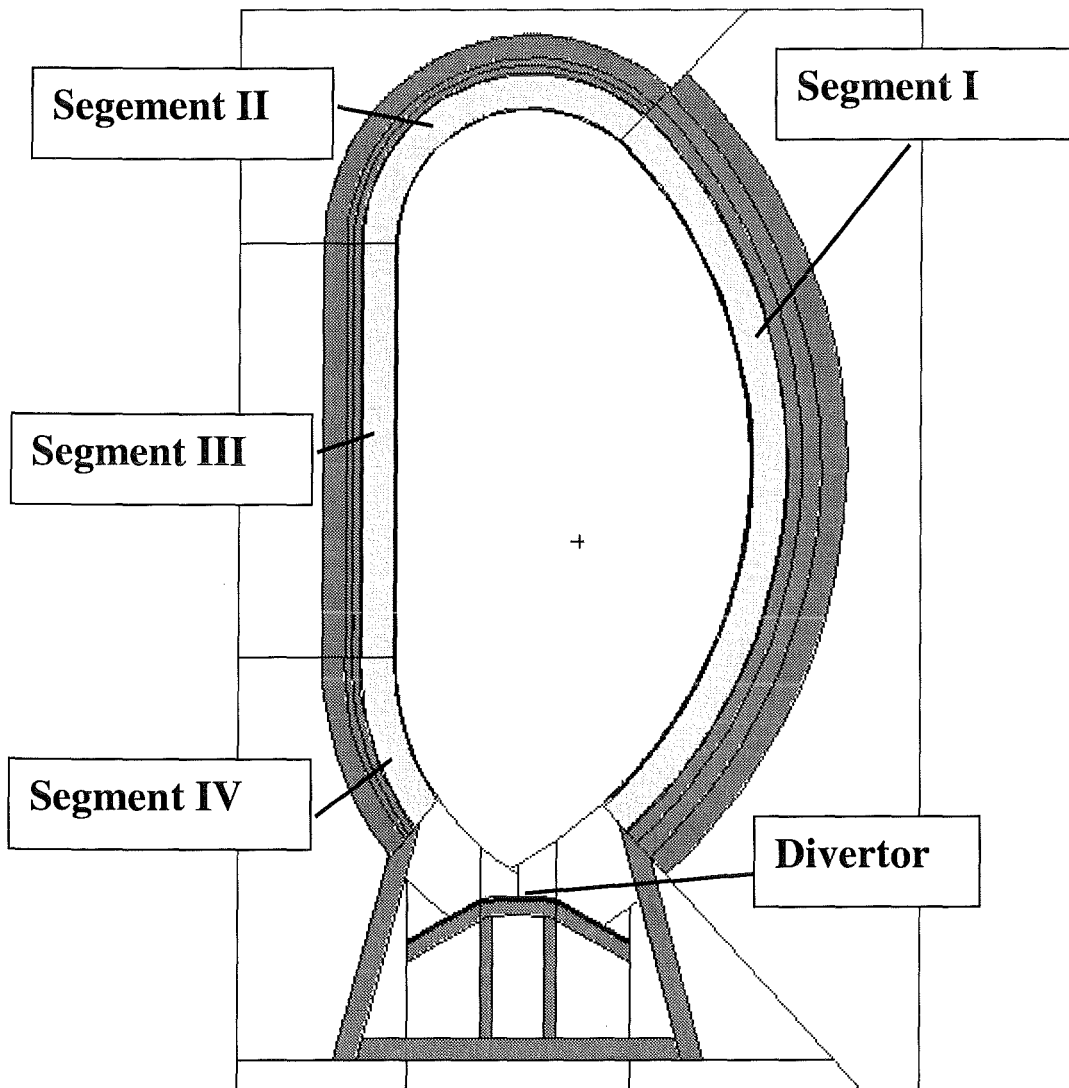


**Fig. 1:** Vertical cross-section of MCNP torus sector model (PPA1 reactor with HCPB blanket segments included)

**Table III** Neutron wall loadings and first wall surface areas for the PPA reactor models.

	PPA1		PPA2	
	Neutron wall loading [MW/m <sup>2</sup> ]	Surface area [m <sup>2</sup> ]	Neutron wall loading [MW/m <sup>2</sup> ]	Surface area [m <sup>2</sup> ]
Pol. Segment I (outboard)				
Average	2.27	530	2.51	716
Peak	2.57	-	2.79	-
Pol. Segment II (top)	1.56	143	1.62	182
Pol. Segment III (inboard )				
Average	1.92	152	2.05	215
Peak value	2.28	-	2.55	-
Pol. Segment IV (bottom inboard)	1.26	58	1.37	73.6
Total of blanket segments	2.03	882	2.22	1187
Divertor port	0.755	190	0.903	280
Total including divertor port	1.80	1072	1.97	1467

### III. Approach for nuclear heating calculations

The nuclear calculations for the three blanket variants have been performed by making use of the generic PPA1 reactor model as noted above. To allow the assessment for the PPA2 reactor model, the following extrapolation rules have been established:

#### Nuclear power density at outboard torus mid-plane

$$P_{PPA2} [\text{W/cm}^3] = P_{PPA1} [\text{W/cm}^3] \cdot WL_{PPA2,\text{max}}/WL_{PPA1,\text{max}} \cong P_{PPA1} [\text{W/cm}^3] \cdot 1.10$$

with  $WL [\text{MW/m}^2]$  = neutron wall loading.

#### Nuclear power generation in the blanket

$$P [\text{MW}] = WL [\text{MW/m}^2] \cdot S_{FW} [\text{m}^2] \cdot M_E$$

with  $S_{FW}$  = first wall area and  $M_E$  = energy multiplication of the blanket.

We have e. g. for the outboard blanket segment (poloidal segment I, 7.5° torus sector):

$$P_{PPA1,1} = WL_{PPA1,1} \cdot S_{FW,PPA1,1} \cdot M_E = 2.27 \text{ MW/m}^2 \cdot 14.92 \text{ m}^2 \cdot M_E = 25.1 \text{ MW} \cdot M_E$$

$$P_{PPA2,1} = WL_{PPA1,1} \cdot S_{FW,PPA1,1} \cdot WL_{PPA2,1} / WL_{PPA1,1} \cdot S_{FW,PPA2,1} / S_{FW,PPA1,1} \cdot M_E \\ = 25.1 \text{ MW} \cdot 2.51 \text{ MW/m}^2 / 2.27 \text{ MW/m}^2 \cdot 14.92 \text{ m}^2 / 11.04 \text{ m}^2 \cdot M_E$$

$$P_{PPA2,1} = 25.1 \text{ MW} \cdot 1.10 \cdot 1.35 \cdot M_E$$

For the outboard blanket segment of the PPA1 reactor, the following multiplication factors  $M_E$  have been derived for the considered PPA blanket concepts:

PPA blanket concept	DCLL	IHCPB	AHCPB
Energy multiplication $M_E$ (outboard blanket segment)	1.11	1.34	1.19

The specified rules have also been used to extrapolate to higher neutron wall loadings when assessing the design limits of the investigated PPA blanket concepts.

## IV. Nuclear calculations for the PPA blanket concepts

### IV.A DCLL blanket concept

#### IV.A.1 Blanket lay-out

A technical description of the DCLL blanket concept is given in Section 2 of this report. The large-sized liquid metal flow channels provide a good Tritium breeding potential when using the Pb-17Li liquid metal at a  ${}^6\text{Li}$  enrichment of 90 at% as breeder material. The total radial thickness of the blanket amounts to 78.5 and 47 cm including first and back wall, outboard and inboard, respectively. Fig. 2 show a horizontal cross-section of the outboard blanket segment at torus mid-plane. Note that there is included a toroidal gap of 1.5 cm between the blanket sectors. As for the structural material, the low-activation steel EUROFER '97 [6] has been used to simulate the ODS in the neutronic calculation.. The assumed elemental composition is displayed in Table IV. There is also taken into account 1 cm thick SiC/SiC layers in the model foreseen as electrical insulation.

Table IV: Elemental composition of the LA steel EUROFER as used in the neutronics calculations

Element	Fe	Cr	Mn	W	Ta
W%	89.1	9.0	0.4	1.1	0.07

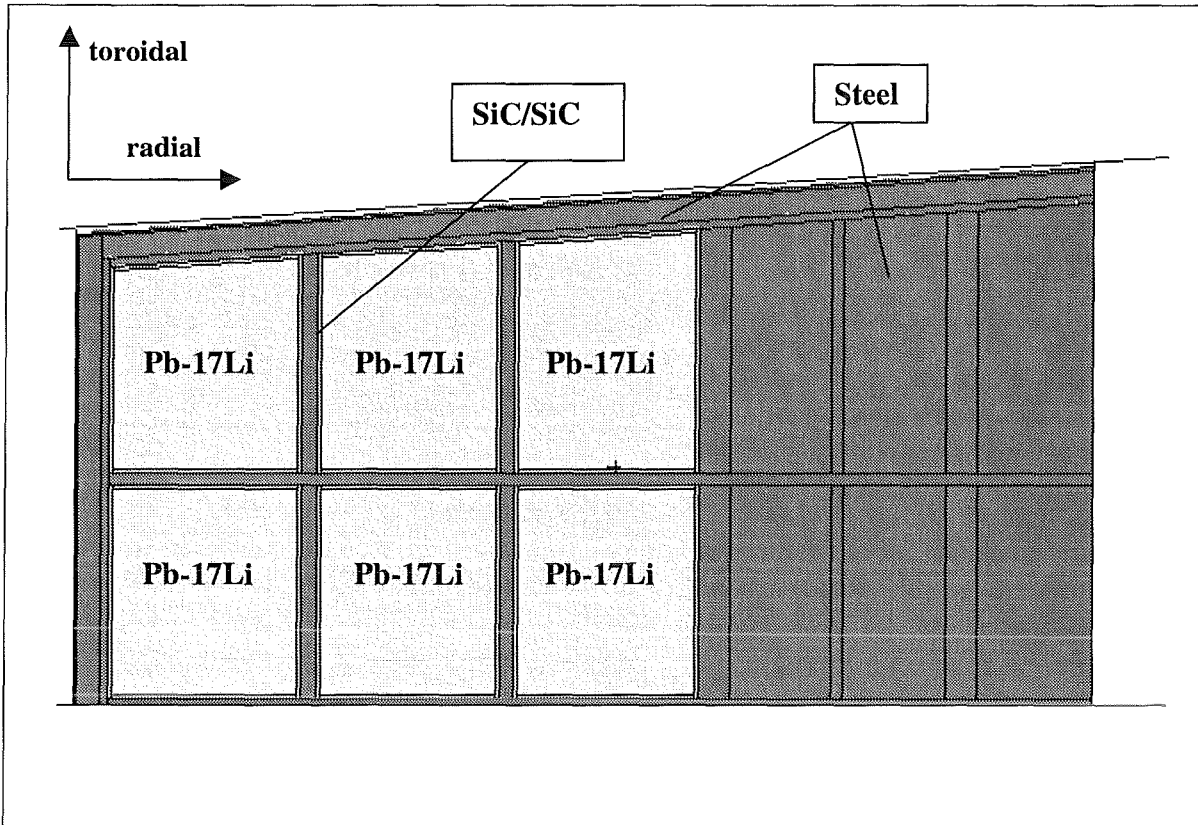


**Fig. 2:** DCLL blanket: horizontal cut through outboard blanket segment (PPA1 reactor, torus mid-plane)

#### IV.A.2 Tritium breeding performance

With the assumed boundary conditions, the global Tritium Breeding Ratio (TBR) amounts to 1.09 for the DCLL blanket concept, see Table V. Note that the outboard blanket segment (poloidal segment I) provides 70 % of the Tritium breeding. The neutron multiplication factor is at 1.59.

Table V: Tritium breeding ratio of the DCLL blanket (PPA1 reactor model).

Poloidal segment	I	II	III	IV	Total
TBR	0.76	0.14	0.14	0.05	1.09

#### IV.A.3 Nuclear heating

Nuclear heating calculations include Monte Carlo calculations of the nuclear power generated in the various reactor components (first wall, blanket, shield, divertor etc.) and of the nuclear power density distribution. For the purpose of the PPA study, the radial power density profile at torus mid-plane of the outboard blanket segment has been considered where there are the highest nuclear and thermal loadings.

The nuclear power generation is shown in Table VI as calculated for a 7.5 ° toroidal sector of the PPA reactor with an fusion power assumed as specified above (Table I). The total nuclear power generated in the reactor amounts to 2290 and 3420 MW, PPA1 and PPA2, respectively. This corresponds to a global energy multiplication factor of 1.18 when taking into account all reactor components, i. e. including blanket, shield and divertor. Fig. 3 shows the radial power density profile in the outboard blanket segment at torus mid-plane, normalised to the PPA2 reactor conditions.

**Table VI** Power generation [MW] in a 7.5 ° toroidal sector of the PPA reactor with DCLL blanket segments.

<b>PPA1</b>						
Poloidal segment	I	II	III	IV	Divertor	Total
Pb-17Li	20.6	3.92	3.94	1.3	-	29.7
Steel	6.36	2.25	2.61	0.96	-	12.2
SiC/SiC	0.62	0.15	0.17	0.05	-	0.99
<b>Total sector</b>	<b>27.5</b>	<b>6.31</b>	<b>6.72</b>	<b>2.31</b>	<b>4.79</b>	<b>47.7</b>

<b>PPA2</b>						
Poloidal segment	I	II	III	IV	Divertor	Total
Pb-17Li	30.6	5.22	5.97	1.8	-	43.6
Steel	9.46	2.99	3.96	1.34	-	17.8
SiC/SiC	0.93	0.19	0.26	0.07	-	1.45
<b>Total sector</b>	<b>41.0</b>	<b>8.41</b>	<b>1.02</b>	<b>3.22</b>	<b>8.46</b>	<b>71.3</b>

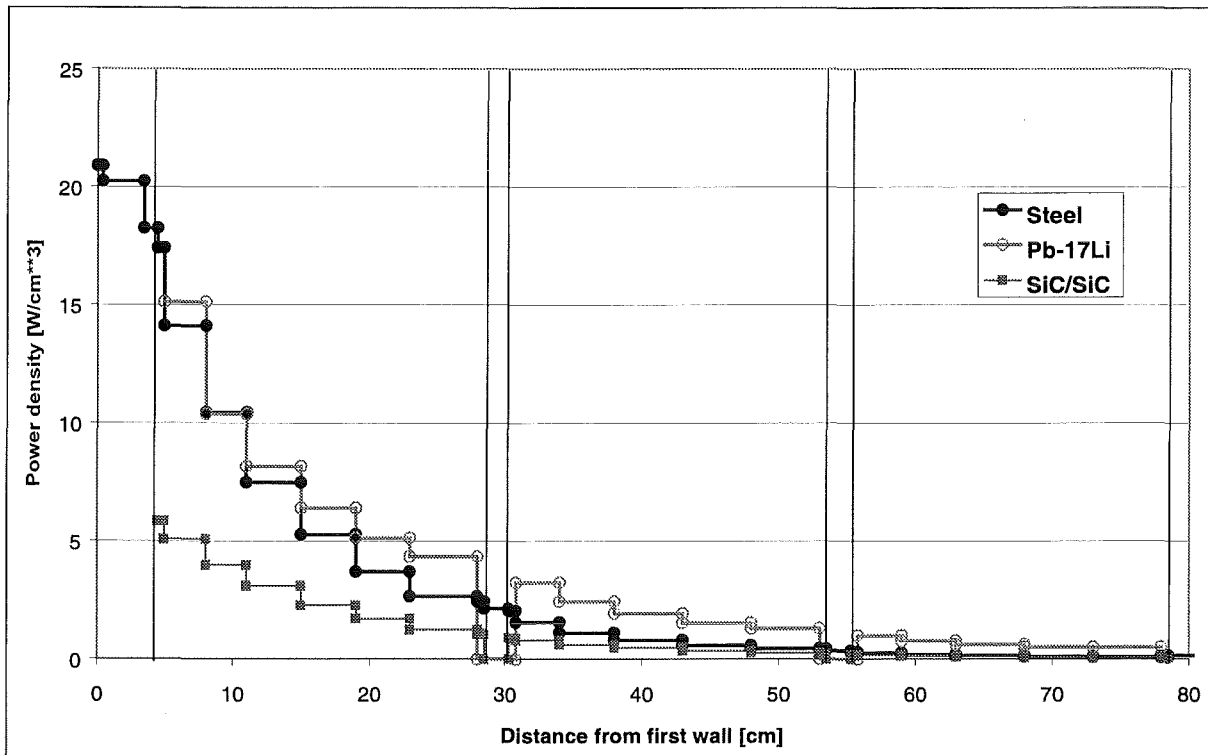


**Fig. 3** DCLL blanket: Radial power density profile in the outboard blanket segment (PPA2 reactor, torus mid-plane).

### References

- [1] F. Briesmeister (ed.): MCNP - A General Monte Carlo N-Particle Transport Code, Version 4A, LA-12625-M, November 1993, Version 4B March 1997
- [2] P. Vontobel: A NJOY Generated Neutron Data Library Based on EFF-1 for the Continuous Energy Monte Carlo Code MCNP, PSI-Bericht Nr. 107, September 1991
- [3] I. Cook, , UKAEA Culham, PPA geometry etc, e-mail of 21 January, 1999.
- [4] N. Taylor, UKAEA Culham, Neutron source distribution, e-mail of 16 February, 1999.
- [5] I. Cook, , UKAEA Culham, PPA parameters, e-mail of 12 March, 1999.
- [6] R. Lindau, Forschungszentrum Karlsruhe, private communication, 1997

## **Appendix 2**

DRAFT-01 (21/05/1999)

***On the Use of SiC<sub>f</sub>/SiC as Structural Materials for Fusion Blankets  
CEA Comments and Suggestions concerning  
« Dual-Coolant » and « He-Cooled Ceramic » Blankets  
L. Giancarli, G. Aiello, H. Golfier, Y. Poitevin, J.F. Salavy  
CEA/Saclay, DRN/DMT/SERMA, 91191 Gif-sur-Yvette, France***

### **1. Introduction**

The CEA is involved since several years on design activities specific for ceramic-matrix composite structural materials and is contributing to the activity an European working group which involves also the SiC<sub>f</sub>/SiC major industrial manufacturer, the SEP (Société Européenne de Propulsion, today division of SNECMA). The fabrication method considered at present the « reference » industrial manufacturing method for SiC<sub>f</sub>/SiC is the Chemical Vapor Infiltration technique (CVI).

The CEA contribution has been aimed to identify the major needs in terms of R&D for present-day SiC<sub>f</sub>/SiC composites by proposing and analyzing various blanket design proposals. This activity has also led to the development of the TAURO blanket concept [1], which a self-cooled Pb-17Li blanket concept using SiC<sub>f</sub>/SiC as structural material.

Because of such experience, within the framework of the European pre-studies for Power Reactor Plant, the CEA is contributing to the evaluation of the blanket concepts using SiC<sub>f</sub>/SiC as structural material from the viewpoint of the SiC<sub>f</sub>/SiC structure long-term feasibility.

In particular, the sub-tasks PPA2.5.2 and PPA2.6.2 concern two blanket concepts, respectively the « Dual-coolant » and the « He-cooled ceramic » blankets, proposed by FZK for which the CEA is charged to give support on all items concerning the SiC<sub>f</sub>/SiC, that is for instance, the identification of reasonable extrapolation of present-day SiC<sub>f</sub>/SiC characteristics, possible manufacturing issues and specific R&D issues.

This report is therefore aiming to make comments and suggestions for the design of such two blanket concepts starting from a list of questions which has been prepared by the task coordinators of the corresponding blanket.

### **2 Recall of the major blankets features**

Two blanket concepts are considered in this report : the Dual-Coolant Pb-17Li blanket concept and the He-Cooled ceramic pebble-bed blanket concept.

#### **2.1 Dual-Coolant Pb-17Li blanket (DC)**

The DC blanket (see Fig. 1) is formed essentially by a stiffened martensitic steel box which act as Pb-17Li container. The stiffeners act also as flow separator, forming roughly square channels (335 mm x 240 mm). The Pb-17Li, besides the function of tritium breeder and neutron multiplier, acts also as coolant. The Pb-17Li is flowing at relatively high velocity (~1 m/s), The Pb-17Li outlet temperature is dictated by compatibility issues and, for efficiency reasons, needs to be maximized. Because of the high Pb-17Li velocity and of the high magnetic field present in the blanket region (~7 Tesla), the Pb-17Li need to be electrically insulated from the steel wall. This is obtained by adding SiC<sub>f</sub>/SiC channel inserts (about 5 mm-thick) which act also as thermal insulators (in order to maximize the Pb-17Li temperature without having too high steel temperatures, ~600°C for ODS steel).

The steel-box (including the FW) and the stiffeners are directly cooled by Helium (p=8 MPa) which allows to keep sufficiently low the steel temperature.

In this concept the most important specific requirements for SiC<sub>f</sub>/SiC, which has not direct structural functions, are low electrical conductivity and low thermal conductivity, together with compatibility with high-T Pb-17Li.

#### **2.2 Helium-Cooled ceramic pebble-bed blanket (HC)**

The HC blanket (see Fig. 2) uses SiC<sub>f</sub>/SiC structures, ceramic pebble-beds as breeder, Beryllium pebble-beds as multiplier, Helium (8 MPa) as coolant, and also Helium (0.1 MPa) as purge gas for Tritium extraction from ceramic and Beryllium.

Essentially, there are two SiC<sub>f</sub>/SiC components : a He-cooled box formed by a series of parallel tubes attached together in order to form a container, and a SiC<sub>f</sub>/SiC tube bundle (a sort of tube serpentine called herewith as « meander ») located in an appropriate way in order to form separate regions able to segregate the ceramic pebbles from the Be-pebbles.

In this concept the most important specific requirements for SiC<sub>f</sub>/SiC, which is the only structural material, are high thermal conductivity, high-T compatibility with ceramic and Be, and high hermeticity to Helium both in the container wall (need of avoiding leakage to the plasma region) and in the breeder zone (need of avoiding a pressurization of the box which is not stiffened).

### 3 Comments and Suggestions

The task coordinators of the activities related to both DC and HC blankets have released a list of questions concerning directly the use of SiC<sub>f</sub>/SiC in the two concepts. Following a meeting held in Bordeaux between FZK, CEA, and SiC<sub>f</sub>/SiC manufacturer (SNECMA, division SEP), these questions were addressed both to CEA and to industry. Starting from these questions (which are reported herewith for clarity), the present section gives the CEA comments and suggestions, based on present available data and reasonable extrapolation, concerning the various issues which were indicated. It is expected that, at a second stage, industry will give its own comments based on present-day industrial knowledge of the composite.

#### 3.1 Generic questions

*Question nb.1 - Can sheets and tubes be manufactured of SiC<sub>f</sub>/SiC ? (straight, bents, junctions, flanges, stiffening ribs...) - Can SiC be machined by wire erosion ?*

Sheets of SiC<sub>f</sub>/SiC can easily be manufactured (at present, the maximum achievable thickness is about 6 mm, however thickness up to about 10 mm could be reasonably achievable in the future after appropriate R&D). Sheets can have quite complex shape (curved, with relatively sharp angles, etc. ; for instance turbine helix shape can be already achieved). The same of course apply to stiffening ribs. Junctions require special procedure (see next question).

The information available at CEA suggests to avoid machining by wire erosion because of the risk of oxidation of the material (demonstrated for CFC). Machining can preferably be performed mechanically and/or by laser. It is clear that machining (especially in the case of the laser technique) has to be performed prior the application of the last SiC-coating, called « sealcoat » (see question nb.4 below) ; therefore, piece machining should preferentially be performed by the manufacturer.

*Question nb.2 - Is it possible to connect SiC<sub>f</sub>/SiC plates (stiffening ribs) and tubes to other SiC<sub>f</sub>/SiC pieces ? How can direct connections be made ? (brazed, EB-welded)*

Connections between SiC<sub>f</sub>/SiC pieces are possible by three main techniques (depending on required strength of the joint and on its accessibility within the concerned component) :

- 1) assembling by sewing at textile stage followed by the densification phase in the furnace ;
- 2) sticking of two finished pieces and then co-infiltration in the furnace ;
- 3) after manufacturing of each finished piece by brazing (external process).

The third option, brazing, cannot be avoided (it is required at least for closing the box...). Therefore, a brazing technique NEEDS to be available before considering any possibility of appropriate blanket design. It has been, and still it is, one of the priority of the present EU R&D (at very low level !) on SiC<sub>f</sub>/SiC. The best results have been obtained from a brazing technique developed at CEA-Grenoble [2], codenamed Brasic<sup>®</sup>. Preliminary tests have shown that the properties of the brazing are similar to that of the SiC<sub>f</sub>/SiC itself. Compatibility with other materials and behavior under irradiation has not yet been tested.

In order to improve the joining efficiency it has been agreed with the SEP experts that the best way for having a good junction between, for instance, stiffener ribs and flat walls is to prepare the ends of the rib to be joined with a T-shape or L-shape in order to have a larger surface of contact between the two pieces. If one extrapolate this idea to tubes, the requirement will be to modify the diameter at the ends of each tube in order to insert the end of one tube into the beginning of the following one and putting the brazing in between. Another possibility would be to machine at each end a complementary step through half of the thickness.

*Question nb.3 - How can SiC work-pieces be connected with non SiC (metal) pieces : flanges, fixing devices, covers ?*

Connections between SiC<sub>f</sub>/SiC and other materials (other composites and/or metals) can be assumed to be possible provided relevant R&D will be performed. The major problem is expected to be the differential thermal expansion which could require the use of compliant materials (TBD).

Mechanical attachment (ex. : bolts) can also be envisaged (differential thermal expansion to be checked, of course).

*Question nb.4 - Is leak tightness achieved by CVD cover on the inside/outside ? Will a leak-tight outer shell peel off at elevated pressure ? Speed of deposition limited by what ?*

It is important to recall that porosity is essential for allowing the SiC<sub>f</sub>/SiC to accommodate stresses (avoiding fragile behavior). Therefore, the only way of achieving leak tightness is to add some coating. It is expected that a final SiC coating, as last step of the CVI process (and therefore without problem of differential thermal expansion), can be added in order to achieve leak tightness to Helium. This process can be adapted to both outside and inside walls (of a

tube, for instance). A major expected problem during operation is the appearance of cracks on the coat, especially due to thermal cycling. If a crack appears, and an high pressure is present (for instance, inside the tubes) the cracks will tend to increase. Experiments are required on this issue : it appears to be one of the most severe issues of the He-cooled concepts.

*Question nb.5 - What is the maximum temperature for SiC<sub>f</sub>/SiC as structural material ?*

Present-day composites (e.g., the 3D CERASEP<sup>®</sup> N3-1, using Nicalon NL207 fibers) can accept about 1100°C. Future composites with advanced fibers (Hi-Nicalon, Hi-Nicalon S) can operate to higher temperature. It is suggested to use a value between 1300°C and 1400°C as a good guess for reactor studies purposes. This temperature is also the expected limit value for the Brasic<sup>®</sup> brazing.

*Question nb.6 - Three different kinds of SiC are used : whisker, powder, CVD. How many parameters are available to describe mechanical properties needed for FEM modeling ?*

Whiskers have been rejected many years ago because of public health problem related to the fabrication process (e.g., lung cancer). Moreover, at present the most developed methods within industry is CVD.

The simultaneous and complementary presence of matrix and fibers are, in fact, the main reasons of the difficulties encountered for performing a simple FEM modeling.

In fact, SiC<sub>f</sub>/SiC composites exhibit a strongly non linear mechanical behavior because of fibers/matrix interaction during loading. Damage is the main mechanical phenomena in these composites and it affects the composite's properties long before the reaching of the rupture limit (300 MPa for Cerasep<sup>®</sup> N3-1, Table I). A specific damage model is then necessary if one wants to carry out analyses beyond the elastic limit (see later on design criteria).

In the absence of a specific model, and remaining in the linear-elastic domain, an orthotrope modeling of the composite could be sufficient. In this case, appropriate values of the SiC<sub>f</sub>/SiC properties should be used for each of the orthotropy axes. At present, not all the values of these properties are known. Some have been deducted from previous composites (i.e., the Cerasep<sup>®</sup> N2-1), while others have been assumed equal along each of the orthotropy axes. The proposed values are reported in Table I.

Taking into account such a specific behavior, the CEA is currently involved in the implementation of specific appropriate models in the main CEA FEM code (i.e., CASTEM 2000 code). In parallel, specific design criteria are required. Preliminary criteria proposed by CEA are given in **Appendix 2A** but further and lengthy R&D is required to establish acceptable agreed criteria, especially for using SiC<sub>f</sub>/SiC in a nuclear environment.

*Question nb.7 - Can electrical insulating effect be varied independently or will a change in electrical insulation affect the thermal conductivity as well ?*

It is expected that an increase of the thermal conductivity will inevitably lead to an increase of the electrical conductivity. However, the change is not necessarily proportional and therefore acceptable solutions may exist. Moreover, it is mainly required to increase the thermal conductivity through the thickness of the composite. An increase of the electrical conductivity only through the thickness (keeping constant those in the composite plane) may be acceptable (to be checked in future MHD analyses).

It must be stressed that this issue is a typical « fusion » issue, therefore no experimental work related with these subjects has never been performed. The value of SiC<sub>f</sub>/SiC CERASEP<sup>®</sup>N2-1 electrical conductivity has been measured for the first time in 1997 at JRC/Ispra [6]. As a consequence, only « speculations » are possible today.

Another issue is that while the thermal conductivity tends to decrease with the neutron fluence, the electrical conductivity is expected, as for other ceramics, to increase (at least, in-pile under neutron flux).

*Question nb.8 - How can damages occurring during manufacturing be recognized and how can they be avoided ? (Testing Procedure)*

In nuclear industry, the problem of non-destructive tests is already well-known for metallic structures. For SiC<sub>f</sub>/SiC structures it may be even more complex. Available control procedures for composites (at present, known only the composites manufacturers) are likely be insufficient. Significant R&D will be required. However, at present, it can be considered as a second priority requirement.

*Question nb.9 - Chemical compatibility : SiO<sub>2</sub> layers will not exist in contact with Li or Pb-17Li. What will the chemical behavior of non-oxidized SiC be in contact with Li<sub>4</sub>SiO<sub>4</sub> or Be ?*

Experiments on compatibility between Li<sub>4</sub>SiO<sub>4</sub> and SiC<sub>f</sub>/SiC have been performed at ENEA-Casaccia in the framework of the EU program on Advanced Materials in the last few years.

Experiments have been carried out using flowing Helium (Pure He) simulating the purge gas. The results are quite favorable (to be completed).  
No data are available (at least, within CEA) on compatibility between SiC<sub>f</sub>/SiC and Beryllium.

*Question nb.10 - Is material with higher elongation at rupture available (possible) ?*

Yes, but it would have higher porosity and therefore worst mechanical properties (to be checked).

*Question nb.11 - Are permeability data for <sup>3</sup>T and He at elevated temperatures available ?*

Without SiC-coating, He-permeability is certainly unacceptable. Detailed values have to be found.

Permeability to Tritium is also expected to be high, however it is not yet evaluated the level of acceptability (which may be large).

*Question nb.12 - Will He-leak tightness be below 10<sup>-8</sup>Pa m<sup>3</sup>s<sup>-1</sup> for a 3m<sup>2</sup> surface ?*

Answer directly related to the previous question. (to be checked)

*Question nb.13 - What is the state of the art of SiC<sub>f</sub>/SiC production nowadays - which are the predictable developments within the next years ?*

Characteristics of present-day best performing SiC<sub>f</sub>/SiC are given in Table I together with uncertainties and values assumed in the CEA calculations (which are therefore to be interpreted as « suggested values »).

From the point of view of available industrial products (and limiting to products developed by SEP, which is, at present, the only manufacturer able to produce 3D composites), the situation is described hereafter.

Two different SiC<sub>f</sub>/SiC industrial composites are available from SEP : the 2D Cerasep® N2-1 and the 3D Cerasep® N3-1. Both of them use the Nicalon NL207 fibers produced by Nippon Carbon and are densified by CVI [3].

The Cerasep® N2-1, developed in the eighties, is well known and characterized. Its main drawbacks are the delamination problems and the consequent difficulties to obtain complex shapes such as, for instance, those required in the TAURO blanket [1]. In fact, the TAURO manufacturing sequence is based on the use of the more recent Cerasep® N3-1. This new composite uses the same raw components of the previous 2D version, but its 3D GUIPEX® texture avoids delamination problems and confers it a higher resistance to inter-laminar shear stresses (44 MPa instead of 30 MPa).

The limits of this composite for Fusion Power Reactor (FPR) applications are mainly its low thermal conductivity and its low resistance to irradiation damage. The use of low oxygen content fibers like the Hi-Nicalon fibers (Nippon Carbon) could solve those two problems. Actually the thermal conductivity of this new fiber is higher than the one of Nicalon NL207 (see Table II), and its properties changes due to neutron irradiation are lower [4]. Also the maximum operating temperature increases (1300°C instead of 1100°C). A new composite, the Cerasep® N4-1, which uses the Hi-Nicalon fibers is currently under development by SEP [1]. This new composite appears very promising for FPR applications.

Further R&D works on SiC<sub>f</sub>/SiC composites will take in to account the use of new, high purity fibers (e.g., Hi-Nicalon-S) as well as studies on Hi-Nicalon fibers treatments. Other short terms developments foreseen by SEP include improvements in the Guipex® texture (Unlinked Guipex® Textures and variable Guipex® thickness) which will allow to realize even more complex geometry.

*Question nb.14 - Which are the testing facilities available at SEP / at FZK ?*

To be answered by SEP / FZK.

### **3.2 HC blanket concept (SiC<sub>f</sub>/SiC as structural material)**

#### **3.2.1 Specific questions for the proposed HC blanket concept on SiC<sub>f</sub>/SiC properties**

*Question nb.15 - Is it possible to achieve high thermal conductivity (>15 W/mK) ?*

Measured data for 3D CERASEP® N3-1 are given in Table I. The major issue is the thermal conductivity through the thickness. Present measured value at 800°C is about 7 W/mK ; neutron irradiation (for few dpa, after which saturation is expected) leads to a further reduction of a factor 2-3. Major R&D is clearly required to improve these values. The objective of achieving a value of 15 W/mK appears reasonable.

It is suggested to assume this value for the present design (plus a parametric study around this value).

*Question nb.16 - Is it possible to achieve relatively low electrical conductivity ( $<10^3 \Omega^{-1} m^{-1}$ ) to avoid electro-mechanical effect of plasma disruption ?*

Recently measured value at JRC/Ispra for CERASEP<sup>®</sup>N2-1 is about  $500 \Omega^{-1} m^{-1}$  which fulfill the requirement.

*Question nb.17 - Is it possible to achieve high Helium hermeticity especially in the First Wall ?*

It is clear (see previous section) that acceptable hermeticity to Helium can be achieved only with a specific coating. The related problems are already discussed in the previous section. It must be stressed that high hermeticity is also required in the breeder region in order to avoid the pressurization of the box which is not able to sustain significant pressure because no stiffener ribs are present (by the way, this may be a severe problem for this concept in case of accidental break on a cooling tube).

*Question nb.18 - Compatibility with  $Li_4SiO_4$  and Beryllium ?*

Answer already given in the previous section.

*Question nb.19 : Do the mechanical properties remains satisfactory up to  $1000^\circ C$  ?*

The mechanical properties remain satisfactory up to the maximum allowable temperature given in the previous section.

### **3.2.2 Specific questions for the proposed HC blanket concept on component feasibility**

*Question nb.20 - feasibility of long tubes in form of meander ?*

At present, tubes are manufactured by weaving the fibers around a solid core, putting the whole system in the oven for densification, and finally dissolving the core for having the tubes as final products. Moreover, the achieved diameters are greater than 40 mm and the homogeneity of the SiC<sub>f</sub>/SiC properties cannot be guaranteed.

It is clear that such a manufacturing procedure cannot be applied to long tubes in form of meander. New manufacturing procedures have therefore to be at first developed and then industrialized. In all cases, the assumption of completely avoiding joints between tubes appears not reasonable. It is suggested to take into account a certain number of joints between curved tubes in the rear part of the blanket (located in a relatively low fluence).

*Question nb.21 - feasibility of cooling plates and First Wall (FW) made by tube assembly ?*

At present, this type of procedure has never been applied. It appears difficult to force and control the matrix densification to specific locations in order to form plates. Moreover, the idea of weaving further fibers around the already identified tubes for the final plate densification (two-step procedure) has never been tested (not even at a laboratory scale). A campaign of R&D needs to be defined and launched.

*Question nb.22 - feasibility of connection between large (in the FW) and small tubes (in the cooling plates) in the back part of the blanket ?*

This connection appears feasible by brazing provided the tubes are manufactured in the way already described in the previous section.

### **3.3 DC blanket concept (SiC<sub>f</sub>/SiC as channel inserts)**

#### **3.3.1 Specific questions for the proposed DC blanket concept on SiC<sub>f</sub>/SiC properties**

*Question nb.23 - Is it possible to achieve low thermal conductivity ( $<2 W/mK$ ) ?*

In general, for SiC<sub>f</sub>/SiC, a major issue is the low thermal conductivity. It appears therefore relatively easy to achieve a value of  $2 W/mK$  or lower. Moreover, neutron irradiation will tend to improve the situation. The transient situation (below 1 dpa) could be improved by the use of an insulating coating which is allowed to disappear in a relatively short time.

*Question nb.24 - Is it possible to achieve low electrical conductivity for the insert ( $<1.0 \Omega^{-1} m^{-1}$ ) leading to an uniform velocity distribution of the Pb-17Li flow ?*

Recently measured value at JRC/Ispra for CERASEP<sup>®</sup>N2-1 is about  $500 \Omega^{-1} m^{-1}$  [6]. The requirement of a lower value is therefore matter of future R&D. The fact the these inserts have no structural function could make acceptable the use of composites with characteristics very close to those of the SiC matrix (bad mechanical properties but very low electrical conductivity).

*Question nb.25 - Is a sealed surface achievable ? (infiltration of Pb-17Li would increase the thermal conductivity and increase also the electrical conductivity leading to unallowable high MHD pressure losses).*

The possibility of applying a SiC-coating during the densification phase, as a final step, has already been proved by the industry. R&D is required in order to verify the lifetime of such a coating (need of limiting the appearance and the size of cracks). The infiltration of Pb-17Li appears however less likely than the He-leaks in the previous concept.

*Question nb.26 - Is compatibility with Pb-17Li achievable at high temperature (interface at 750°C) ?*

The only experimental data available (obtained in JRC/Ispra) have shown a compatibility between SiC<sub>f</sub>/SiC and static Pb-17Li at 800°C for few thousands hours [5].

Pb-17Li infiltration was not fully checked in the experiment. Further R&D is therefore required to check the effects of Pb-17Li velocity and to verify if infiltration occurs. Longer operating times have also to be achieved.

### **3.3.2 Specific questions for the proposed DC blanket concept on channel insert fabrication and installation**

*Question nb.27 - What is the maximum achievable length of the channel inserts ?*

Present available furnace within industry would allow a length of about 3.5 m. However, there are, in principle, no problems in achieving a much larger length. It is just a matter of constructing a sufficiently large furnace. The major problem will be the investment cost which cannot be evaluated at the present stage and may become irrelevant in the very long term.

*Question nb.28 - Is there the possibility of joining separate portions of SiC<sub>f</sub>/SiC channel inserts together, the thickness of the SiC<sub>f</sub>/SiC insert remaining constant ? ?*

Yes, it is possible to join separate portions of SiC<sub>f</sub>/SiC channel inserts by using the specific brazing technique discussed above. It is also possible to maintain the thickness constant : this can be achieved by machining at the end of each portion a complementary step through half of the thickness. This method is in fact the reference method proposed in TAURO for joining top cap and bottom to the main body of the module [1].

*Question nb.29 - Is there the possibility of the integration of the channel insert spacers in order to provide defined Pb-17Li gaps between the inserts and the steel structures ?*

This point is a specific design question for the DC blanket which does not involve the specific characteristics of SiC<sub>f</sub>/SiC. It has therefore to be answered by the designers after establishment of the gap thickness and the acceptable uncertainty on its dimension.

*Question nb.30 - Is there the possibility of supporting the whole channel inserts construction in the blanket interior ?*

As for the previous question, this point is a specific design question for the DC blanket which does not involve the specific characteristics of SiC<sub>f</sub>/SiC. Spacers and support are part of the same problem whose solution is independent from the actual material the inserts are made of.

Anyway, in general it can be anyway said that joints between steels and SiC<sub>f</sub>/SiC inserts are not directly possible because of the very different thermal expansion. Compliant materials have therefore to be found.

*Question nb.31 - Is possible to make joints between the channel inserts and the coolant access tubes, what is the proper seal material for those high temperatures (700°C), and under neutron irradiation ?*

This question is related to the previous ones. The answer depends on the material of which the coolant access tubes are made of and the functions of the required joints. At a first glance, it appears that flow channel inserts present in the blanket have to be connected with flow channel inserts located within the coolant access tubes. In this case, both materials being SiC<sub>f</sub>/SiC, the joints, if necessary, can be made of Brasic<sup>®</sup>. Again, direct joints between steel and SiC<sub>f</sub>/SiC are not directly feasible.

Anyway, in general it can be said that joints between steels and SiC<sub>f</sub>/SiC inserts are not directly possible because of the very different thermal expansion. Compliant materials have therefore to be found.

## **4 Conclusions**

This report gives a preliminary list of data and assumptions to be applied to designs using SiC<sub>f</sub>/SiC composites in the framework of the pre-study for the EU power plant.

The use of these data and assumptions guarantees the homogeneity and the coherence between the studies performed by different laboratories (in particular, CEA and FZK).

At the same time, the comparison of assumptions and requirements with available industrial materials characteristics and technology gives an idea of the level of R&D required in order to consider SiC<sub>f</sub>/SiC as candidate for FPR in-vessel components structural material.

From the comments made in the previous sections, it appears clear that the use of SiC<sub>f</sub>/SiC for making « flow channel inserts » considerably reduce the R&D demands.

## 5 References

- [1] L. Giancarli, et al., Fusion Eng. & Design 41 (1998) 165-171.
- [2] A. Gasse, et al., Progress on SiC<sub>f</sub>/SiC Structures Joining Techniques and Modeling for Design Analysis, Fusion Technology 1988, Proc. of SOFT-20, 7-11 Sept. 1998, Marseille, France, pp. 1235-1238.
- [3] A. Caso, et al., A New SiC<sub>f</sub>/SiC Composite as Low-activation Structural Material, Proc. of the SiC<sub>f</sub>/SiC Composites Workshop, JRC/Ispira (I), 28-29 October 1996.
- [4] S. Sharafat, et al., Fusion Eng. & Design 29 (1995) 411-420.
- [5] P. Fenici, H.W. Scholtz, Journal of Nuclear Materials 212-215 (1994).
- [6] R. Scholtz, et al., Electrical Conductivity of Silicon Carbide Composites, Proc. of the 2<sup>nd</sup> IEA « SiC<sub>f</sub>/SiC Composites » Workshop, Sendai (Japan), October 23-24, 1997.

**Table I** Cerasep® N3-1 main characteristics

Property	T (°C)	Measured Value (SEP data)	Value assumed for the analyses
Density	20	>2.4 g/cm <sup>3</sup>	2.5 g/cm <sup>3</sup>
Porosity	20	(10±2)%	10%
Fiber Content	20	40%	40 %
Thickness	-	0.8 - 6 mm	6 - 10 mm
Tensile Stress (in plane)	20	(300±20) MPa	-
Tensile Strain	20	(0.80±0.25)%	-
Trans-Laminar Shear Stress	20	(200±20) MPa	-
Inter-Laminar Shear Stress	20	44 MPa	44 MPa
Young's modulus (in plane)	20	(200±20) GPa	200 GPa
Young's modulus (through the thickness)	20	-	200 GPa <sup>1</sup>
Shear modulus (in plane)	20	-	80 GPa <sup>#</sup>
Shear modulus (through the thickness)	20	-	50 GPa <sup>#</sup>
Poisson's ratio (in plane)	20	-	0.18 <sup>#</sup>
Poisson's ratio (through the thickness)	20	-	0.18 <sup>#1</sup>
Thermal Conductivity (in plane)	1000	15 W/m*K	15 W/m*K
Thermal Conductivity (through the thickness)	20	(13±2) W/m*K	15 W/m*K
	800	7.6 W/m*K	15 W/m*K
	1000	7.5 W/m*K	15 W/m*K
Thermal expansion coefficient (in plane)	20	4*10 <sup>-6</sup> /K	4*10 <sup>-6</sup> /K
Thermal expansion coefficient (through the thickness)	20	-	2.5*10 <sup>-6</sup> /K <sup>#</sup>

<sup>1</sup> value not available, the same value have been assumed through the thickness and in plane

<sup>#</sup> corresponding value for the 2D composite

**Table II** Main properties of the SiC fibers produced by Nippon Carbon

Property			Nicalon NL207	Hi-Nicalon
Chemical composition	wt-%	Si	56.6	62.4
		C	31.7	37.1
		O	11.7	0.5
Tensile strength	GPa	20°C	3	2.8
Young modulus	GPa	20°C	220	270
Strain	%	20°C	1.4	1.0
Thermal conductivity	W/mK	20°C	2.97	7.77
		500°C	2.20	10.1
Electrical resistivity	Ω·cm	20°C	10 <sup>3</sup> -10 <sup>4</sup>	1.4
Industrial level			standard product	standard product

**List of Figures:**

Fig. 1: The Dual-Coolant Pb-17Li blanket concept (DC)

Fig. 2: The Helium-Cooled ceramic pebble-bed blanket concept (HC)

## **APPENDIX 2A**

### ***Proposed Design Criteria for SiC<sub>f</sub>/SiC Structural Material***

#### **A1 Introduction**

In the past, typical design criteria for SiC<sub>f</sub>/SiC based blankets (used for instance in the ARIES-I study) were the following :

- i) primary stresses (i.e. stresses due to the mechanical loads) limited to 140 MPa (Von Mises stress);
- ii) secondary stresses (i.e. stresses due to thermal loads) limited to 190 MPa.

This approach, common for metals, is however not satisfactory for composite materials like the SiC<sub>f</sub>/SiC because : i) the distinction between primary and secondary stresses is not well suited, and ii) composite materials present different properties (and therefore different strengths) depending on the loading direction. Also tensile and compression strengths are strongly different.

The Von Mises stress is therefore inadequate as long as these differences are not taken into account.

A new approach for evaluating stress levels in SiC<sub>f</sub>/SiC composites has recently been proposed by CEA [A1]. Starting from an orthotropic monolayer modeling of the composite, where the orthotropy directions correspond to the fibers' directions, the stress levels were separately investigated along each orthotropy axis for each of the basic parts of the blanket. The maximum values of the obtained stresses were then compared with the corresponding rupture limits.

While this approach gives a better description of the loading status of the structure, its main drawback is the particular mechanical behavior of SiC<sub>f</sub>/SiC composites. The stress-strain relation of these composites up to the rupture limit is in fact highly non-linear because of the progressive material damage. Stress levels predicted assuming elastic behavior are therefore inaccurate (although pessimistic). Also the rupture limits for all of the orthotropy directions are not known. Moreover, the mechanical tests required to determine them are not always easy to perform for the 3D composite.

#### **A2 Improved design criteria proposed**

More accurate design criteria, although still preliminary, are presented hereafter. Because of the lack of data for the current 3D composite (the Cerasep® N3-1), they have been inferred on the basis of the mechanical behavior of the 2D composite (Cerasep® N2-1).

For this material the stress-strain relation under tensile strength is linear up to 110 MPa [A2], when the micro-cracking of the matrix starts. The bridging effect of the fibers however prevents the opening of the cracks, and the mechanical behavior remains elastic, although not linear, up to 145 MPa.

Above this limit the anisotropic nature of the composite starts to appear and the mechanical behavior is no longer elastic.

Plane stress states can therefore be evaluated with the Von Mises stress as long as stress levels do not exceed 110 MPa. Possibly stress levels up to 145 MPa can be accepted taking into account that they should decrease when the non-linear behavior of the composite will be taken into account.

For complex 3D stress states, like those due to thermo-mechanical loads in the TAURO blanket, this criterion is no longer valid because of the great differences between the composite properties in plane and through the thickness. However if one can accept to uncouple the stresses through the thickness and the stresses in plane, then the Von Mises criterion can be retained for the latter, while stresses through the thickness can be separately investigated.

Therefore the design criteria adopted at present in CEA analyses are the following :

- starting from the 3D stress tensor as obtained from CASTEM 2000 FEM code, the components in plane are combined to express the Von Mises stress : the assumed limit is 110 MPa ;
- for the shear stress through the thickness a limit of 44 MPa (rupture limit - SEP data) has been assumed ;
- no data is instead currently available for the tensile strength through the thickness. A limit of 110 MPa has been assumed.

#### **A3 Required improvements**

Further improvements in the design criteria are still needed. A behavioral model capable to simulate the non linear stress-strain relation and to predict the damage status of the composite is required. Also it must be noticed that the current resistance criterion does not distinguish between compressive and tensile stresses in plane.

#### **A4 References**

- [A1] G. Aiello, et al., A New Approach for Evaluating Stress Levels in the TAURO SiC<sub>f</sub>/SiC Breeding Blanket, CEA/DMT Internal Report, SERMA/LCA/RT/98-2351/A (1998).
- [A2] X. Aubard (SEP), private communication (PhD thesis).

## Appendix 3

### Abstract

# MHD Flow in the Dual Coolant Blanket Concept

L. Bühler

## 1 Introduction

The idea of using liquid metals as breeding material and removing a major fraction of heat by a separate helium cooling has been presented some years ago by Malang, Bojarsky, Bühler, Deckers, Fischer, Norajitra and Reiser (1993). In their proposal the authors assumed that an electrically insulating coating covers the duct walls so that magnetohydro dynamic pressure losses are minimized to those in insulating ducts. It has been shown that the pressure drop in such a blanket concept is not a crucial issue and results in about  $\Delta p = 0.4 \text{ MPa}$  for the outboard blanket. It has been shown in the summary report compiled by Malang and Schleisiek (1994) that even with the technology of so-called flow channel inserts pressure drop in the blanket stays within design limits. These flow channel inserts consist of an insulating layer that is protected from the corrosive liquid metal by thin sheets of stainless steel. The steel layers are electrically conducting, but as long as they are thin the pressure drop is acceptable.

Now in the improved dual coolant, concept it is proposed to use a silicone carbide composite material as insulating insert. This material seems to be compatible with the liquid breeder *PbLi* (see e.g. Pérez, Giancarli, Molon and Salavy (1995), where SiC is used as structural material). The electrical conductivity of SiC is very low. Values for the electrical conductivity of the insert material

$$\sigma_i = 4 \cdot 10^{-5} \frac{1}{\Omega m}$$

are given by Pérez et al. (1995), while more recently a value of

$$\sigma_i = 10^2 - 10^3 \frac{1}{\Omega m}$$

for SiC has been reported (M. C. Billone, 1998, included in Tillack, Wang, Pulsifer, Malang, Sze, Billone and Sviatoslavsky (1999)) or values

$$\sigma_i = 2 - 10^2 \frac{1}{\Omega m}$$

are published by a SiC manufacturer (<http://www.mortoncvd.com/sicpropl.htm>). These values are several orders of magnitude lower than that of the fluid at 600 °C,

$$\sigma = 7.2 \cdot 10^7 \frac{1}{\Omega m}$$

(Malang and Tillack (1995)) and promise small MHD pressure drop. Nevertheless, one should keep in mind that the values reported above hold for unirradiated material, " that the electrical resistivity of SiC varies by at least six orders of magnitude depending on the fabrication technique, impurity content, etc." (personal communication with C. Billone, 1999), and that the degree of irradiation degradation of the electric resistivity is unknown at present day. On the other hand there are indications that a SiC/SiC composite has a conductivity different from that of the pure material.

## 2 Analysis

It can be seen from the geometry of the dual coolant blanket that all relevant cross sections are of rectangular shape. The liquid metal flows, electrically insulated from the conducting walls, inside the SiC inserts. There may be a small gap between the insert and the steel wall that is filled with almost stagnant breeding material.

The fully developed laminar incompressible flow of the electrically conducting fluid inside the SiC insert is governed by the equations for momentum along the axis, here the x-direction

$$M^{-2} \nabla^2 u + K = j_z, \tag{1}$$

and Ohm's law

$$j_y = -\partial_y \phi, \quad (2)$$

$$j_z = -\partial_z \phi + u. \quad (3)$$

Conservation of electric charge requires

$$\partial_y j_y + \partial_z j_z = 0. \quad (4)$$

It is assumed that the poloidal extension of the blanket is large enough that in most part of the blanket fully developed flow will establish. The kinematic boundary conditions are as usual in hydrodynamic flows. At the walls there is no-slip

$$u = 0. \quad (5)$$

It is further assumed that the inserts are good insulators, say they do not carry a significant amount of current in the tangential direction compared to the current flow within the Hartmann layers. Nevertheless, it is known that the wall material is not a perfect insulator. This is taken into account by the fact that currents may cross the relatively thin insert and enter the much better conducting wall. This condition reads

$$j_n = -\frac{1}{\kappa}(\phi_w - \phi). \quad (6)$$

The currents that enter the wall create there a distribution of wall potential  $\phi_w$ , that is, according to the thin-wall condition (see e.g. Walker (1981)), determined by

$$j_n = -c \nabla^2 \phi_w. \quad (7)$$

In the equations displayed above  $u$ ,  $K$ ,  $j$ , and  $\phi$  denote the velocity, the pressure gradient, the current density and potential, scaled by the reference quantities the average 2 velocity  $u_0$ ,  $\sigma u_0 B^2$ ,  $\sigma u_0 B$ , and  $u_0 a B$ , respectively and

$$M = \alpha B \sqrt{\frac{\sigma}{\rho \nu}} \quad (8)$$

is the Hartmann number. A characteristic scale of the duct geometry is  $a$  that may be chosen e.g. as the half width of the duct, measured along the magnetic field lines. It is assumed that the fluid is incompressible with constant density  $\rho$ , electrical conductivity  $\sigma$  and kinematic viscosity  $\nu$ . The parameter

$$\kappa = \frac{\sigma_i t_i}{\sigma_i a} \quad (9)$$

denotes the wall-normal electric resistance of the insert, with thickness  $t_i$  and conductivity  $\sigma_i$  (compare e.g. Bühler and Molokov (1993)). It can be seen that  $\kappa$  may become small if  $t_i \ll a$ , a fact that becomes important when very thin layers (coatings) are considered.

The conductivity of the walls may be characterized by the wall conductance ratio

$$c = \frac{\sigma_w t_w}{\sigma a}. \quad (10)$$

For the case that the inserts carry some small amount of current in the tangential direction and assuming a stagnant liquid breeder in the gap of thickness  $t_g$  one could modify the wall conductance ratio as

$$c = \frac{\sigma_w t_w + \sigma_i t_i + \sigma_g t_g}{\sigma a}. \quad (11)$$

The governing equations can be solved by asymptotic techniques valid for high Hartmann numbers,  $M \gg 1$ , and one finds finally

$$u = u_c(z) \{1 - \exp[M(|y| - 1)]\} \quad (12)$$

where the core velocity  $u_c$  is given by

$$u_c(z) = K \left\{ (M - \eta) \frac{\cosh(\beta z)}{\cosh(\beta b)} + \eta \right\} \quad (13)$$

with coefficients

$$\beta = \sqrt{\frac{cM + 1}{c\kappa}}, \eta = \frac{c + 1}{c + M^{-1}} \quad (14)$$

as shown by Bühler and Molokov (1993). The velocity profile is nearly uniform along magnetic field lines and exhibits very thin viscous boundary layers of exponential type near the walls that are perpendicular to the field, called Hartmann walls. These viscous layers are known as the Hartmann layers and their thickness scales as  $\delta \sim M^{-1}$ . The velocity outside the viscous layers, in the core, depends on  $z$  only. There is the possibility of higher velocities near the sides, where the magnetic field is tangential to the so-called side walls. Results will be displayed in the next section where the analysis is applied for the Dual Coolant Blanket data.

The pressure drop is obtained by the condition for volumetric flux

$$\int_0^d \int_0^1 u dy dz = d. \quad (15)$$

One obtains the result for pressure gradient as

$$k = \frac{\beta d}{(M - \eta) \tanh(\beta d) + \eta \beta d}. \quad (16)$$

## 2.1 Flow in the first duct

According to the geometry described above one can evaluate the nondimensional parameters. They are

$$M = 2.96 \cdot 10^4, c = 5.8 \cdot 10^{-2}, \kappa = 2.35 \cdot (10^4 - 10^2). \quad (17)$$

Since there are uncertainties for the conductivity of the inserts a range of the resistance parameter  $r$ , is specified according to the conductivity

$$\sigma_i = 10^0 - 10^2 \frac{1}{\Omega m}$$

to cover the range to be expected. The liquid metal properties are taken at an average temperature of  $T = 600^\circ C$ , using the polynomial dependencies on temperature as published by Malang

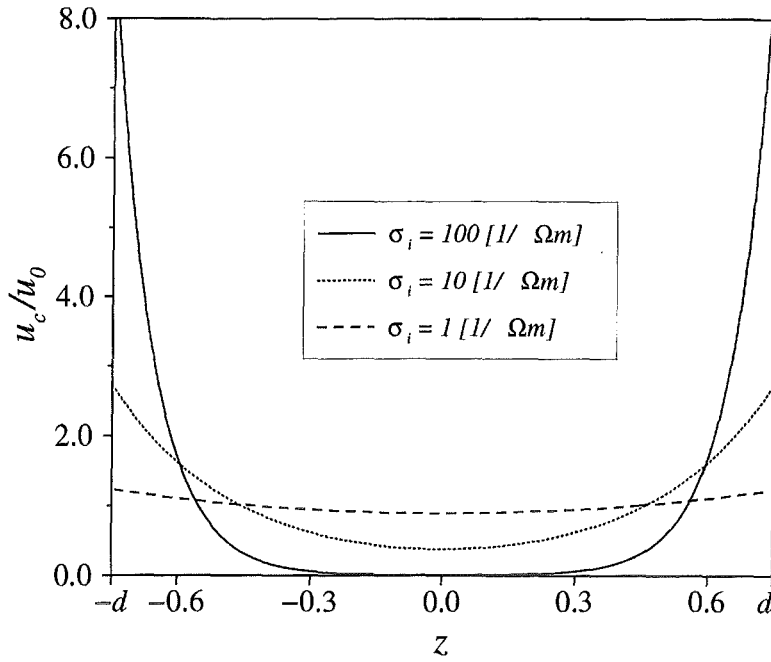


Figure 1: Pressure drop in the first row of rectangular poloidal ducts as a function of the conductivity of the insert.

and Tillack (1995). For the geometry of the first row of rectangular ducts one finds pressure drops which are relatively small. Results are shown in figure 1. For small conductivity of the inserts the pressure drop approaches values as in insulating ducts. If  $\sigma_i$  becomes larger than about

$$\sigma_i \approx 10 \frac{1}{\Omega m}$$

the pressure drop becomes proportional to  $\sigma_i^{1/2}$ . The points on the pressure drop line indicate special values for which velocity profiles are shown below.

Velocity profiles for three different values of  $cTi$  are shown in figure 2. If the insert provides high insulation,

$$\sigma \lesssim 1 \frac{1}{\Omega m}$$

the velocity is almost uniform in the whole cross section. For higher conductivities, in the range as to be expected, one finds an increase of velocity when approaching the side walls which are parallel to the applied magnetic field. The magnitude of nondimensional velocity at the side wall may reach relatively high values depending on the insert conductivity. Such strongly expressed velocity profiles can not be excluded with the present knowledge about the insulation properties of the SiC material. The increased velocities near the side walls, especially near the first wall, increase the heat transfer in regions of high volumetric power density. The very low velocity near the duct center may be unfavorable for heat transfer reasons for which a uniform velocity profile would be desirable. On the other hand, unlike in circular pipes, rectangular ducts allow for MHD instabilities that promote a vortex motion with main vorticity aligned with the B-field. Such vortices could homogenize the average velocity and temperature field without increasing the pressure drop too large. The answer to this question requires more detailed nonlinear calculations and experiments are required that are beyond the scope of the present laminar study. Nevertheless, the idea of vortex generation near the side walls is reasonably supported by the analytical work performed by Ting, Walker, Moon, Reed and Picologlou (1991a), by experiments of Ting, Walker, Moon, Reed and Picologlou (1991b), or by recent experiments performed by Burr (1998) and should be kept in mind for future research.

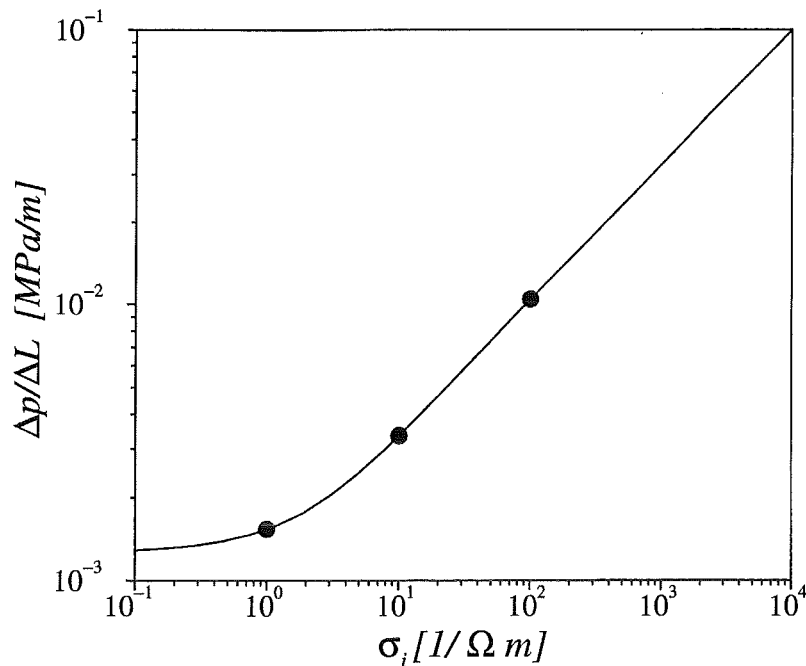


Figure 2: Velocity profile  $u(z)$  measured along the radial coordinate  $z$  for three values of  $\sigma_i$ . The velocity is scaled by the average velocity  $\sigma_o$ .

So far the calculations for one duct. Since the other ducts have half the velocity than the one considered above one should just multiply the current results by 1.5 to get the total pressure drop per 1m blanket length. The bends at the bottom of the blanket turn the flow in a plane perpendicular to the magnetic field lines. Such flows do not cause higher MHD pressure drop than the flow in a straight duct of same average length Molokov (1995).

#### References

- Bühler, L. and Molokov, S.: 1993, Magnetohydro dynamic flows in ducts with insulating coatings, Technical Report KW 5103, Kernforschungszentrum Karlsruhe.
- Burr, U.: 1998, Turbulente Transportvorgänge in magnetohydrodynamischen Kanalströmungen, PhD thesis, Universität Karlsruhe. Techreport Forschungszentrum Karlsruhe FZKA 6038.
- Malang, S., Bojarsky, E., Bühler, L., Deckers, H., Fischer, U., Norajitra, P. and Reiser, H.: 1993, Dual coolant liquid metal breeder blanket, in C. Ferro, M. Gasparotto and H. Knoepfel (eds), Fusion Technology 1992, Proceedings of the 17<sup>th</sup> Symposium on Fusion Technology, Rome, Italy, 14-18 September 1992, Elsevier Science Publishers B. V., pp. 1424-1428.
- Malang, S. and Schleisiek, K.: 1994, Dual coolant blanket concept, Technical Report KW 5424, Kernforschungszentrum Karlsruhe.
- Malang, S. and Tillack, M. S.: 1995, Development of self-cooled liquid metal breeder blankets, Technical Report FZKA 5581, Forschungszentrum Karlsruhe.
- Molokov, S.: 1995, Liquid metal flows in insulating elements of self-cooled blankets, Fusion Engineering and Design 27, 642-649.
- Pérez, A. S., Giancarli, L., Molon, S. and Salavy, J. F.: 1995, Progress on the design of the TAURO breeding blanket concept, Technical Report DIVIT 95/575 (SERMA/LCA/1829), CEA.
- Tillack, M. S., Wang, X. R., Pulsifer, I., Malang, S., Sze, D. K., Billone, M. and Sviatoslavsky, L.: 1999, Fusion power core engineering for the ARIES-ST power plant, Fusion Engineering and Design p. to be published.
- Ting, A. L., Walker, J. S., Moon, T. 1, Reed, C. B. and Picologlou, B. F.: 1991a, Linear stability analysis for high-velocity boundary layers in liquid-metal magnetohydrodynamic flows, Int. J. Engng. Sci. 29(8), 939-948.
- Ting, A. L., Walker, J. S., Moon, T. 1, Reed, C. B. and Picologlou, B. F.: 1991b, Linear stability results for high-velocity boundary layers in self-cooled liquid-metal blankets, Fusion Technology 19, 1036-1039.
- Walker, J. S.: 1981, Magnetohydrodynamic flows in rectangular ducts with thin conducting walls, Journal de Mécanique 20(1), 79-112.